

UNIVERSITÀ DEGLI STUDI DI PADOVA

Department of Civil, Environmental and Architectural Engineering

Corso di Laurea Magistale in Ingegneria Civile

Tesi di Laurea

Investigation on the seismic assessment of Reinforced Concrete frames based on fragility curves

Relatore:

Prof. Ing. Carlo Pellegrino

Correlatore:

Dr. Ing. Riccardo Morbin

Laureando:

Xingyong Yang

Anno Accademico 2013-2014

TABLE OF CONTENTS

ABSTRACT	1
Chapter 1 INTRODUCTION	2
1.1 SICHUAN EARTHQUAKE.....	2
1.2 GREAT HANSHIN EARTHQUAKE.....	3
1.3 Organization of the Thesis	7
Chapter 2 DEFINITION AND BACKGROUND	9
2.1 Background and the scientific meaning.....	9
2.2 Seismic Damage of RC frame structure.....	10
2.3 Performance-Based Earthquake Engineering (PBEE).....	12
2.3.1 The Overview of the Performance-Based Earthquake Engineering	12
2.3.2 The basic framework for the Performance-Based Earthquake Engineering (PBEE).....	13
2.3.3 The relationship between the PBEE and structural vulnerability	17
2.4 Structural seismic vulnerability overview	17
2.5 Previous studies on seismic vulnerability for RC buildings	18
Chapter 3 THE ANALYSIS METHOD OF STRUCTURAL SEISMIC RESPONSE	24
3.1 Introduction	24
3.2 IDA methods and basic principles of the seismic vulnerability.....	24
3.2.1 Incremental dynamic analysis method.....	24
3.2.2 The basic principles of the seismic vulnerability.....	25
3.3 The problems of Seismic Fragility analysis based on IDA method.....	27
3.3.1 How to select ground motion records	27
3.3.2 Scale factor and algorithm	29
3.3.3 Intensity measures (IM) and Damage measures (DM)	30
3.3.4 Defining limit states.....	30
3.3.5 The Interpolation and Statistics of IDA curves.....	31
3.3.6 Theoretical derivation of seismic vulnerability analysis.....	32
Chapter 4 MODEL OF RC FRAME STRUCTURE	33
4.1 Introduction	33
4.2 The design of RC frame structure model.....	34

4.2.1 Engineering situation	34
4.2.2 Design of the basic model.....	34
4.3 Nonlinear Finite Element Modeling	35
4.3.1 Introduction of OpenSees Software	35
4.3.2 Constitutive relations of materials	36
4.3.3 The finite element models.....	37
4.4 Nonlinear Dynamic Analysis	37
4.5 Analysis result.....	38
4.6 Algorithm Analysis	38
4.6.1 Single Ground Motion record of IDA curve	38
4.6.2 Number of Ground Motion records of IDA curve	41
4.6.3 probabilistic seismic demand model.....	43
4.6.4 Seismic Vulnerability Analysis	44
Chapter 5 INFLUENCE OF STRUCTURE PARAMETERS ON THE SEISMIC VULNERABILITY	46
5.1 Introduction	46
5.2 Longitudinal reinforcement strength	46
5.2.1 The analysis model based on the seismic vulnerability analysis of IDA method	47
5.2.2 Results analysis.....	55
5.3 Strength of Concrete	58
5.3.1 The analysis model based on the seismic vulnerability analysis of IDA method	59
5.3.2 Results analysis.....	70
5.4 The aspect ratio of the column cross-section.....	72
5.4.1 The analysis model based on the seismic vulnerability analysis of IDA method	72
5.4.2 Results analysis.....	81
Chapter 6 CONCLUSION AND PROSPECTION	83
6.1 The main results and conclusions of this paper	83
6.2 Prospect	84
REFERENCES	85
APPENDIX	88

ABSTRACT

In the recent years, the inadequacies of the traditional seismic design concept and design method attract more and more attention because of their possibilities to induce enormous casualties and property losses. Therefore, a problem has been raised about how to guarantee the quality of the building structures to resist collapse due to earthquake. Considering that the earthquake can be described as a process that uncertainties (structure and earthquake) are introduced to couple with non-linear variables, this paper is mainly to employ IDA method to analyze the earthquake uncertainties. After discussing the seismic vulnerability on 2D frame structure, this paper intends to study the impact of three factors (the longitudinal reinforcement strength, the concrete strength, and the aspect ratio of cross-section column) on the seismic performance of RC frame structure, especially against the influence of the collapse.

First, Incremental Dynamic Analysis (IDA) – based seismic fragility curves analysis are introduced. 10 ground motion records with $Sa(T_1, 5\%)$ as the indicator for seismic action and θ_{max} as the indicator for structural damages are selected. When dealing with the threshold, not only the simple and convenient DM rules, but also IDA method which is eligible for collapse critical point judgment are adopted. So a reasonable set of critical points of various levels can be achieved. Second, the finite element modeling method on OpenSEES-based RC plane frame construction is analyzed and 6-storey RC 2D frame structure is chosen for study.

From the results, RC frame structure which are in strict accordance with current Italian code (NTC 2008) aspect ratio of cross-section column influence on seismic resistance is ambiguous on the premise of a similar axial compression ratio, elevation of concrete strength levels is tantamount to that of seismic resistance. With the increase in the beam-column longitudinal reinforcement strength, there is a higher possibility to reach IO and LS state for the structure with B 450C steel than FeB38k and FeB32k under the same seismic intensity. However, when it is about to collapse, the structure with B 450C steel shows better resistance ability than the other two. This research provides theoretical reference to evaluate the longitudinal reinforcement strength, Concrete strength, Aspect ratio of cross-section column on construction seismic resistance on a quantitative basis, as well as a quantitative reference to performance-based design of RC frame structures.

Chapter 1 INTRODUCTION

1.1 SICHUAN EARTHQUAKE

The 2008 Sichuan Earthquake or the Great Sichuan Earthquake, measured at 8.0 Ms and 7.9 Mw, and occurred at 02:28:01 p.m. China Standard Time at epicenter on Monday, May 12 in Sichuan province, killed 69,195 people and left 18,392 missing.

It is also known as the Wenchuan earthquake (Chinese: 汶川大地震; pinyin: Wènchuān dà dìzhèn), after the location of the earthquake's epicenter, Wenchuan County, Sichuan. The epicenter was 80 kilometers west-northwest of Chengdu, the provincial capital, with a focal depth of 19 km. The earthquake was also felt in nearby countries and as far away as both Beijing and Shanghai—1,500 km. and 1,700 km. away—where office buildings swayed with the tremor. Strong aftershocks, some exceeding magnitude 6, continued to hit the area even months after the main quake, causing new casualties and damage.

Official figures stated that 69,197 were confirmed dead, including 68,636 in Sichuan province, and 374,176 injured, with 18,222 listed as missing. The earthquake left about 4.8 million people homeless, though the number could be as high as 11 million. Approximately 15 million people lived in the affected area. It was the deadliest earthquake to hit China since the 1976 Tangshan earthquake, which killed at least 240,000 people, and the strongest in the country since the 1950 Chayu earthquake, which registered at 8.5 on the Richter magnitude scale. It is the 21st deadliest earthquake of all time. On November 6, 2008, the central government announced that it would spend 1 trillion yuan (about \$146.5 billion) over the next three years to rebuild areas damaged by the earthquake, as part of the Chinese economic stimulus program.



Figure 1.1 Miaoziping Bridge damaged in 2008 earthquake



Figure 1.2 A bank in Beichuan after the earthquake

Miaoziping Bridge is located where Duwen Highway (connecting Chengdu and Wenchuan) crosses the Zipingpu dam reservoir and Min River. In total, the structure is 1,440m long and consists of a three-span continuous prestressed box girder bridge with prestressed concrete girder approach bridges of two, four, and five spans as shown in Figure 1.1. The first floors of many building were crushed during the Wenchuan earthquake.

1.2 GREAT HANSHIN EARTHQUAKE

The Great Hanshin earthquake occurred at 5:46 a.m. on Tuesday, January 17, 1995. This earthquake is also called by the following names: Kobe, South Hyogo, Hyogo-ken Nanbu.

The 1995 Great Hanshin Earthquake had a local magnitude of 7.2. The duration was about 20 seconds. The focus of the earthquake was less than 20km below Awaji-shima, an island in the Japan Inland Sea. It was one of the most devastating earthquakes ever to hit Japan.

More than 5,500 people were killed and over 26,000 people injured. The economic loss has been estimated at about USD 200 billion. The proximity of the epicenter, and the propagation of rupture directly beneath the highly populated region, help explain the great loss of life and the high level of destruction.

The cities of Kobe and Osaka are connected by an elevated highway. The earthquake caused several portions of the highway to collapse. Most of the deaths and injuries occurred when older wood-frame houses with heavy clay tile roofs collapsed. Note that homes and buildings are designed to be very strong in the vertical direction because they support their own static weight. Furthermore, many of the structures in Kobe built since 1981 had been designed to strict seismic codes. Most of these buildings withstood the earthquake.




Figure 1.3 Bridge damaged in Hanshin earthquake





Figure 1.4 Highway damaged after the earthquake


EXTENT OF TREMORS


Places ordered by distance from epicenter (or time of propagation) :


 China (Mainland): All provincial-level divisions except Xinjiang, Jilin and Heilongjiang were physically affected by the quake.


 Hong Kong: Tremors were felt approximately three minutes after the quake, continuing for about half a minute. This was also the most distant earthquake known ever to be felt in Hong Kong. The intensity reached MM III in Hong Kong.


 Macau: Tremors were felt approximately three minutes after the quake.

 Vietnam: Tremors were felt approximately five minutes after the earthquake in Northern parts of Vietnam. The intensity was MM III in Hanoi.


 Thailand: In parts of Thailand tremors were felt six minutes after the quake. Office buildings in Bangkok swayed for the next several minutes.


 Taiwan: It took about eight minutes for the quake to reach Taiwan, where the tremors continued for one to two minutes; no damage or injuries were reported. The intensity was MM III in Taipei.


 Mongolia: Tremors were felt approximately eight minutes after the earthquake in parts of Mongolia.

 Bangladesh: Tremors were felt eight and a half minutes after the quake in all parts of Bangladesh.

 Nepal: Tremors were felt approximately eight and a half minutes after the quake.

 India: Tremors were felt approximately nine minutes after the earthquake in parts of India.

 Pakistan: In parts of Northern Pakistan tremors were felt ten minutes after the quake.

 Russia: Tremors were felt in Tuva, no casualties reported.

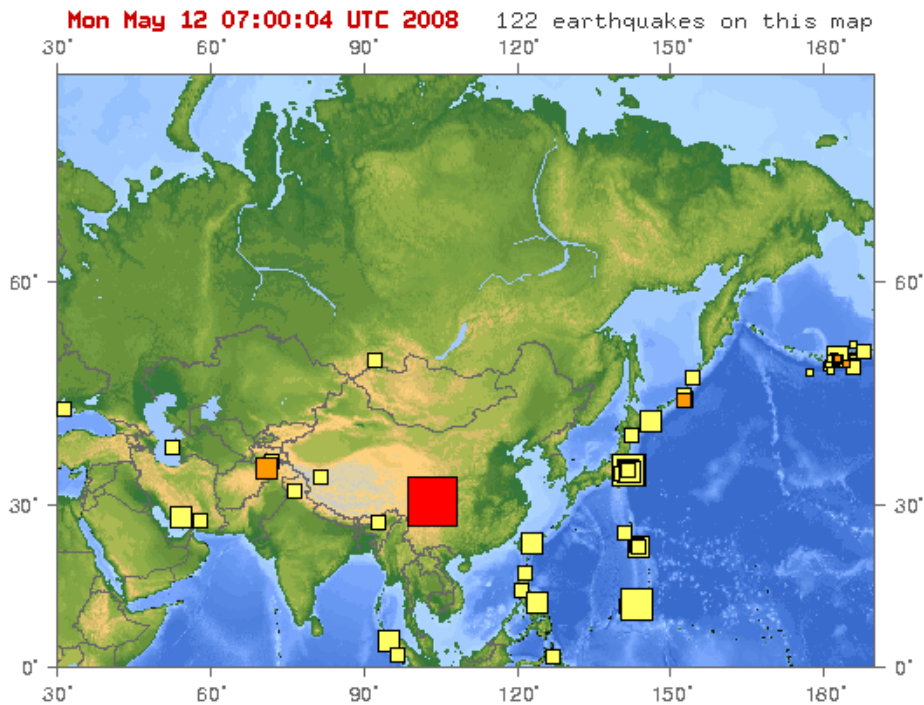


Figure 1.5 Map of epicenter of May 12, 2008 earthquake in Sichuan province, China

The USGS provided a map of Asia in May 2008, which showed a total of 122 earthquakes occurring on the continent. The large red square near the center of the map depicts the 7.9 magnitude Chengdu earthquake in Sichuan province.

PROPERTY DAMAGE

The earthquake left at least 5 million people without housing, although the number could be as high as 11 million. Millions of livestock and a significant amount of agriculture were also destroyed, including 12.5 million animals, mainly birds. In the Sichuan province a million pigs died out of 60 million in total. Catastrophe modeling firm AIR Worldwide reported official estimates of insurers' losses at US\$1 billion from the earthquake; estimated total damages exceed US\$20 billion. It values Chengdu, at the time having an urban population of 4.5 million people, at around US\$115 billion, with only a small portion covered by insurance.

The massive damage of properties and houses in the earthquake area was because China did not create an adequate seismic design code until after the devastating 1976 Tangshan earthquake. If the buildings were older and built prior to that 1976 earthquake, chances are they weren't built for adequate earthquake forces.

In the days following the disaster, an international reconnaissance team of engineers was dispatched to the region to make a detailed preliminary survey of damaged buildings. Their findings show a variety of reasons why many constructions failed to withstand the earthquake.

The earthquake occurred in the rural part of China. Presumably, many of the buildings were just built; they were not designed, so to speak. There are very strong building codes in China, which take care of earthquake issues and seismic design issues. But many of these buildings presumably were quite old and probably were not built with any regulations overseeing them.

Even with the five largest cities in Sichuan suffering only minor damage from the quake, some estimates of the economic loss run higher than US\$75 billion, making the earthquake one of the costliest natural disasters in Chinese history.

1.3 Organization of the Thesis

The structure uncertainty to resist earthquake action has been studied in this work. Compared to the ground motion uncertainty, the structure uncertainty does not play a leading role in the structural seismic performance. However, the impact of uncertainty resulting from the structure calculation model, structure and components size, and the strength of materials still cannot be ignored on the seismic performance of structures, which is very important in the earthquake.

In this paper, 10 ground motions have been selected to conform to the site requirements.

IDA analysis has been performed with a reasonable ground motion intensity index of random variables, through seismic vulnerability analysis of RC plane frame structure. The effects of three uncertainty factors (the longitudinal reinforcement strength, the concrete strength, and the aspect ratio) on the seismic performance of RC frame structure have been studied.

The main work can be described as follows:

The first chapter briefly introduces the historical earthquakes, the Sichuan earthquake (China) and Kobe earthquake (Japan).

The second chapter introduces the dangers of earthquakes and Seismic Hazard of RC frame structure, including the theory of the seismic design of structure, the basic knowledge of the structure seismic vulnerability analysis, and the previous studies on the seismic vulnerability for RC buildings.

The third chapter discusses the basic principles of IDA method and seismic vulnerability analysis, including the detailed discussions for the problems of the seismic vulnerability based on IDA method, the introduction of the concept of reliability theory to derive formulas of seismic vulnerability, and the description of the RC frame structure based on IDA method of seismic vulnerability analysis steps.

The fourth chapter, in accordance with the current Italian code specification of basic analysis model for the structural design, presents the finite element modeling of RC pane frame structure with OpenSEES software to discuss the problems with material constitutive relation, the cross section of restoring force model, and the element model. For example, detailed instructions were given about the six story RC frame structure, to analyze the seismic vulnerability based on IDA method.

The fifth chapter mainly studies the influence of the uncertainty parameters on seismic performance of structure, including the longitudinal reinforcement strength, the concrete

strength and the aspect ratio, to analyze the seismic vulnerability for the RC plane frame structure model based on IDA method and to evaluate the seismic performance.

Chapter six is the conclusion and prospect of the paper.

Chapter 2 DEFINITION AND BACKGROUND

2.1 Background and the scientific meaning

Earthquake is a sudden, very strong destructive natural disaster, a strong earthquake in the moment can give a modern city a devastating blow. On people's lives and property caused serious harm. For example, in 2008 Sichuan earthquake, 2009 Indonesian earthquake, 2010 Haiti, Chile, Yushu, Indonesia, New Zealand earthquake and the 2011 earthquake in Japan, particularly large earthquakes, resulting in a large number of houses destroyed and collapsed, bring about tens of thousands of people casualties, leading to huge economic losses and serious social problems.

Table 2.1 Part of major earthquakes since the 20th century

Rank	Location	Magnitude	Property damage USD
1	Tohoku, Japan	9.0	122 billion
2	Great Hanshin, Japan	6.9	100 billion
3	Sichuan, China	8.0	75 billion
4	Chile, Chile	8.8	27 billion
5	Northridge, United States	6.7	20 billion
6	Tangshan, China	7.8	19 billion
7	Emilia, Italy	6.1	12 billion
8	Christchurch, New Zealand	6.3	11 billion
9	Taipei, Taiwan	7.6	10 billion
10	San Francisco, United State	7.8	9.5 billion

Destruction of all kinds of structures collapsed during the earthquake, and is the main cause to harm people's lives and property. According to statistics of casualties caused by various types of structures covering 95% of the total casualties. Therefore, study on the performance of the structure is one of the main objectives of structural engineering.

RC frame structure building layout flexibility to satisfy Building requirements, increasingly to use in civil engineering. According to data provided by the National Bureau of Statistics in 2008, suffered the greatest impact in the earthquake in Sichuan, Gansu and Shaanxi

provinces in RC frame structure of urban residential accounted for 30%、 48.3% and 33.3% of the total. In the earthquake, RC frame structures suffered varying degrees of damages, people's lives and property were caused great harm. Therefore, it is very important to study on the RC frame structure and analyze the seismic capacity.

2.2 Seismic Damage of RC frame structure.

Under the effect of strong earthquakes, the structural damage mechanism and the process is extremely complex, the researchers at home and abroad is still not fully use the theoretical and computational analysis to explain them. Therefore, summarizes the characteristics of typical structure in the earthquake damage, it is necessary to learn from. In wenchuan earthquake, beichuan county, many framework structure destruction in the city, the main damage is: Collapse of structure, underlying damage of the framework, the extremity of beam damage, the filler wall damage, etc.

1. Collapse and underlying damage of the framework

Figure 2.1 is an example of the whole structure collapsed. Figure 2.2 is an example of the collapse of the underlying framework. For the underlying framework, the upper part of housing construction masonry structures in the earthquake, which destroyed almost all appear in a different structure transition of storey. This is due to the stiffness of the frame structure and masonry structure quite different, due to the rigidity of the mutation, the transition layer is very serious in the earthquake damage, a lot of damage in the form of complete collapse, for such construction, housing construction in the future, we should carefully choose.



Figure 2.1 Example of the whole structure collapsed



Figure 2.2 Example of collapse of the underlying framework

2. Extremity of column damage

In the earthquake, a large frame structure appeared column end damage, rather than the designer desired that the extremity of beam damage, which did not form a "strong column weak beam" yield System. The general performance of concrete spalling, stirrups out even fracture, column longitudinal reinforcement bending, "strong beam weak column" phenomenon caused Chinese scholars reflection to the 2001 version of the seismic code.



Figure 2.3 The extremity of column damage in the earthquake.

3. The filler wall damage

The main reasons of the damage of filler wall are:

- 1) The lack of a reliable connection between the wall and the main structure.
- 2) Between the wall and column not even placed sufficient number reinforcement.
- 3) Infill walls of brick and mortar tensile strength is low. Infilled damage phenomenon mainly is horizontal cracks, vertical cracks, diagonal cracks and cross cracks, etc. Shown in figure 2.4



Figure 2.4 The filler wall damage

2.3 Performance-Based Earthquake Engineering (PBEE)

2.3.1 The Overview of the Performance-Based Earthquake Engineering

Each occurrence of a strong earthquake, not only to the people's lives and property brought disaster, but also can expose a lot of defect of building structure design ,to provide the most reliable information for the further improvement of seismic design methods. After the 2008 earthquake as our country according to the 2001 edition of the problems found "Seismic Design of Buildings" has been modified; 2010, based on experience and earthquake damage new technology to produce large earthquakes occurred in recent years in China and abroad, our has revised 2010 seismic design code as people in-depth study of the seismic action, seismic design ideas have been considered from the earliest completely rigid development of the structural system to the current national seismic codes in the generally accepted three level of seismic fortification , has made great progress, this design idea in the actual earthquake also verified with good seismic performance.

Although according to design code or reinforced buildings in earthquake has caused a number of casualties obviously decrease, but the structure of the normal use of loss of function caused huge economic losses by the seismic excitation are often beyond the capacity of the owners, especially with the rapid economic development, the costs of renovation of the building's internal structure as well as high-tech equipment, etc. often exceeds the cost of the structure of the building itself.

For example, the 1995 Great Hanshin 7.2M earthquake in Japan, the death of 55 people, economic losses of up to \$ 100 billion, and the restoration and reconstruction work after the earthquake lasted for more than two years .1999, 7.6M earthquake occurred in Taiwan, China , resulting in 2405 deaths and 11,306 people were injured, the economic losses of nearly \$ 10 billion; 2010 Haiti earthquake caused 11.3 million deaths and economic losses of about \$ 7.75 billion.

More and more instances of the earthquake disaster prompted scholars from various countries on the existing seismic design ideas and methods for profound review found that the current ideological of anti-seismic in nature to protect the lives and safety purposes, although it can be guarantee structure does not collapse when a major earthquake to temporarily and to protect the safety of life, but the structure may have significant plastic deformation and damage, causing serious damage to people 's property. Because in today's society and the owners of the building have different levels of anti-seismic performance requirements, so the modern building structures not only to be able to avoid collapse, but also to meet user demand for

multi-level buildings. However, the boundaries between the three fortification levels rather vague, in the actual engineering ,the designer is difficult to control, such as damage to what state considered "repairable", allowing the structure to produce how much damage in the earthquake , these are not specifically quantified. Therefore, There are some problems for the existing norms in the design concept and satisfy to social needs, etc., in the further explore more sophisticated seismic design ideas and methods is an urgent need.

The early 1990s, American scholar Moehle first proposed the idea Displacement Base Seismic Design (DBSD). he was improved based on force Design method is put forward the structure of the plastic deformation capacity to meet the scheduled deformation under earthquake excitation. DBSD theoretical is achieved by controlling the structure of the interlayer displacement angle limit, to be more precise evaluation of the structural response under seismic action. DBSD theoretical emergence and development to the Performance Based Seismic Design (PBSD) has laid a good foundation, the United States, Japanese scholars on the basis of performance-based seismic design an in-depth study and subsequently cause the States widespread attention.

Although many research institutions, scholars PBSD gives definitions are not identical, but are considered in the design of buildings using the term, when subject to certain seismic force , structural damage should not exceed its corresponding performance level. Compared to conventional design, performance-based seismic design concept more widely and directly meet the needs of individuals and society according to their own requirements for use of the building, and the designer can choose different ways and means to achieve these requirements, so that we can more easily to apply to the new structure system, new design methods and new materials, etc.

2.3.2 The basic framework for the Performance-Based Earthquake Engineering (PBEE)

Essence of the performance-based seismic design theory is an attempt to control the deformation of the structure, damage states and reaction design. depending on the fortification of its general level, the seismic performance of the structure is divided into different levels, depending on the specific needs and then designer according to the specific requirements of owner, determine a reasonable seismic performance objectives and reasonable structural measures.

Performance-based seismic design elements include:

- Seismic fortification levels
- Seismic performance levels
- Seismic design
- Anti-seismic design objectives and analysis methods

1. Seismic fortification levels

Seismic fortification level refers to the level of the building site in the future may be subjected to seismic action and can also be understood as how much should be selected as the seismic intensity for structural defense objects. It is directly related to seismic safety and the risk of earthquake damage suffered extent of the building, usually with different return periods and exceedance probability of the earthquake to represent. China's 2010 edition of the code for seismic design of buildings used in the 89 edition and 2001 edition to keep the three-level of seismic fortification. and the United States U.S. FEMA273, SEAOC Vision 2000 recommends a four-level of seismic fortification in the performance of design structural.

Table 2.2 China's three-level of seismic fortification.

Level of seismic fortification	Meaning	50-year exceedance probability	Return period(year)
First level	Small earthquake	63.2%	50
	Dose not destroy Moderate		
Second level	Earthquake Repairable	10%	475
Third level	Major earthquake Dose not collapse	2%-3%	1642

Table 2.3 U.S FEMA273 four-level of seismic fortification

Seismic level	Exceedance probability	Return period(year)
Frequent	30 year 50%	43
Occasional	50 year 50%	72

Rare	50 year 10%	474
Very Rare	100 year 10%	970

Table 2.4 U.S SEAOC four-level of seismic fortification

Seismic level	50-year exceedance probability	Return period(year)
Frequent	50%	72
Occasional	20%	225
Rare	10%	474
Very Rare	2%	2475

2. Seismic performance levels

Seismic performance level is expected to describe the maximum damage of buildings in a specific seismic design standards, we can use the structure of vulnerability, the function of structure and personnel security to reflect. Compared to conventional design, performance-based seismic performance level considering the structural elements, non-structural components, equipment and interior decoration and other factors, making the structure more specific seismic performance standards, people's choice and more flexible.

3. Seismic design

The objective of seismic design is aimed at a certain seismic fortification levels and structure to achieve the desired level of seismic performance, is the premise and foundation of structure design process. To control the different structures and the extent of damage fortification non structural components under earthquake, should be made to adapt to different types of multi-level buildings seismic targets. Figure 2.5 is the relationship between earthquake performance level and earthquake design level.

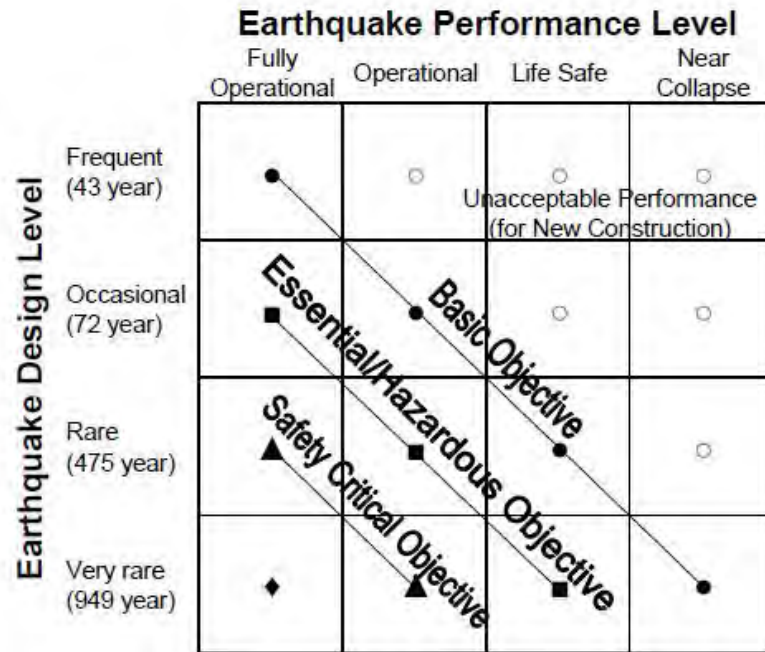


Figure 2.5 Vision 2000 recommended seismic performance objectives for buildings(after SEAOC, 1995)

4. Anti-seismic design objectives and analysis methods

Along with the experience accumulation and the efforts of the researchers, the seismic design structural analysis methods are constantly developing and improving, has gone from static analysis to dynamic analysis, the development process from the linear analysis to non linear analysis . At present, the most commonly used analysis methods for seismic design of structures have static pushover analysis (SPO) method and incremental dynamic analysis (IDA) method.

Static pushover analysis is carried out in elasto-plastic analysis of the structure under lateral static monotonic loading, the method can predict the structure and components of a given peak response and seismic performance under seismic action, compared with the dynamic time history analysis, the structural analysis and calculation is simple, greatly reducing the amount of time, but can be approximated to obtain structure elastic-plastic seismic response. However, SPO adopted level loading mode does not match with the actual earthquake, its essence is still one kind of static analysis methods. Although there are many scholars have proposed a number of improved methods to try to compensate for this deficiency, making the method to calculate the accuracy has increased, but from an accurate description of the dynamic response of structures under earthquake is still a big gap.

Due to the incremental dynamic analysis rely on a large number of the elasto-plastic time history of computing, computing power requirements are relatively higher , in recent years with

the development of computer technology the incremental dynamic analysis (IDA)method began to be a large number of applications. IDA method is a kind of traditional dynamic elastic-plastic time history analysis method based on elasto-plastic seismic response dynamic parameter analysis methods , its advantages is that it can fully grasp the dynamic characteristics of the system, when there are a sufficient number of ground motion, this the method can reflect the response of structures subjected to vibrations in the time. IDA analysis results are usually expressed by IDA curve, IDA curve can reflect the structural system from linear elastic to elastic-plastic under different ground motion intensity, to the overall collapse of the whole response process, so you can better understand the earthquake especially strong effect on the performance of the structure and the characteristics of structural response anywhere the vibration intensity of the laws of growth and change.

2.3.3 The relationship between the PBEE and structural vulnerability

ATC-40 principles based on FEMA273 criteria focus on the research of assessment method based structural performance in performance-based seismic design. The principles adopted static nonlinear analysis method to evaluate the seismic capacity spectrum and demand structure of the spectrum, and to simplify the method to obtain seismic vulnerability of structures. Therefore, the vulnerability of structure is an important part of the seismic performance-based design, and it is inevitable continuation of ideas based on the performance of the design .

2.4 Structural seismic vulnerability overview

Structural seismic vulnerability refers to the probability of structure of different degree of damage at different levels of earthquake .From the sense of probability quantitatively characterize the seismic performance of engineering structures, macroscopic description of the relationship between ground motion intensity and extent of structural damage. Usually seismic vulnerability curves with respect to different performance levels of structural failure probability and ground motion intensity gathers, in order to describe the seismic vulnerability of structures.

There are two commonly used methods to obtain the structural seismic vulnerability curves:

- (1) The empirical method, namely, through the previous structure of the earthquake damage investigation statistics, describe the structure under the effect of different intensity earthquake damage probability curve. This approach is limited by the number of samples

obtained, and influenced by the experience of experts, the credibility of the research results are often subject to certain restrictions.

- (2) Analysis method, namely the seismic fragility curves obtained by theoretical methods, typically, through a lot of time history analysis and time-history analysis of data by finite element numerical simulation on the structure to obtain seismic fragility curves.

2.5 Previous studies on seismic vulnerability for RC buildings

The last fifteen years a large number of studies on the production of seismic fragility curves for RC buildings have been carried out in Europe. Several assessment procedures were followed; not based on EC8 Part3 though. Some of these studies, based on analytical or hybrid assessment methods, are presented in the following paragraphs.

Singhal & Kiremidjian [1995] produced vulnerability curves and damage probability matrices for low-rise, mid-rise and high-rise RC frame structures using the Park and Ang damage index. The ground motion characterization parameters used are the spectral acceleration and the root mean square acceleration. Nonlinear dynamic analyses were performed. Constrained Monte Carlo simulation techniques were used for evaluating the fragility curves.

Mosalam et al. [1997] produced vulnerability curves for low-rise bare and infilled RC frames designed for gravity loads. Pushover analyses were performed, assuming variability of concrete, steel and masonry properties, in order to obtain trilinear capacity curves. The characteristic values were assumed to follow a lognormal distribution with assumed coefficients of variation. Nonlinear analysis of the trilinear SDOF systems were performed for 800 artificial accelerograms. The Monte Carlo technique was employed to sample 200 capacity curves for each accelerogram. Reasonable agreement was found with fragility curves obtained from the ATC-13 damage probability matrices (better agreement for low levels of damage).

Dumova-Jovanoska [2000] performed non-linear dynamic analyses of a schematic 6-storey RC frame and a 16-storey RC wall-frame structure, both with seismic design, for 240 artificial accelerograms. The results were presented in terms of damage index vs. intensity for different damage states and also as damage probability matrices.

A.Masi [2003] evaluated the seismic vulnerability of some framed structural types representative of post-1970 RC existing buildings in Italy, designed only to vertical loads. Three main types were examined: bare frames, regularly infilled frames and open ground storey (pilotis) frames. Each masonry panel was modelled by using plane elements having elastoplastic behavior. The evaluation of the seismic vulnerability was carried out on the basis

of a set up procedure proposed by Masi et al. (2001a). The seismic resistance was evaluated by means of fragility curves relevant to some structural and non-structural parameters. The vulnerability class of each type, according to EMS98, was defined taking into account the increasing damage degrees computed by applying increasing seismic intensities. A correlation between PGA values and EMS98 intensities, proposed by Margottini et al. (1985), was adopted. The seismic response was calculated through non-linear dynamic (time-history) analyses on bases of: normalised base shear, interstorey drift and curvature ductility demand. The evaluation of the ductility capacities was obtained from analytical formulations adopting suitable values of the ultimate deformations of materials (Calvi and Priestley 1998). The results shown a high vulnerability for the pilotis buildings; low vulnerability was attributed to the regularly infilled buildings and an intermediate seismic behavior was shown by bare buildings.

Kappos et al. [2003], within the RISK-UE project, applied the capacity spectrum method on several configurations of regular RC buildings with and without infills (the case of soft ground storey was also examined) and with different levels of seismic design. As the capacity spectrum method assumes a bilinear response, when the displacement demand is higher than the capacity of regularly infilled frames or pilotis buildings with good seismic design, it was suggested to use the capacity curve for the bare frame. The uncertainty in the definition of damage state and the variability of the capacity were taken from HAZUS. The dispersion for all damage states of a given structural class was the mean of the dispersions for each damage state, so as to avoid intersecting fragility curves. Reference was made to the cost of replacement and to a damage index. The vulnerability curves were produced following the hybrid method, where analytical and observational capacity curves are combined.

Milutinovic & Trendafiloski [2003], presented the vulnerability curves for buildings developed within the RISK-UE project. Building typologies were identified from the stock in the project application sites, i.e. Barcelona, Bitola, Bucharest, Catania, Nice, Sofia and Thessaloniki. Both empirical and analytical methods were used. Different damage scales for each approach were employed and a correlation between the two was proposed. For steel, wood and reinforced masonry structures, the HAZUS vulnerability curves were adopted. Empirical curves were produced from damage probability matrices. Damage probability matrices were produced using a vulnerability index that accounts for structural characteristics and local conditions (weights by expert judgement). Pushover capacity curves distinguish between materials of construction, construction tradition, experience and technology used, as well as prescribed (by code) and achieved (in practice) levels of seismic protection. The characteristic points of the bilinear capacity curve (period, strength, ductility) may be obtained by code

requirements, expert judgement, or analysis. CIMNE used the capacity spectrum method. IZIIS performed inelastic dynamic analysis of RC frame structures using recorded accelerograms. UNIGE estimated the lognormal standard deviation of vulnerability curves for masonry structures as a function of ductility. UTCB used the capacity spectrum method. A probabilistic approach (Monte Carlo for seismic input, variability of concrete and steel properties) was used to define the properties of low and moderate-code RC buildings and then pushover analyses were performed to obtain their capacity curves. A code-based approach, applicable to new buildings, is mentioned. Characteristic values for capacity and fragility curves for all building types are given.

Erberik & Elnashai [2004] produced vulnerability curves for a 5-storey schematic flat-slab building with masonry infills designed according to current US seismic codes. Ten recorded accelerograms from various regions that were compatible with the code spectrum were selected and scaled to obtain all damage levels. Four limit states were assigned to the building in terms of interstorey drift ratio. Damage states were calculated for all elements of each storey and the most critical storey defined the damage state of the structure. The material uncertainty was treated by Monte Carlo analysis; normal and lognormal distributions were used to describe the statistical variation of material properties. The developed curves were compared with those in the literature, derived for moment-resisting RC frames and justified why using vulnerability curves of moment-resisting frames to assess seismic damage of flat slab buildings is non-conservative.

Akkar et al [2005] presented vulnerability curves for low-rise and mid-rise infilled frame RC buildings. Pushover analyses of 32 existing buildings in Duzce were performed to define the intervals of base shear capacity, period and ultimate drift of 2, 3, 4 and 5-storey buildings with low-level of seismic design. Nonlinear dynamic analyses were then performed for 82 recorded accelerograms and bilinear structures with properties within the identified intervals. The number of stories was found to have a significant effect on the probability of exceeding the moderate and the severe damage limit states. Spectral displacement correlated better with peak ground velocity than peak ground acceleration, particularly for higher levels of damage.

There was good agreement of the vulnerability curves with observed damage after the 1999 Duzce earthquake.

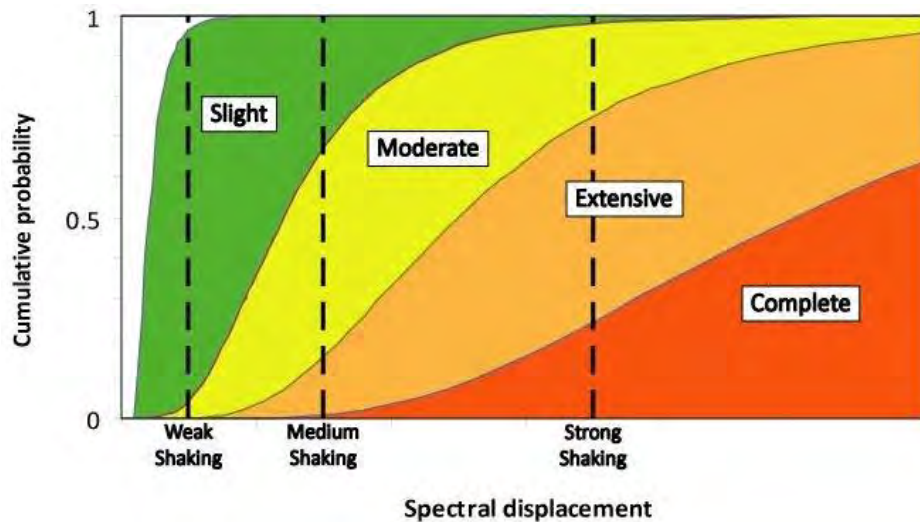


Figure 2.6 Ragility curves based on HAZUS Damage Functions

Kappos et al. [2006] produced vulnerability curves for RC frame and wall-frame buildings, as well as for unreinforced masonry (URM) structures, according to a hybrid method developed at AUTH. This method combines statistical data with appropriately processed results from non-linear dynamic or static analyses, that permit extrapolation of statistical data to PGAs and/or spectral displacements for which no data are available. Vulnerability curves were derived in terms of PGA, as well as spectral displacement S_d . Analyses of several different RC building configurations were performed, representing most of the typologies of buildings in S. European countries. Low-rise, mid-rise and high-rise buildings were considered; each one was assumed to have three different configurations (bare, regularly infilled and soft ground storey building). Four classes of seismic design were considered: no code, low code, moderate code and high code. Inelastic static and dynamic time-history analyses were carried out.

Kircil & Polat [2006] performed nonlinear dynamic analyses of representative RC buildings, designed with the 1975 code, using 12 artificial accelerograms with increasing intensity in order to define the parameters of lognormal vulnerability curves. Fragility curves for different steel grades were summed (sum weighted by the population of each sample) to provide a single curve for all buildings. A relationship was established between number of storeys and mean and standard deviation of the curves, so as to obtain curves for structures with number of storeys not in the examined range.

Erberik [2008] studied 28 RC frame buildings that were inspected after the Düzce earthquake. The buildings were constructed between 1973 and 1999. Pushover analyses were performed to obtain the bilinear capacity curves and the distribution of their characteristic properties.

2800 nonlinear dynamic analyses of randomly sampled SDOF structures were performed for a set of 100 recorded accelerograms. The effect of post-yield to initial stiffness ratio variability (negligible), simulation (negligible) and sampling (negligible) techniques, sample size (negligible), limit state variability (important) and degrading hysteretic behaviour (important) was studied by means of parametric analyses. The predictions of the analytical curves were in satisfactory agreement with the observed damage.

Özer & Erberik [2008] produced vulnerability curves for RC frame structures in Turkey. 3-, 5-, 7- and 9-storey RC frames with poor, medium and good seismic designed were considered. Concrete and steel strength and modulus of elasticity were variables. Four damage states were introduced as slight or no damage (DS1), significant damage (DS2), severe damage (DS3) and collapse (DS4). The seismic demand statistics in terms of maximum interstorey drift ratio were obtained for different sets of ground motion records by performing non-linear time-history analyses. Figure presents an example of fragility curves, plotted versus PGV, that were developed in this study.

Polese et al. [2008] studied RC frame and masonry buildings constructed in Naples before seismic codes were introduced. The bilinear capacity curves of 400 RC frame buildings, with 1, 4 and 7 storeys and varying plan dimensions were obtained by pushover curves. Sample buildings were generated by Monte Carlo simulation and the properties of their capacity curves were obtained from the database of the 400 buildings. The capacity spectrum method was applied for the EC8 spectrum with increasing values of peak ground acceleration. The variability in yield and ultimate rotation and in the evaluation of seismic demand was found to have a significant effect on the fragility curves.

Rossetto & Elnashai [2005] produced vulnerability curves for low-rise infilled RC frames, designed with the old Italian seismic code. Building design, material properties (variability of concrete, steel and masonry) and ground motion were selected to be representative of the region. Adaptive pushover analysis was performed and a trilinear idealisation of the capacity curve of infilled frames was considered more representative. The performance point was obtained by means of nonlinear dynamic analysis of the equivalent SDOF structure, instead of the graphic method. Ten accelerograms are sufficient to account for ground motion variability (Wen & Wu, 2001). The results of the analyses were used to construct response surfaces, from which the vulnerability curves were produced by entering random values of material properties and spectral displacement to obtain the maximum drift. The analytical curves were in reasonable agreement with empirical curves.

Vacareanu et al [2004] focused on the seismic vulnerability assessment of representative residential RC buildings in Bucharest using HAZUS and ATC-40 methodology. The buildings were designed with low-level and medium-level seismic codes. A relationship was established between interstorey drift and Park & Ang damage index. The demand corresponded to a single recorded accelerogram. Monte-Carlo simulation was used to calibrate the fragility function parameters.

Chapter 3 THE ANALYSIS METHOD OF STRUCTURAL SEISMIC RESPONSE

3.1 Introduction

Current earthquake engineering major mitigation measures of earthquake disaster is risk analysis, the specific including seismic hazard analysis, seismic vulnerability analysis and earthquake losses estimated three aspects. The seismic vulnerability analysis of building can be used before the earthquake disaster prediction, designer depend on different structure seismic vulnerability, and to improve the seismic capacity of structure; At the same time can also be used for earthquake damage assessment.

Provide the basis for the estimate earthquake losses, and proposed measures to avoid or reduce casualties and to achieve the goal of earthquake disaster reduction. Provide the basis for estimating earthquake losses, and put forward the measure of avoid or reduce the loss of life, realize the goal of protecting and mitigating earthquake disasters.

Structural seismic vulnerability study is actually an important part of the performance-based design concept is based on the performance of the design ideas inevitable continuation. In recent years, the analysis of seismic vulnerability based on the IDA method becomes a hot spot to study and research.

Incremental dynamic analysis IDA method was developed by Bertero first proposed in 1977, Vamvatsikos and Cornell was carried out systematic research and summarize it into a practical use.

Now is the Federal Emergency Management Agency (FEMA) summarized using analytical methods as the whole structure collapsed seismic capacity assessment.

The method can examine the structure at different intensity levels seismic demand and overall resistance to collapse ability to realize the structure from linear elastic to elastic-plastic, and then the whole process of the collapse of the entire response analysis, and comprehensive evaluation on the seismic performance of the structure, therefore non-linear structural analysis has been widely used in the earthquake.

3.2 IDA methods and basic principles of the seismic vulnerability

3.2.1 Incremental dynamic analysis method

Incremental dynamic analysis (IDA) involves performing multiple nonlinear dynamic analyses of a structural model under a suite of ground motion records, each scaled to several

levels of seismic intensity. The scaling levels are appropriately selected to force the structure through the entire range of behavior, from elastic to inelastic and finally to global dynamic instability, where the structure essentially experiences collapse. Appropriate postprocessing can present the results in terms of IDA curves, one for each ground motion record, of the seismic intensity, typically represented by a scalar Intensity Measure (IM), versus the structural response, as measured by an Engineering Demand Parameter (EDP).

Possible choices for the IM are scalar (or rarely vector) quantities that relate to the severity of the recorded ground motion and scale linearly or nonlinearly with its amplitude. The IM is properly chosen well so that appropriate hazard maps (hazard curves) can be produced for them by probabilistic seismic hazard analysis. Possible choices are the peak ground acceleration, peak ground velocity or Arias intensity, but the most widely used is the 5%-damped spectral acceleration at the first-mode period of the structure.

The EDP can be any structural response quantity that relates to structural, non-structural or contents' damage. Typical choices are the maximum (over all stories and time) interstory drift, the individual peak story drifts and the peak floor accelerations.

3.2.2 The basic principles of the seismic vulnerability

Seismic vulnerability refers to a certain area due to the extent of the losses caused by the earthquake.

Its research object can be a single structure or a class structure, it can be a region. The structural seismic vulnerability refers to the structure at different intensity earthquake excitation, the possibility of different degrees of damage or a structure reaches a probability with a certain limit state (performance level).

Seismic vulnerability can be formulated (ground motion intensity S_a)

$$P_{DV|IM}(0|S_a) = \sum P_{DV|LS}(O|C) P_{DM|IM}(Z > C)$$

Where DV is a description of the structure reaches a limit state binary indicator variable, when $DV = 0$ means the structure reached the limit state.

$P_{DV|IM}(0|S_a)$ is the probability when the structure reaches the limit state with the intensity of the ground motion S_a .

LS is the indicators of the capacity of structure.

$\sum P_{DV|LS}(O|C)$ represents the probability of the structure reached the limit state when the capacity of structure is C.

$P_{DM|IM}(Z > C)$ represents the probability when the ground motion intensity is S_a , the seismic responses of the structure Z is greater than the capacity of structure C .

Every limit state has a certain critical value C , when the response of structure reaches the critical value is considered the structure must be damage. That is $P_{DV|IM}(0|C) = 1$. Critical value C can be obtained from the general statistics and experimental data, when the lack of damage data and test data can only be obtained by theoretical analysis method (numerical simulation). This paper is the IDA analysis based on the analysis model, on the summary of IDA curves defined on the critical value corresponding to the different damage limit state.

3.3 The problems of Seismic Fragility analysis based on IDA method

3.3.1 How to select ground motion records

Ground motion that earthquake ground motion, which is released by the source of seismic wave caused by the soil near the surface, is the cause of earthquake damage external cause, it is a bridge between seismic and seismic. Because of the earthquake ground motion is the non-stationary random process with wider frequency band, the earthquake seismogenic mechanism, propagation medium, field condition factors, has a great deal of uncertainty, makes the seismic time history simulation of different ground is very difficult. According to the current of real seismic records, found that even with earthquakes, in the same field of different directions of seismic records are also different. Different ground motion inputs, displacement and internal force of structure is different, sometimes can reach several times or even dozens of times. Therefore, analysis of IDA, reasonably selected ground motion is particularly important.

U.S. ATC-63 (2008) report gives recommendations to select 22 far field and 28 near-field ground motion. To select these seismic waves based on the following principles:

(1) Selected earthquake magnitude greater than 6.5, because of the small magnitude earthquakes have too less energy, and the extent of damage to the structure is usually not enough to cause the collapse of the structure.

(2) Venue for rock or hard soil site, American standard IBC2006 will be divided into A-F6 class field. Class A and Class B for hard rock, a small number of strong motion records in this sites, E and F class for soft soil, if the structures built on soft soil, it may appear foundation damage in the earthquake, rather than the structure their destruction. In this paper, we study the structure of using class C and D only recorded on the site seismic waves.

(3) Epicentral distances greater than 10 km. Near-field earthquake ground motions recorded with the general record is quite different. In recent years attracted the attention of national researchers. Its long pulse period, significant and similar pulse wave velocity peaks, making the increase in displacement ductility demand levels and the long-period seismic structure of short-period structure. Studies have shown that the site should generally be nearly field and far field distinguish treatment, avoid seismic response of discrete too much. In summary, all ground motion records selected from this paper the epicenters are greater than 10km.

(4) Avoid from the same seismic event more than two seismic waves, have to make choice of seismic waves have broader applicability.

(5) PGA greater than 0.2g , PGV greater than 15 cm/s.

(6) Effective period seismic waves reach at least 4s.

(7) Strong motion seismograph placed in free space or a small building on the ground floor, placement should be considered the structure of the building - the coupling effect of soil on the impact of seismic waves.

In addition, the experience of earthquake damage, the structure of low cyclic fatigue structure, the cumulative effect of the structure and the experimental study have shown that the duration of the ground motion has important influence on the damage of the structures . The study found that:

(1) When the earthquake holding general for non-degenerate nonlinear system has little effect;

(2) When holding for degenerative strong nonlinear system a greater impact;

(3) The duration have a great impact for degradation or no degradation of nonlinear systems of the cumulative loss of the energy. Visible, the impact of the duration of earthquake for the structural response mainly in the nonlinear stage. Determine the duration, the most intense part of the ground motion records should be included in the selected duration, and generally duration of the ground motion greater than or equal to 10 times the basic period of the structure T_1 .

Literature study shows that moderate height of the building, when using a relatively suitable and effective seismic intensity index, the 10-20 seismograms usually accurate enough to assess the seismic demand structure. Therefore, the paper selects 16 ground motion be in progress incremental dynamic analysis.

In this paper, all models are in the second category selected venues, and U.S. seismic surveys Center (USGS) division on grounds similar in the S2 site, V_s take 180 ~ 360 m/s. Reference ATC-63 election wave principle , from the PEER Strong Motion Database pick out 10 ground motion records to meet the requirements of the velocity range and the epicenter .

As shown in Table 3.1 The duration of earthquake taken 20s.

Table 3.1 Analysis of the input ground motion records

No.	Name of ground motion	Station	Component	PGA (g)
1	Morgan Hill	Gilroy Array #5	G03090	0.395
2	Loma Prieta	Gilroy Array #3	G030090	0.200
3	Superstition Hills	EICentroImp.Co.Cent	ICC090	0.258
4	Westmorland	Westmorland Fire	WSM090	0.368
5	Imperial Valley	117 El Centro Array #9	I-ELC270	0.215
6	Landers	Yermo Fire Station	YER270	0.245
7	Loma Prieta	57382 Gilroy Array #4	G04090	0.212
8	Northridge	LA-Hollywood Stor FF	HOL360	0.358
9	San Fernando	LA-Hollywood Stor Lot	PEL090	0.210
10	Whittier Narrows	Hollywood-Coldwater Can	A-CWC270	0.250

3.3.2 Scale factor and algorithm

The Scale Factor (SF) of a scaled accelerogram, a_β , is the non-negative scalar $\beta \in [0, +\infty]$ that produces a_β when multiplicatively applied to the unscaled (natural) acceleration time history a_1 .

Note how the SF constitutes a one-to-one mapping from the original accelerogram to all its scaled images. A value of $\beta = 1$ signifies the natural accelerogram, $\beta < 1$ is a scaled-down accelerogram, while $\beta > 1$ corresponds to a scaled-up one.

Although the SF is the simplest way to characterize the scaled images of an accelerogram, it is by no means convenient for engineering purposes as it offers no information of the real ‘power’ of the scaled record and its effect on a given structure. Of more practical use would be a measure that would map to the SF one-to-one, yet would be more informative, in the sense of better relating to its damaging potential.

Once the model has been formed and the ground motion records have been selected, we need a fast and automated way to perform the actual dynamic analyses needed for IDA. This entails appropriately scaling each record to cover the entire range of structural response, from

elasticity, to yielding, and finally global dynamic instability. Our task is made significantly easier by using an advanced algorithm, like hunt & fill (Vamvatsikos and Cornell, 2002a). This ensures that the record scaling levels are optimally selected to minimize the number of required runs: Analyses are performed at rapidly increasing levels of IM until numerical non-convergence is encountered (signalling global dynamic instability), while additional analyses are run at intermediate IM-levels to sufficiently bracket the global collapse and increase the accuracy at lower IMs. The user only needs to specify the desired accuracy for demand and capacity, select the maximum tolerable number of dynamic analyses, and then wait for a few hours to get the results. Since the algorithm has been implemented in software able to wrap around most existing analysis programs it renders IDA almost effortless, needing no human supervision.

3.3.3 Intensity measures (IM) and Damage measures (DM)

Usually we use the IDA curves to reflect the results of IDA method, while IDA curves need to through the intensity measures (IM) and damage measures (DM) to describe, to illustrate the response of the structure with the enhance role of the external. So the most important to select a suitable IM and DM. There are several issues of efficiency and sufficiency associated with the IM selection. Since there are no directivity influenced records in our suite and the building is of medium height (hence first-mode dominated), the 5%-damped first-mode spectral acceleration $S_a(T1,5\%)$ will be our choice; it has been proven to be both efficient, by minimizing the scatter in the results, thus requiring only a few ground motion records to provide good demand and capacity estimates, and sufficient, as it provides a complete characterization of the response without the need for magnitude or distance information. Similarly, selecting a DM can be application-specific; for example, the peak storey accelerations are well-correlated with contents' damage, while the maximum peak interstorey drift ratio θ_{max} is known to relate well to global dynamic instability and several structural performance limit-states upon which we will focus, so θ_{max} will be our DM choice. Still, it cannot be emphasized enough that these choices are by no means limiting. The user can change his mind and reprocess the IDA data anytime by choosing a different IM or DM, without any need to rerun the dynamic analyses.

3.3.4 Defining limit states

In order to be able to do the performance calculations needed for PBEE, we need to define limit-states on the IDAs, three of which are going to be demonstrated: Immediate Occupancy,

Life Safe , and Collapse Prevention., Immediate Occupancy is violated at $\theta_{max} = 1\%$, Life Safe $\theta_{max} = 2\%$ according to FEMA 350. On the other hand, Collapse Prevention is not exceeded on the IDA curve until the final point where the local tangent reaches 20% of the elastic slope (Figure 3.1) or $\theta_{max} = 10\%$, whichever occurs first in IM terms. Finally, global dynamic instability happens when the flatline is reached and any increase in the IM results in practically infinite DM response. In our example of recordYER270, Immediate Occupancy is violated for $Sa(T1,5\%) = 0.14g$ or $\theta_{max} = 2\%$, and Life Safe is violated for $Sa(T1,5\%) = 0.265g$ or $\theta_{max} = 2\%$ while the Collapse Prevention level is exceeded if $Sa(T1,5\%) = 1.3g$ or $\theta_{max} = 6.76\%$. Finally, global dynamic instability occurs at $Sa(T1,5\%) = 1.5g$,which corresponds to $\theta_{max} = +\infty$.

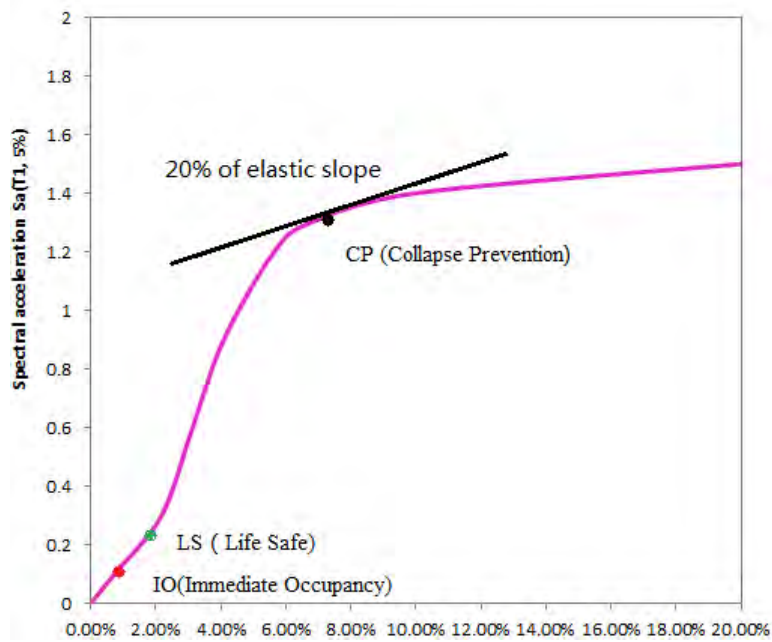


Figure3.1 IDA curves with 3 limit state

3.3.5 The Interpolation and Statistics of IDA curves

Once the desired IM and DM values (in our case $Sa(T1;5\%)$ and θ_{max}) are extracted from each of the dynamic analyses, we are left with a set of discrete points, ten for each record, that reside in the IM-DM plane and lie on its IDA curve, as in Figure 3.1. By interpolating them, the entire IDA curve can be approximated without performing additional analyses. To do so, we may use a basic piecewise linear approximation, or the superior spline interpolation. Based on the concept of natural, coordinate-transformed, parametric splines with a centripetal scheme

for knot-selection , a realistic interpolation can be generated that accurately represents the real IDA curve, as shown in Figure 3.2 for record B-ICC090 of Table 1. Having the complete curve available, it is now possible to calculate DM values at arbitrary levels of IM, allowing the extraction of more IM, DM points with a minimum of computation.

The smooth IDA curve provided by the interpolation scheme offers much to observe. Even for the single record depicted in Figure 1 the IDA curve is not at all simple. It starts as a straight line in the elastic range but then shows the effect of yielding and slightly “softens” at 0.4g by displaying a tangent slope less than the elastic. Subsequently, it “hardens”, having a local slope higher than the elastic, and the building apparently responds with almost the same $\theta_{max} = 5\%$ for $Sa(T1,5\%)$ in the range of 0.51g–0.7g. Finally, it starts softening again, showing ever increasing slopes, i.e., greater rates of DM accumulation as IM increases, reaching the “flatline” at $Sa(T1,5\%) = 1.05g$, where the structure responds with practically “infinite” θ_{max} values and numerical non-convergence has been encountered during the analysis. That is when the building has reached global dynamic instability, when small increments in the IM-level result in unlimited increase of the DM-response.

Table 3.2 three level of limit state on IDA curve

IO		LS		CP	
θ_{max}	$Sa(T1,5\%)$	θ_{max}	$Sa(T1,5\%)$	θ_{max}	$Sa(T1,5\%)$
1.00%	0.14	2.00%	0.263	7.76%	1.3

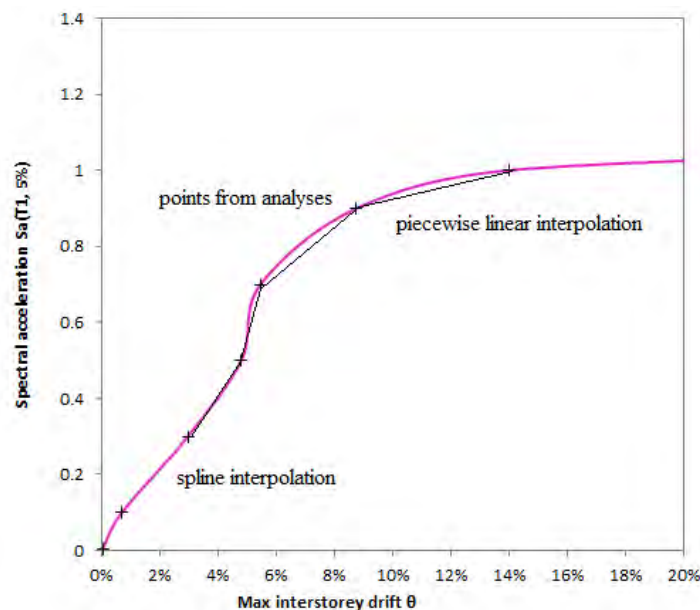


Figure 3.2 The interpolation of the IDA curve

3.3.6 Theoretical derivation of seismic vulnerability analysis

A fragility curve describes the probability of reaching or exceeding a damage state as a function of a chosen ground motion intensity parameter (spectral acceleration). The probability that the demand on the structure exceeds the structural capacity can be computed as follows:

$$P_f = P(S_c - S_d \leq 0)$$

Where

P_f is the probability of exceeding a specific damage state, S_d is the structural demand and S_c is the structure capacity.

If the structural capacity and seismic demand are described by a log-normal distribution, the probability of reaching or exceeding a specific damage state will be log-normally distributed, which can be obtained by a log-normal cumulative probability density function as follows:

$$P_f = \Phi \left[\frac{\ln(S_d/S_c)}{\sqrt{\beta_d^2 + \beta_c^2}} \right] \quad (3-1)$$

Where

β_c is the logarithmic standard deviation for the capacity, β_d is the logarithmic standard deviation for the demand, and $\Phi[*]$ is the standard normal distribution function.

Like Cornell have done for buildings, the Engineering Demand Parameter (EDP) , S_d ,and Intensity Measures (IM) can be represented by a power model:

$$EDP = S_d = \alpha IM^\beta \quad (3-2)$$

$$\ln(S_d) = \ln(\alpha) + \beta \ln(IM) \quad (3-3)$$

$$\ln(S_d) = a + b \ln(IM) \quad (3-4)$$

Where

a and b are unknown regression coefficients, and $\ln(\alpha) = a$, $\beta = b$, IM is the ground motion intensity parameter (S_a). The composite logarithmic standard deviation $\sqrt{\beta_d^2 + \beta_c^2}$, known as the dispersion, is taken from values recommended in HAZUS 99 , $\sqrt{\beta_d^2 + \beta_c^2} = 0.4$, $\Phi[*]$ is the standard normal distribution function, the value checking the table of the standard normal distribution to determine. Obtained the probability of corresponding to different levels of damage, this curve is the fragility curve of structure.

Chapter 4 MODEL OF RC FRAME STRUCTURE

4.1 Introduction

In this chapter, one six-story reinforced concrete building is properly designed considering gravity loads and the lateral seismic loading following the provisions of according to the Eurocode 8. And then the structure is modeled using the open-source software OpenSees. At last, the incremental dynamic analysis (IDA) is used to evaluate the minor damage, moderate damage and collapse risk of the frame.

4.2 The design of RC frame structure model

4.2.1 Engineering situation

The RC frame in this study is designed according to the NTC-08 code. The structure is located Sichuan province in China, anti-seismic is 8 Magnitude (0.2g), the site category S2, the basic snow pressure is 2.3 KN/m^2 , the basic wind pressure is 0.67 KN/m .

When to design a RC frame structure should be consistent with the actual engineering situation in order to have the engineering significance, and finite element modeling, to calculate the internal force, a combination of internal forces, cross-section reinforcement should follow the corresponding norms, in this paper according to NTC-08 (Italian code) designed.

This study is focused on the seismic performance of the structure under horizontal seismic action, and some research show that the wind loads no influence on the structural reinforcement for the multi-storey building structure design when the earthquake is more than 8 Magnitude.

According NTC-08 we take cast in place floor of cement mix, and the thickness of the slab is 24 cm, the roof load is 4.9 KN/m , the load of intermediate floor is 6.1 KN/m , and the variable loads is 2.5 KN/m .

This article is the fifth chapter comparative analysis model needs to design a basic model, other models are in contrast to the fundamental model changing the parameters on the basic model.

4.2.2 Design of the basic model

The structure is a symmetrical six-story reinforced concrete building. The story height is 3 meters for all the stories. The dimensions of the cross-sectional of beam is 400*600 mm, and the dimensions of the cross-sectional of column is 550*550 mm, The concrete is C25/30. The longitudinal reinforcement is B450C Φ 22mm and the transverse reinforcement is Φ 8mm .

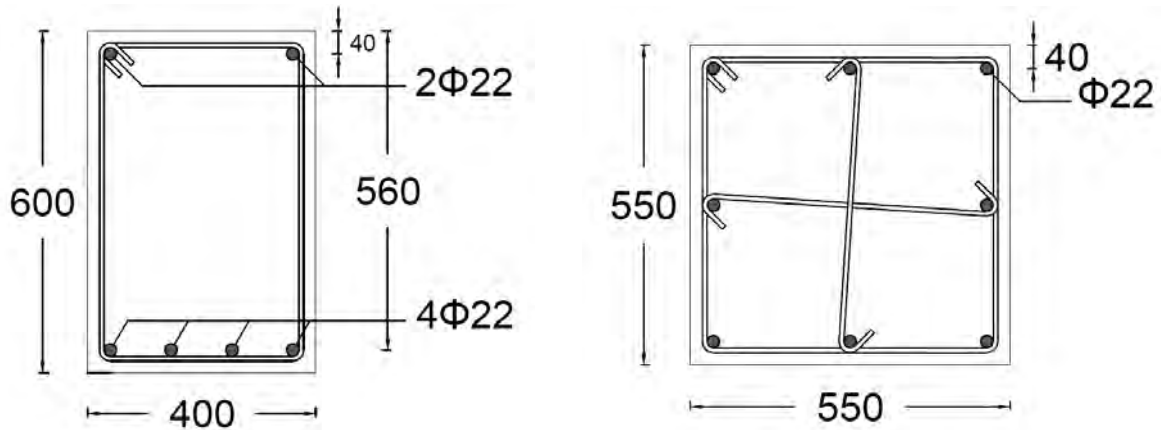


Figure 4.1 Rreinforcement beam and column

The beams in all six stories are with the same section geometry and columns in all stories are also with the same section geometry, Ignoring the influence of the stairs and infill walls, etc., in order to facilitate research in this paper take 2D model to study. Figure 4.1 shows the geometry and reinforcing details of the structure. The structure is symmetrical, thus a planar model is used to stand for the spatial frame in dynamic analysis. The plane model consists of a three-bay frame with the six stories, and the unit is mm. as shown in Figure 4.2

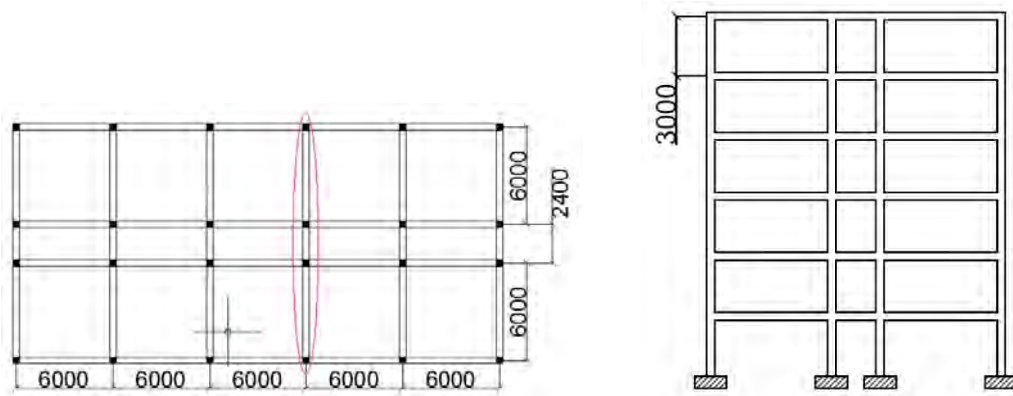


Figure 4.2 Six-story RC frame structure plan and elevation.

4.3 Nonlinear Finite Element Modeling

4.3.1 Introduction of OpenSees Software

Modern earthquake engineering utilizes modeling and simulation to understand the behavior and performance of systems during earthquakes. With the support of the National Science Foundation, the Pacific Earthquake Engineering Research Center (PEER) has developed the Open System for Earthquake Engineering Simulation, OpenSees for short, as a software platform for research and application of simulation for structural and geotechnical systems. The Open System for Earthquake Engineering Simulation (OpenSees) is a software framework for simulating the seismic response of structural and geotechnical systems. OpenSees has advanced capabilities for modeling and analyzing the nonlinear response of systems using a wide range of material models, elements, and solution algorithms. Beams and columns are modeled using the Force-Based Beam-Column Element.

4.3.2 Constitutive relations of materials

The reinforcement adopts the Steel02 Material, which is a uniaxial Giuffre-Menegotto-Pinto steel material object with isotropic strain hardening. The Concrete01 Material developed according to the work of Karsan-Jirsa is used to model the constitutive relation of concrete. An important modeling characteristic is the post-peak response, which captures the strain softening behavior associated with concrete crushing failure. The tensile strength is not considered in this material, which is acceptable in numerical simulation. The confining effect of the transverse reinforcement to the core concrete is considered by adopting the Mander model. The typical hysteretic stress-strain relation of Concrete01 is shown in Figure 4.3 and Figure 4.4

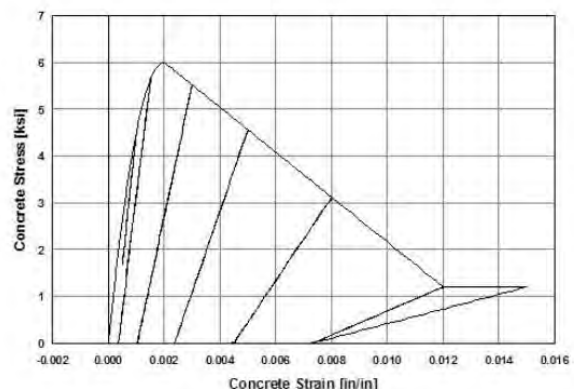
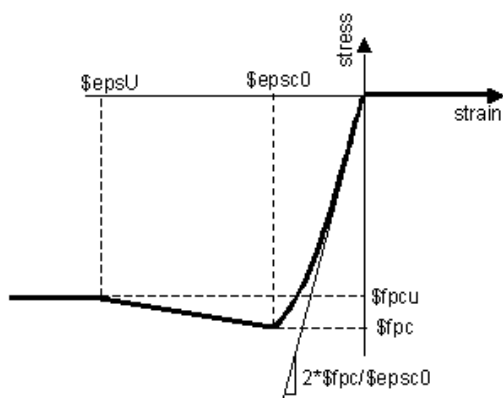


Figure 4.3 Concrete01 Material -- Material Parameters and Typical Hysteretic Stress-Strain Relation of Concrete_1 Model.

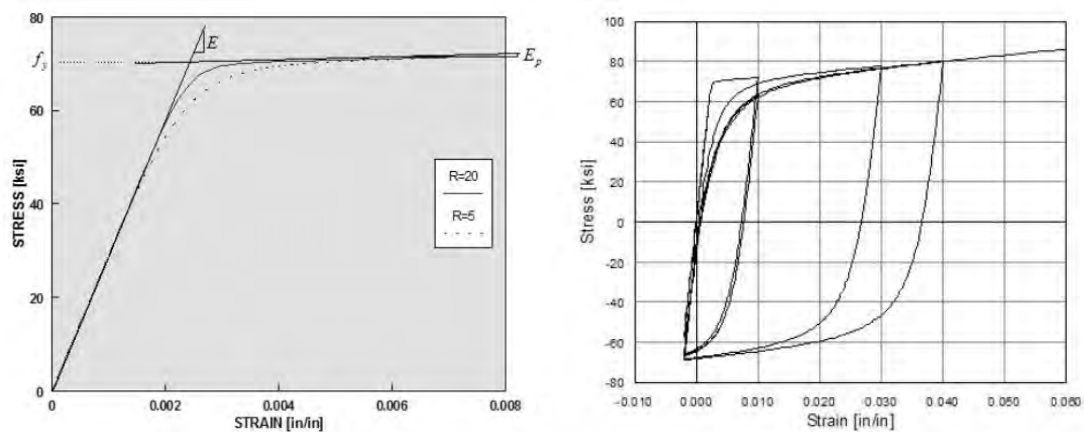


Figure 4.4 Steel02 Material -- Material Parameters of Monotonic Envelope and Steel02 Material -- Hysteretic Behavior of Model w/o Isotropic Hardening

The four parameters in Figure 4.3 are:

- \$f_{pc}\$: concrete compressive strength at 28 days (compression is negative);
- \$\epsilon_{psc0}\$: concrete strain at maximum strength;
- \$f_{pcu}\$: concrete crushing strength;
- \$\epsilon_{psU}\$: concrete strain at crushing strength.

4.3.3 The finite element models

The force-based beam-column Element and fiber section are used to model the beams and columns. In general, the accuracy of one force-based element equals four displacement-based elements. In this study, one force-based element is used to model a beam or column of the frame. P-delta effect is also considered in this model

4.4 Nonlinear Dynamic Analysis

IDA is the dynamic equivalent to a familiar static pushover analysis. Given a structure and a ground motion, IDA is done by conducting a series of nonlinear time-history analyses. The intensity of the ground motion, measured using an IM, is incrementally increased in each analysis. An EDP, such as global drift ratio, is monitored during each analysis. The extreme values of an EDP are plotted against the corresponding value of the ground motion IM for each intensity level to produce a dynamic pushover curve for the structure and the chosen earthquake record. In figure 4.5 show Peak interstorey drift ratio versus storey level of model-4, Gilroy Array #3 station, $S_a(T1) = 0.8g$, and interstorey drift $\theta_{max} = 4.35\%$.

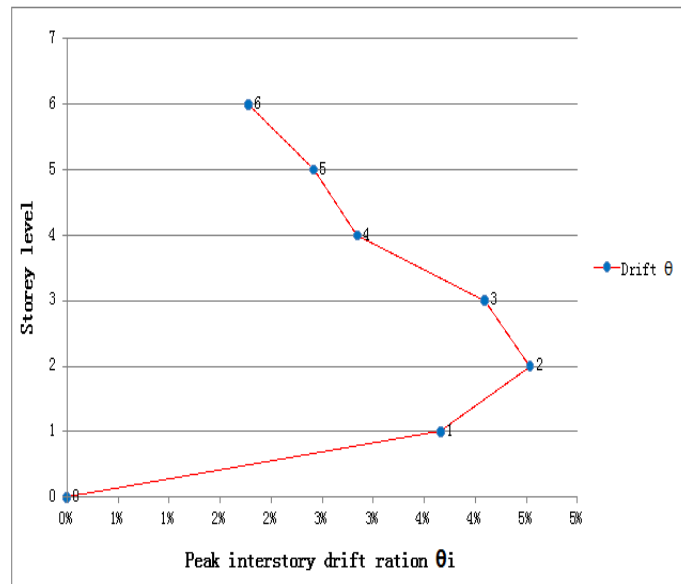


Figure 4.5 Peak interstorey drift ratio versus storey level

4.5 Analysis result

After completing the nonlinear time history analysis of the structure to obtain a large number of structural response data, researchers need to get the data, you need to make the appropriate post-processing work. Recorder program is the main provider of command, the user can customize what you want to output and analysis data are recorded, selectable output, recording options include: displacement, velocity, acceleration, displacement incremental of analysis nonlinear time history in each time, When the drive force of the rod end of each time unit, rod end deformation resistance section, deformation and stiffness changes, and the whole process over time the amount of each envelope mechanism and so on. With these data, the researchers could for data processing and graphics processing.

4.6 Algorithm Analysis

4.6.1 Single Ground Motion record of IDA curve

In IDA, the building analytical model is subjected to a selected earthquake time history while tracking the response of the structure. The input ground motion is scaled to increasing levels of intensity until collapse occurs, as indicated by runaway interstorey drifts. This process is repeated for all earthquake records and for each structure. In this study, the ground motion intensity is scaled by the spectral acceleration at the fundamental period of the structure, $S_a(T_1)$. Figure 6 shows IDA results for the 6-story RC structure subjected to one ground motion.

Take this example WSM90 that observed seismograms recorded by Westmorland Fire station ground motion records.

The whole analysis process is based on IDA method of seismic vulnerability detailed specification

Figure 4.6 shows WSM90 earthquake recorded acceleration time history curve.

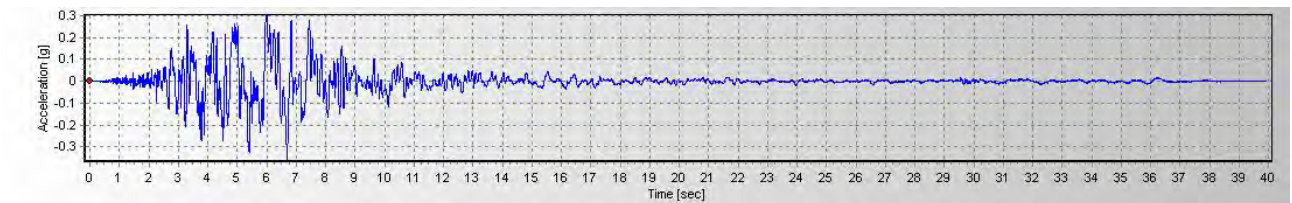


Figure 4.6 WSM90 earthquake recorded acceleration time history curve.

The WSM90 seismic records corresponding damping ratio of 5% of the elastic acceleration response spectrum curve in Figure 4.7.

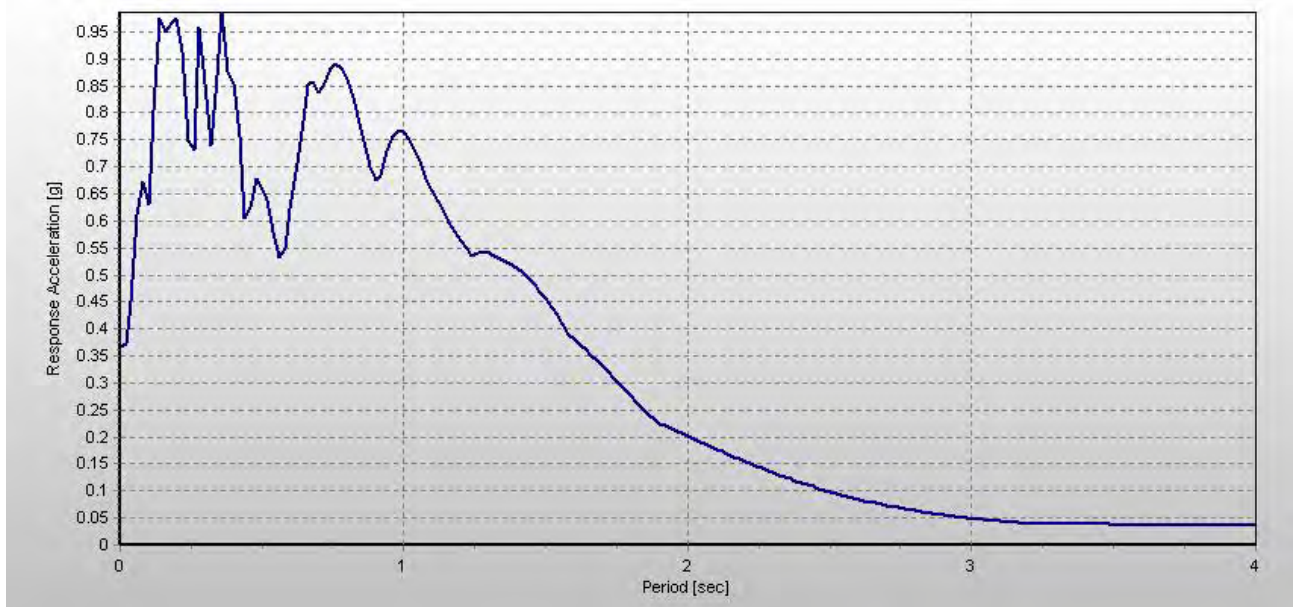


Figure 4.7 The WSM90 seismic records corresponding damping ratio of 5% of the elastic acceleration response spectrum curve.

OpenSEES software calculated Fundamental period of the structure . $T_1 = 1.582$ s, and from Figure 4.62 detected by corresponding damping ratio of 5% of the spectral acceleration values $0.38g$. $S_a(T_1) = 0.38g$, first step we can use $S_a = 0.005g$, we can get the scale factor(SF) $\lambda = 0.005/0.38 = 0.0132$, and multiplied the natural accelerogram by SF. and then we can record the Peak interstorey drift θ_1 . repeat the first step and increase IM by the step scale record, run analysis and extract DM θ_2 , and repeat above step, we can get $\theta_3, \dots, \theta_n$ until collapse is reached. Furthermore, to improve upon the capacity resolution, a simple

enhancement is to add a step-reducing routine, for example bisection, when collapse (e.g. non-convergence or with a tangent slope equal to 20% of the elastic slope) is detected, so as to tighten the bracketing of the Satline. This will enable a prescribed accuracy for the capacity to be reached regardless of the demand resolution.

repeat

Select an IM in the gap between the highest non-collapsing and lowest non-collapsing IM; scale record, run analysis and extract DM(s)

until highest collapsing and lowest non-collapsing IM-gap < tolerance.

When all three pieces are run sequentially, they make for a more efficient procedure, a hunt& fill tracing algorithm, described in detail by Vamvatsikos and Cornell , that performs increasingly larger leaps, attempting to bound the IM parameter space, and then ;fills in the gaps, both capacity and demand-wise. It needs an initial step and a stopping rule, just like the stepping algorithm, plus a step increasing function, a capacity and a demand resolution. The latter two can be selected so that a prescribed number of runs is performed on each record, thus tracing each curve with the same load of resources.

Table 4.6 can show the Algorithm for IDA curve.

Table 4.6 The algorithm for IDA curve

NO.	Sa(T1) g	Scale Factor	θmax
1	0.005	0.013	0.04%
2	0.1	0.263	0.66%
3	0.2	0.526	1.28%
4	0.4	1.053	2.41%
5	0.6	1.579	3.64%
6	0.8	2.105	4.33%
7	1.0	2.632	4.39%
8	1.2	3.158	4.39%
9	1.5	3.947	5.18%
10	1.8	4.737	6.44%
11	2.1	5.526	8.42%
12	2.3	6.053	14.06%
13	2.5	6.579	noconverge
14	2.2	5.789	10.44%

From above table can get 14 efficient point (θ_{max}, Sa), These data points are plotted on a coordinate system DM –IM ,in Figure 4.63 to get a single IDA curve of the model-4 with Westmorland Fire station record.

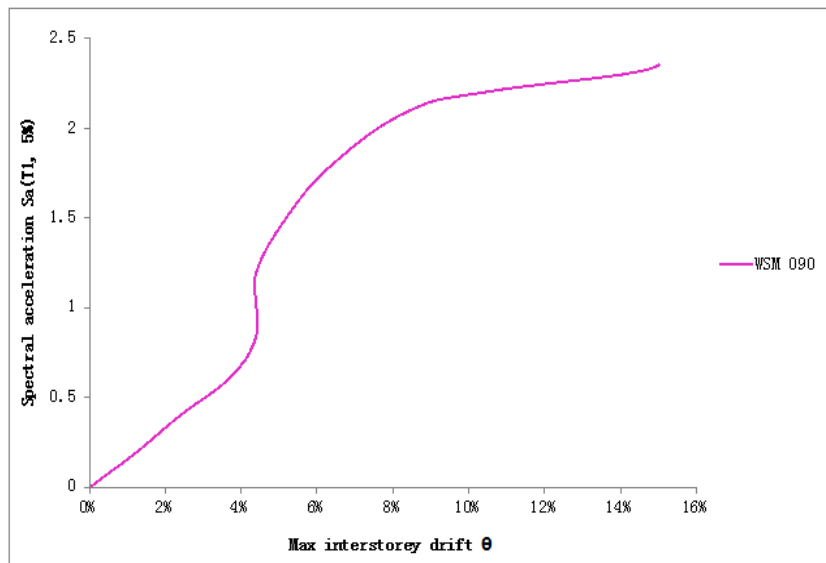


Figure 4.8 The IDA curves of the RC frame subjected to one ground motion

As can be seen from Figure 4.8, IDA curve at the beginning is basically a straight line, this is because the structure of the initial deformation in seismic excitation in the elastic range. When the maximum story drift angle of about 0.04, IDA slope of the curve changes the maximum drift angle between 0.04 to 0.045 segment curve has a relative rise phase, which is the stress hardening performance. Thereafter, the slope of the curve is more greatly reduced, up to 20% of the initial slope of the collapsed structure is in this case may be considered an edge. When the maximum story drift angle tends to infinity, the structure has reached a whole collapsed.

Get the full IDA curve, you need to define the limits of state points on the curve IDA, IDA curves can be applied to performance-based earthquake engineering. In accordance with Chapter 3, section 3.3.4 defines three limit state point can be seen from Figure 4.8.

When $\theta_{max} = 1\%$, $Sa(T1,5\%) = 0.15g$, the structure reaches IO limit state point, $\theta_{max} = 2\%$, $Sa(T1,5\%) = 0.33g$ the structure reaches LS limit state point, and $\theta_{max} = 10\%$, $Sa(T1,5\%) = 2.191g$, the structure reaches CP limit state point.

4.6.2 Number of Ground Motion records of IDA curve

ASCE/SEI 7 suggests that utilizing seven or more randomly selected records provides enough accurate estimate of the EDPs accompanied by reduced record-to-record variability of

the responses.

Due to an IDA curve is not a good predictor of the damage of the structure, so we need to select a series of earthquakes recorded incremental dynamic analysis of structures, access to a number of IDA curves. And get WSM90 ground motion recorded excitation curve the same way as under the IDA, to get the IDA curve from other 9 earthquake excitation, the 10 IDA curves are summarized in the same IM-DM coordinate system, as shown in Figure 4.9.

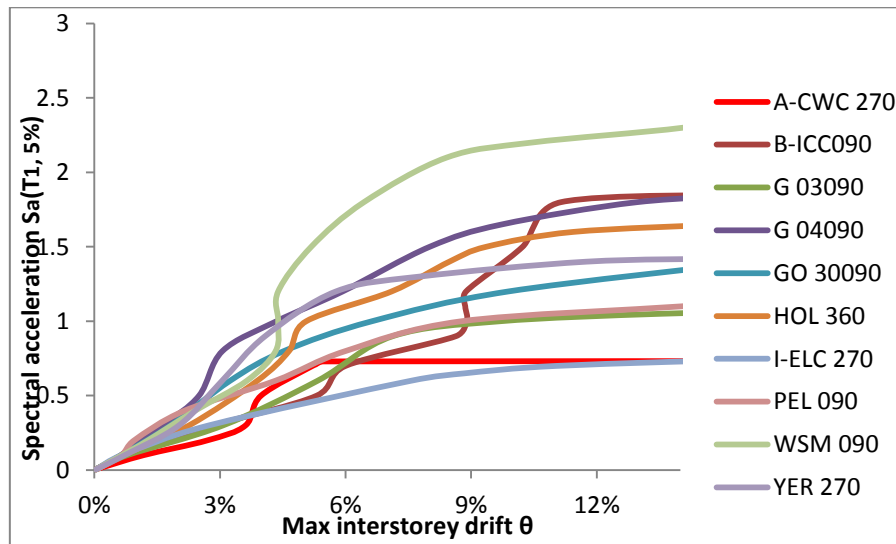


Figure 4.9 10 IDA curve summary of model-4

Due to the shape of the IDA curve are related by the selected made ground motion records, The reaction of the same structure when selected a different ground motion records also have certain discrete, so it is necessary to use the median to summarize these different curves to reduce the difference in Figure 4.10.

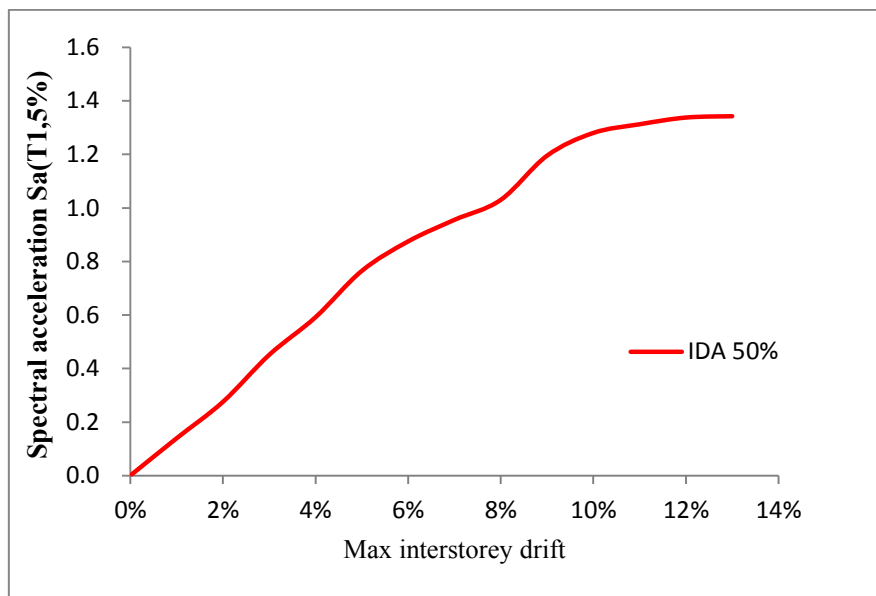


Figure 4.10 Median of IDA curves

Table 4.1 Summary limit state points on IDA curves

IO		LS		CP	
θ_{max} x	Sa(T1,5 %)	θ_{max}	Sa(T1, 5%)	θ_{max}	Sa(T1,5 %)
1.00 %	0.14	2.00%	0.276	10.00 %	1.28

4.6.3 probabilistic seismic demand model

Take logarithmic from each Intensity measure and damage measure, respectively. And according to the formula of the chapter 3 in the form of incremental dynamic analysis of the data obtained by linear regression analysis. Take $\ln(Sa)$ as independent variables and logarithm of structural response $\ln(\theta_{max})$ as the dependent variable establish the coordinate system, $\ln(\theta_{max}) - \ln(Sa)$, and regression analysis results shown in Figure 4.11

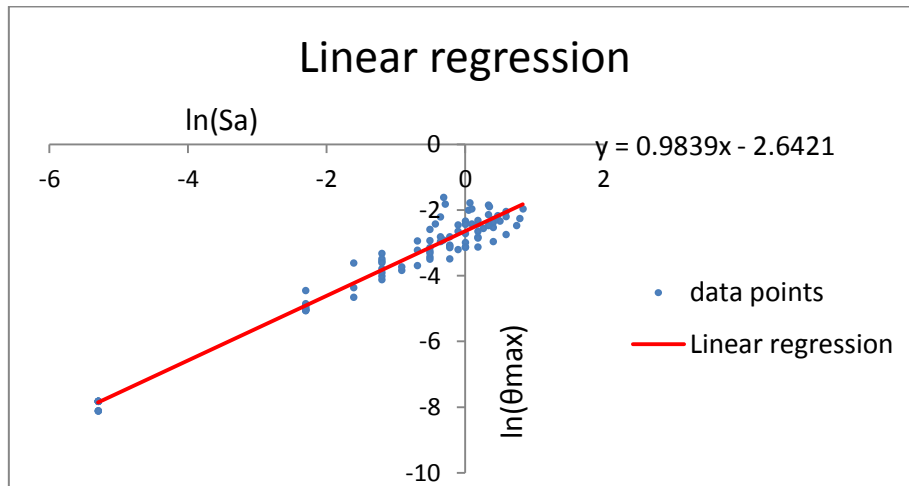


Figure 4.11 The basic model of linear regression analysis

The probability of Seismic demand model is express:

$$\ln(S_d) = a + b \ln(S_a)$$

$$\ln(\alpha) = a \quad \beta = b$$

Table 4.2

$\ln(\theta_{max})=0.9839\ln(Sa)-2.6421$		
$\ln(\alpha)=-2.6421$	α	0.07121
$b=0.9839$	β	0.9839

4.6.4 Seismic Vulnerability Analysis

Statistics from IDA results are used to derive a fragility curve, illustrated in Figure, which defines the probability of collapse as a function of the spectral intensity. The collapse fragility function is defined by the median and standard deviation of the ground motion intensities at which collapse occurs in IDA, assuming a lognormal distribution.

By equation (3-1) (3-2) shows that the probability of failure, $Sa(T1,5\%)$ as the independent variable is calculated as:

$$P_f = \Phi \left[\frac{\ln(\alpha(Sa)^\beta / S_c)}{\sqrt{\beta_d^2 + \beta_c^2}} \right]$$

Table 4.3 Three limit state on IDA curve

$LN(\theta_{max})=0.9839LN(Sa)-2.6421$		
$\ln(\alpha)=-2.6421$	α	0.07121
$b=0.9839$	β	0.9839

The composite logarithmic standard deviation $\sqrt{\beta_d^2 + \beta_c^2}$, known as the dispersion, is taken from values recommended in HAZUS 99, $\sqrt{\beta_d^2 + \beta_c^2}=0.4$, $\Phi[*]$ is the standard normal distribution function, the value checking the table of the standard normal distribution to determine. Obtained the probability of corresponding to different levels of damage, this curve is the fragility curve of structure. The abscissa indicates the intensity of ground motion $Sa(T1,5\%)$, and the vertical axis represents the probability of damage state exceeded. Seismic fragility curves shown in Figure 4.12

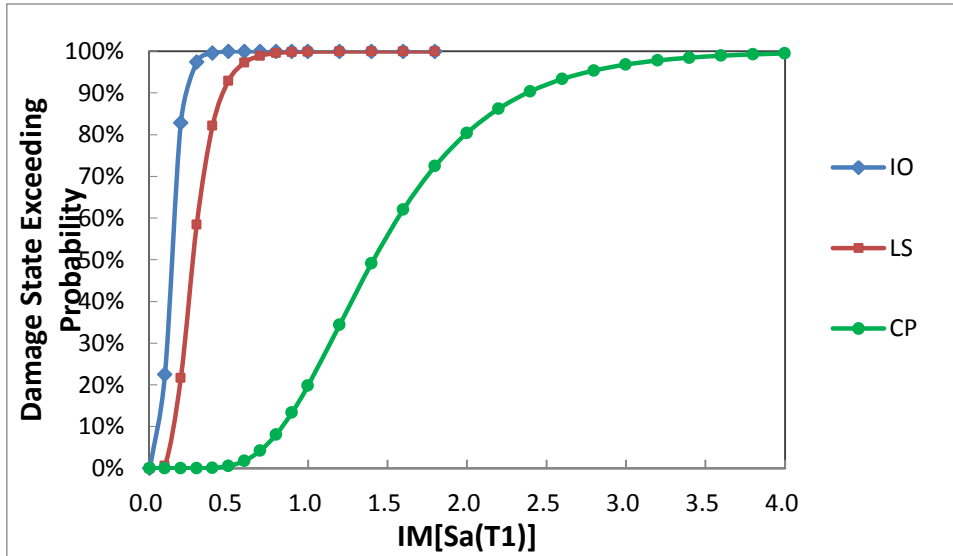


Figure 4.12 The fragility curves of the RC frame subjected to a set of selected ground motions

As can be seen from Figure 4.12, the structural from integrity of the state development to collapse state, fragility curves gradually become flat, the probability of failure is becoming increasingly large. When $S_a=0.355$, the structure reached the probability of IO is 99%, LS is 73% and CP is 0.003%.

Chapter 5 INFLUENCE OF STRUCTURE PARAMETERS ON THE SEISMIC VULNERABILITY

5.1 Introduction

Based on the performance of seismic design makes the structure seismic design from the macroscopic qualitative targets to the concretization of the multiple target transition. This chapter on four groups of RC plane frame structure based on IDA method of seismic vulnerability analysis, discuss the influence of the RC frame structure under different earthquake intensity, with different aspect ration, concrete strength, and the longitudinal reinforcement strength of the structure to achieve the different seismic performance level of the probability. So as to provide q quantitative reference for the RC frame structure based on the performance of seismic design. In order to meet the different levels of demand for the society and the owner of the building.

5.2 Longitudinal reinforcement strength

According to the Italian code (NTC 2008), B 450C steel use mainly for the construction in "Design of Concrete Structures" . with the need of this article, from the old building codes take out other 2 kinds of steel, FeB38k, FeB32k, to study the influence of Longitudinal strength of RC frame structure on the seismic vulnerability, this paper designed 3 RC frame structure according to the Italian code (NTC2008), with the different longitudinal reinforcement strength ,B 450C, FeB38k, FeB32k, in addition to the various the longitudinal reinforcement strength of each model and the basic properties of other materials are kept the same. The longitudinal reinforcement strengty take the yield stress value, due to the elastic modulus of steel discrete very small, in this paper take the value of unity $E = 200000$ MPa, the classification of steel and the yield stress shown in table 5.1.

Table 5.1 The yield stress of steel and elastic modulus

No. model	Model-1	Model-2	Model-3
steel classification	B 450C	FeB38k	FeB32k
f_{yk} / Mpa	450	375	315
E_{cm} [N/mm ²]	200 000	200 000	200 000

5.2.1 The analysis model based on the seismic vulnerability analysis of IDA method

Due to an IDA curve is not a good predictor of the damage of the structure, so we need to select a series of ground motion recorded separately for each model(model-1, model-2, model-3) to analyze based on IDA method, access to a number of IDA curves. to get the 10 different IDA curve from each ground motion, the 10 IDA curves are summarized in the same IM-DM coordinate system, as shown in Figure 5.1 – 5.3.

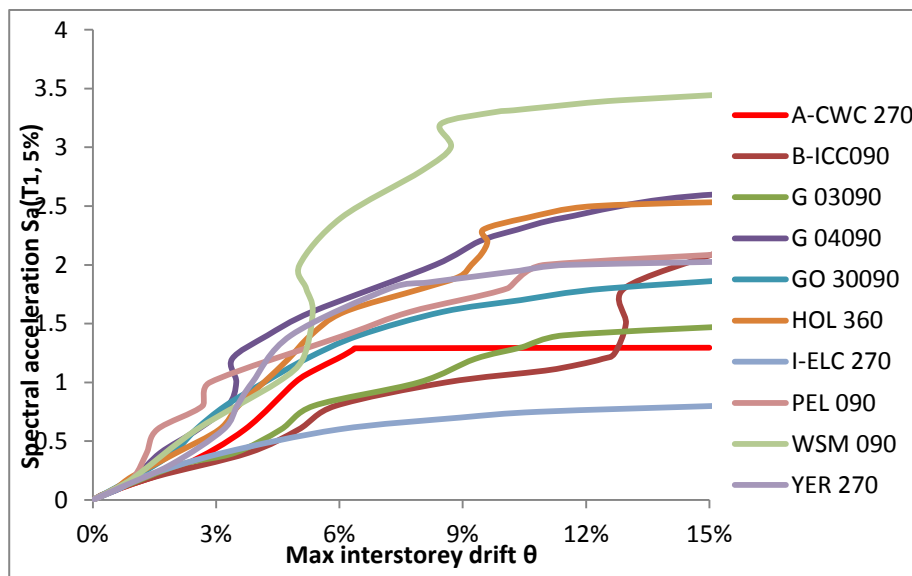


Figure 5.1 IDA curves of model-1

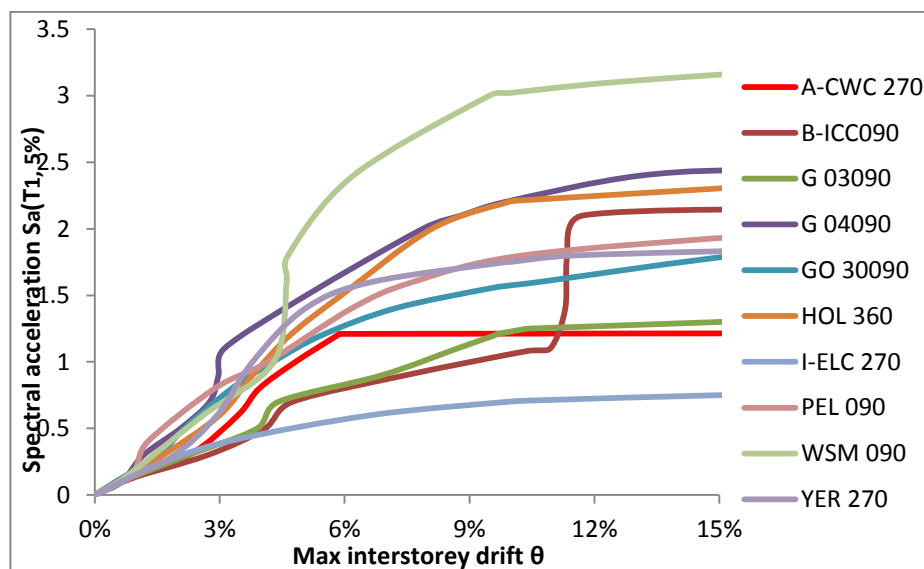


Figure 5.2 IDA curves of model-2

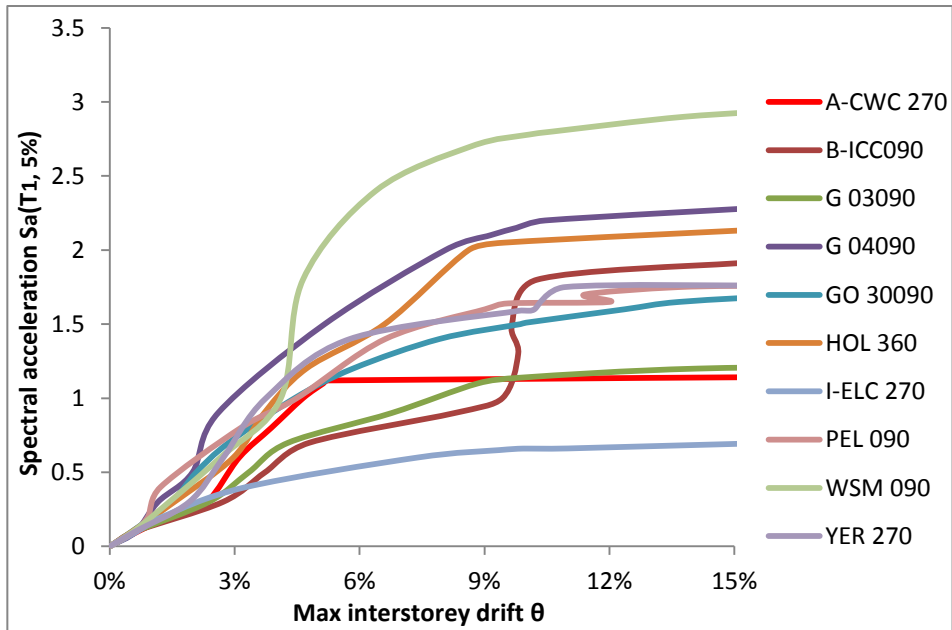


Figure 5.3 IDA curves of model-3

Due to the shape of the IDA curve are related by the selected made ground motion records, The reaction of the same structure when selected a different ground motion records also have certain discrete, so it is necessary to use the median to summarize these different curves to reduce the difference. In Figure 5.4 - 5.6.

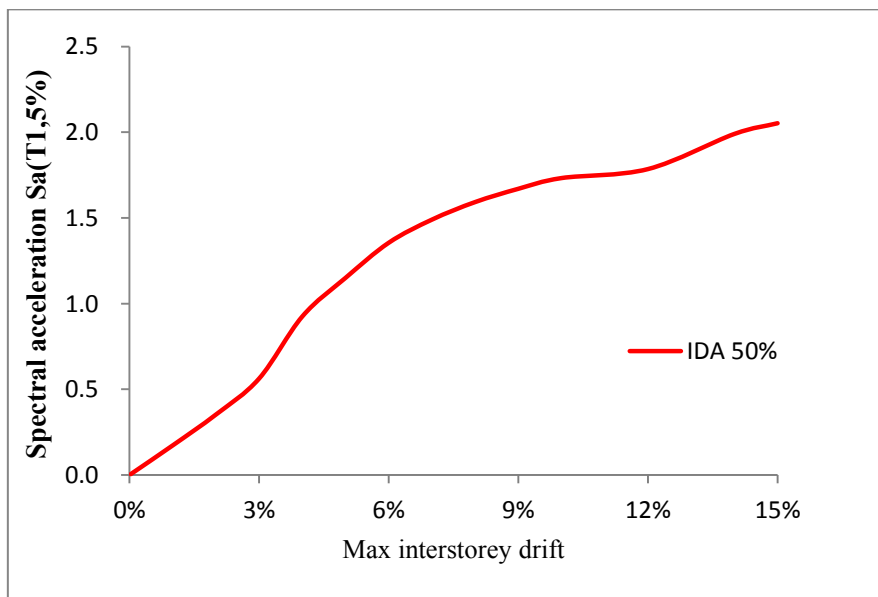


Figure 5.4 Median of IDA curve for model-1

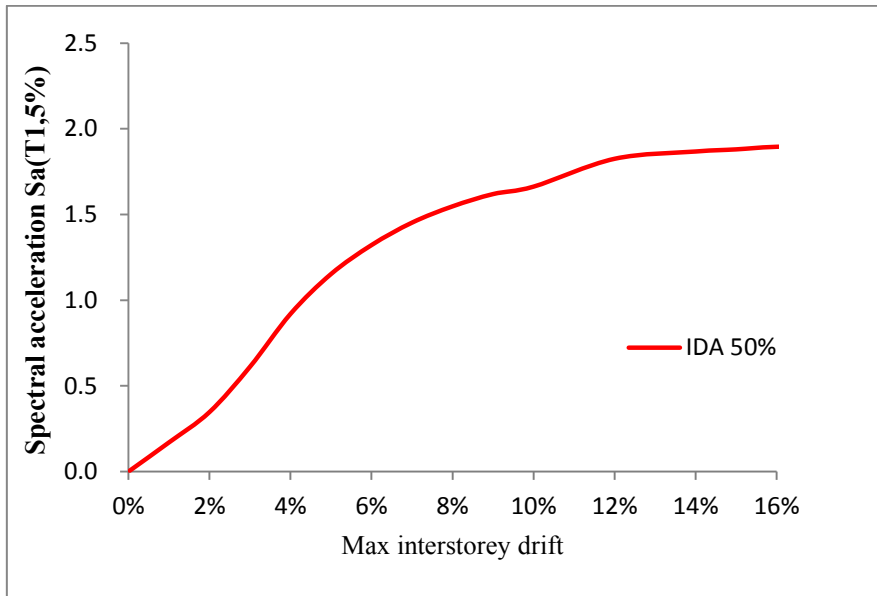


Figure 5.5 Median of IDA curve for model-2

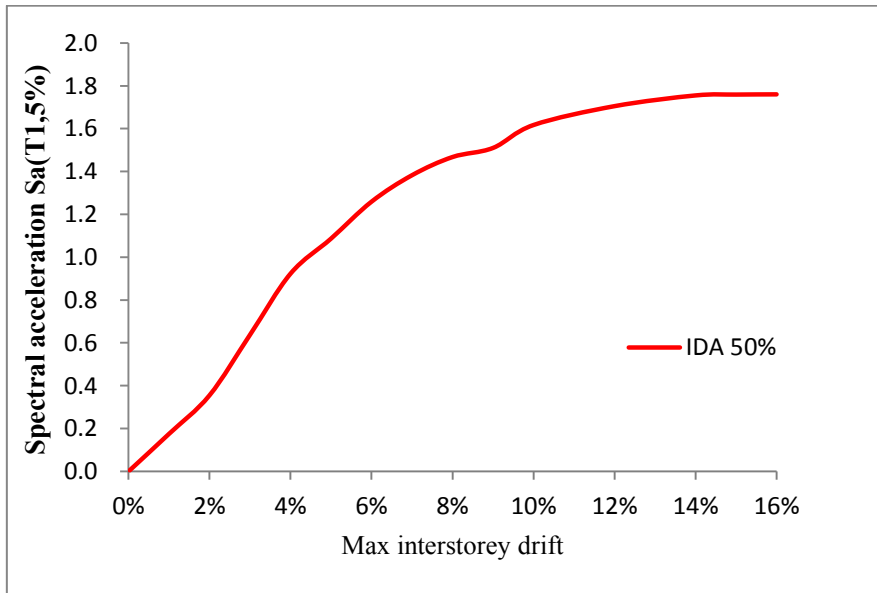


Figure 5.6 Median of IDA curve for model-3

Define the limit of the state point on median of IDA curves, for model-1, model-2,model-3, Respectively. Show on the table 5.2-5.4

Table 5.2 3 limit state point for model-1 on median curves.

IO		LS		CP	
θ_{max}	Sa(T1,5%)	θ_{max}	Sa(T1,5%)	θ_{max}	Sa(T1,5%)
1.00%	0.173	2.00%	0.353	10.00%	1.733

Table 5.3 3 limit state point for model-2 on median curves.

IO		LS		CP	
θ_{max}	Sa(T1,5%)	θ_{max}	Sa(T1,5%)	θ_{max}	Sa(T1,5%)
1.00%	0.175	2.00%	0.347	9.00%	1.619

Table 5.4 3 limit state point for model-3 on median curves.

IO		LS		CP	
θ_{max}	Sa(T1,5%)	θ_{max}	Sa(T1,5%)	θ_{max}	Sa(T1,5%)
1.00%	0.175	2.00%	0.355	8.00%	1.468

Take logarithmic from each Intensity measure and damage measure, respectively. And according to the formula of the chapter 3 in the form of incremental dynamic analysis of the data obtained by linear regression analysis. Take $\ln(Sa)$ as independent variables and logarithm of structural response $\ln(\theta_{max})$ as the dependent variable establish the coordinate system, $\ln(\theta_{max}) - \ln(Sa)$, and regression analysis results shown in Figure 5.7-5.9.

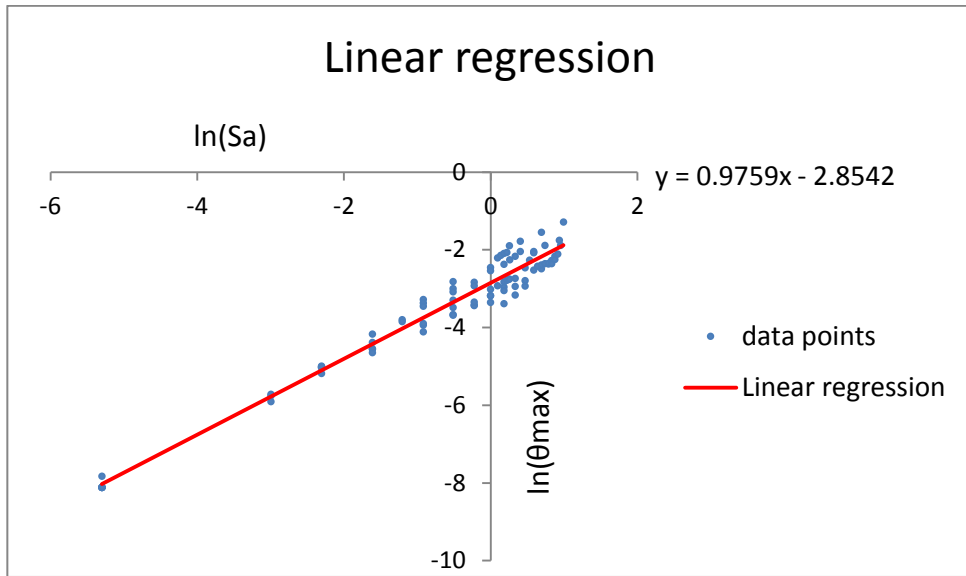


Figure 5.7 regression analysis results on model-1

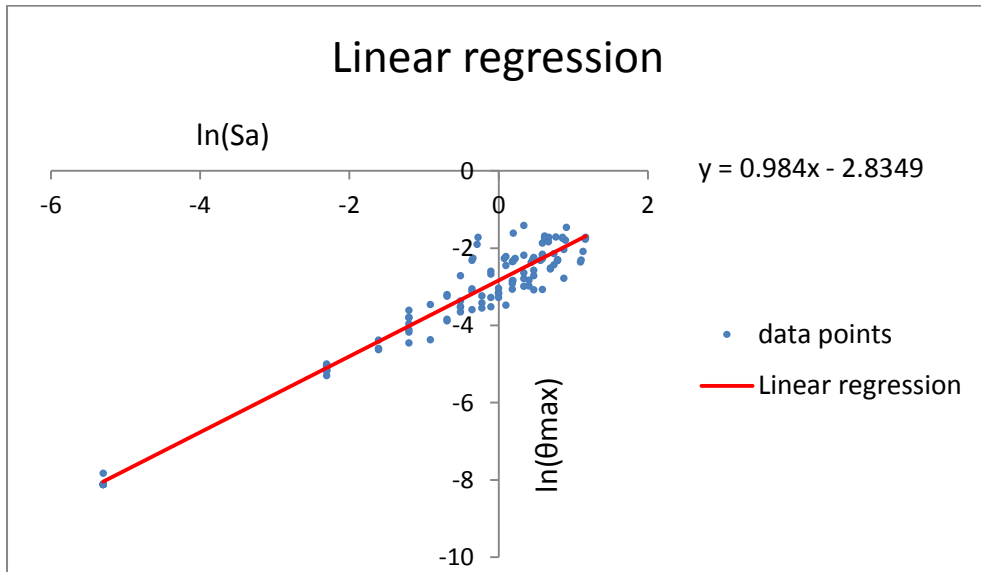


Figure 5.8 regression analysis results on model-2

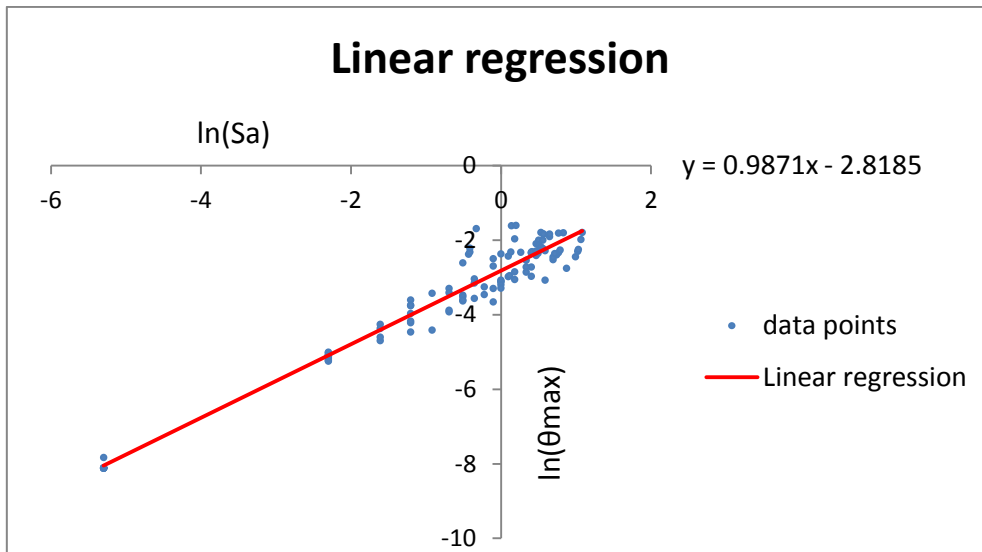


Figure 5.9 regression analysis results on model-3

The probability of Seismic demand model is express on table 5.5-5.7.

$$\ln(\alpha) = a \quad \beta = b$$

Table 5.5 The probability of seismic demand model-4

$LN(\theta_{max})=0.9759LN(Sa)-2.8542$		
$\ln(\alpha)=-2.8542$	α	0.0576
$b=0.9759$	β	0.9759

Table 5.6 The probability of seismic demand model-5

$LN(\theta_{max})=0.9840LN(Sa)-2.8349$		
$\ln(\alpha)=-2.8349$	α	0.05872
$b=0.9840$	β	0.9840

Table 5.7 The probability of seismic demand model-6

$LN(\theta_{max})=0.9871LN(Sa)-2.8185$		
$\ln(\alpha)=-2.8185$	α	0.0597
$b=0.987$	β	0.987

From above table we can get each value of α , β , and then take α , β , into equation (3-1) obtained the failure probability of fundamental period of structure corresponding the acceleration response spectrum $S_a(T_{1,5\%})$ in the limit state. as shown by formula (5-1) and to get the failure probability of the structure for each limit state.

$$P_f = \Phi \left[\frac{\ln \left[\alpha (S_a(T_{1,5\%}))^\beta / S_c \right]}{\sqrt{\beta_d^2 + \beta_c^2}} \right] \quad (5-1)$$

The failure probability of the structure for each limit state on model-1

$$P_f = \Phi \left[\frac{\ln \left[0.0576 (S_a(T_{1,5\%}))^{0.9759} / S_c \right]}{\sqrt{\beta_d^2 + \beta_c^2}} \right] \quad (5-2)$$

The failure probability of the structure for each limit state on model-2

$$P_f = \Phi \left[\frac{\ln \left[0.05872 (S_a(T_{1,5\%}))^{0.9840} / S_c \right]}{\sqrt{\beta_d^2 + \beta_c^2}} \right] \quad (5-3)$$

The failure probability of the structure for each limit state on model-3

$$P_f = \Phi \left[\frac{\ln \left[0.0597 (S_a(T_{1,5\%}))^{0.987} / S_c \right]}{\sqrt{\beta_d^2 + \beta_c^2}} \right] \quad (5-4)$$

The composite logarithmic standard deviation $\sqrt{\beta_d^2 + \beta_c^2}$, known as the dispersion, is taken from values recommended in HAZUS 99 , $\sqrt{\beta_d^2 + \beta_c^2} = 0.4$, S_c is the capacity parameters of structure under the different limit state. $\Phi[*]$ is the standard normal distribution function, the value checking the table of the standard normal distribution to determine. Obtained the probability of corresponding to different levels of damage, this curve is the

fragility curve of structure. The abscissa indicates the intensity of ground motion $Sa(T1,5\%)$, and the vertical axis represents the probability of damage state exceeded. Seismic fragility curves shown in Figure 5.10-5.11.

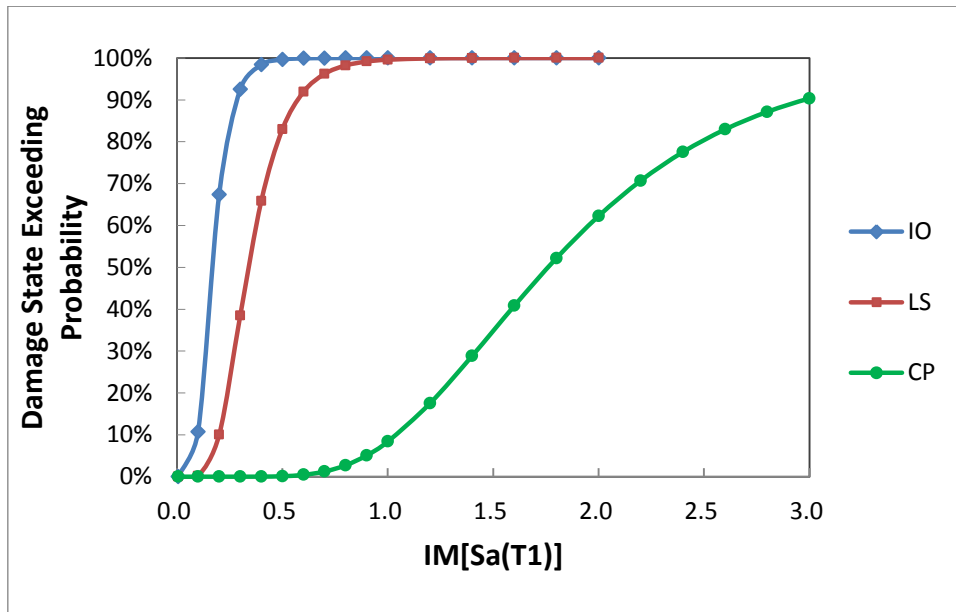


Figure 5.10 Fragility curves of model-1

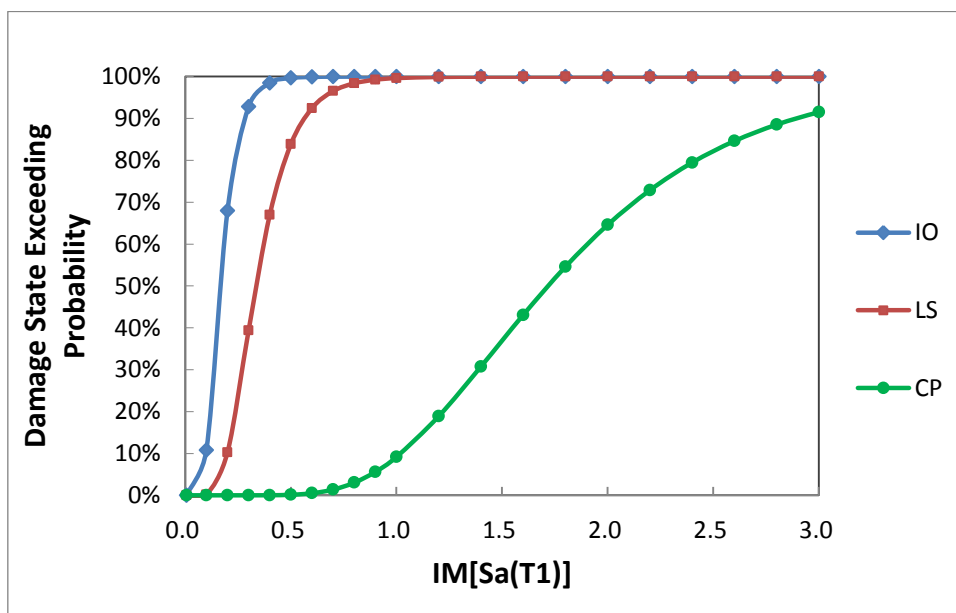


Figure 5.11 Fragility curves of model-2

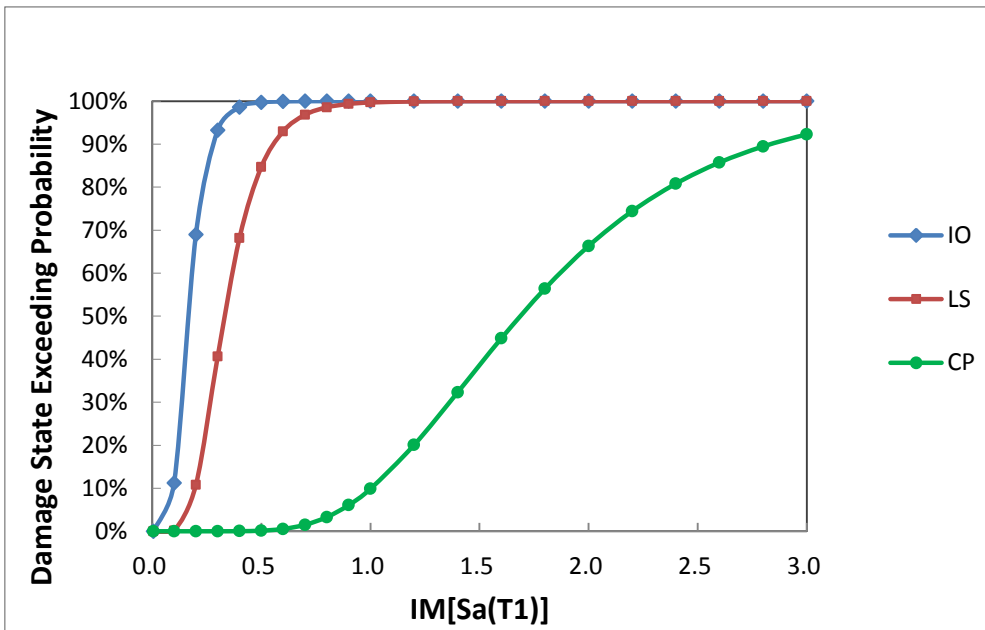


Figure 5.12 Fragility curves of model-3

5.2.2 Results analysis

By comparing the model-1, model-2, and model-3, of the seismic fragility curves, found that, with the increase the concrete strength of RC frame structure, Basically unchanged the probability of the IO state , a little different of the LS state, with the same intensity earthquake. But on the CP limit state the probability of the 3 model are very different. The damage of the structure is similar when under a small earthquake, because the deformation of the structure is also very small, the steel has not yet reached the state yield. And with the increase of steel strength, the probability of CP state is getting lower. Means the smaller the strength of steel, under a great earthquake, the structure of RC frame more prone to collapse. So the Italian code (NTC 2008) suggested the B 450C steel is very good to resist collapse. Compared to the 3 limit state of 3 model as shown in Figure 5.13 – 5.15.

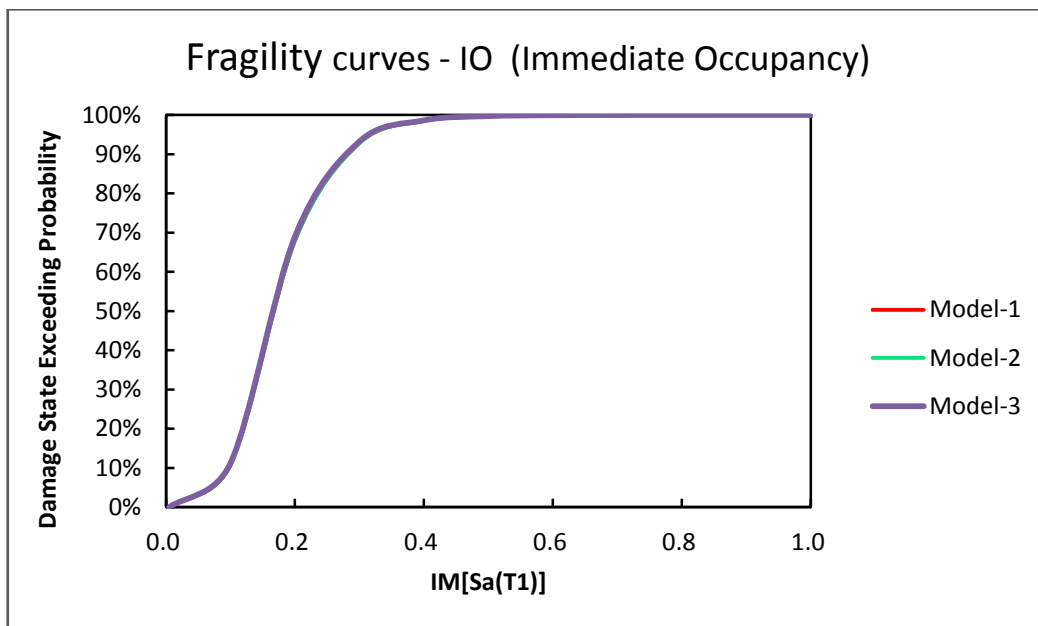


Figure5.13 compare the different steel strength on IO state.

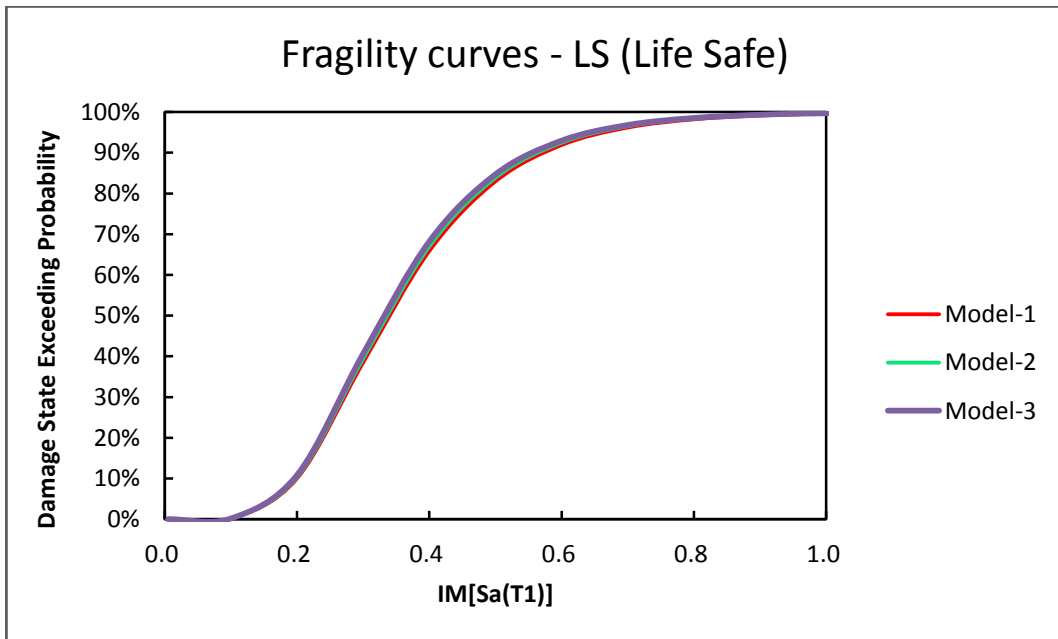


Figure5.14 compare the different steel strength on LS state.

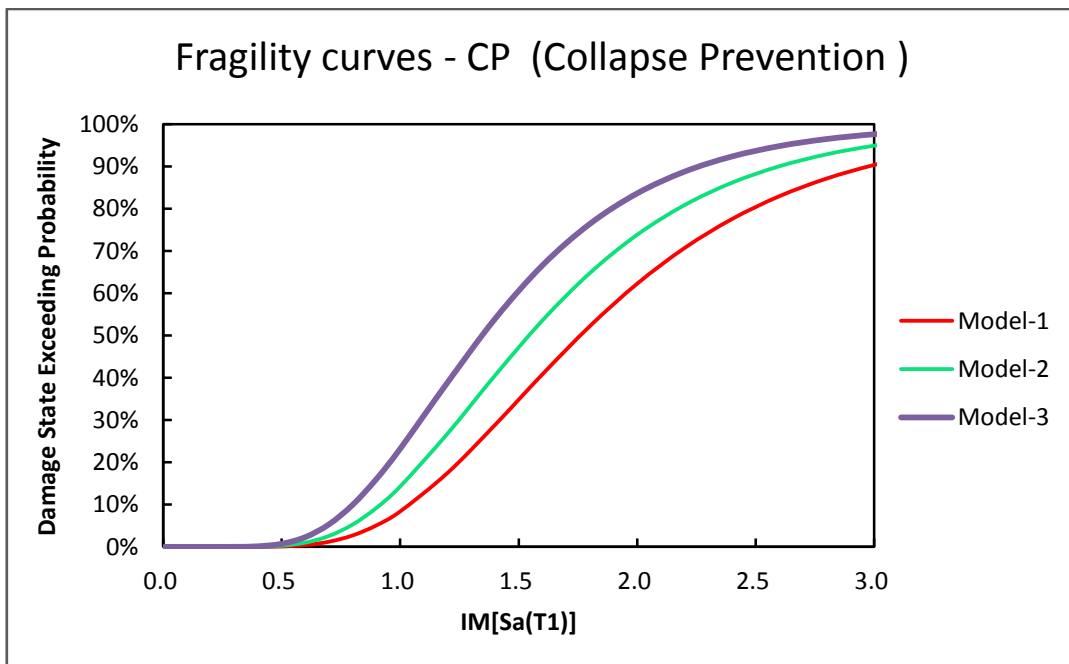


Figure5.14 compare the different steel strength on LS state.

5.3 Strength of Concrete

To study the influence of concrete strength of RC frame structure on the seismic vulnerability, this paper designed 4 RC frame structure according to the Italian code (NTC2008), with the different strength concrete columns, C25/30, C30/37, C40/50, and C50/60, in addition to the various the concret strength of column of each model and the basic properties of other materials are kept the same with basic model-4. C25/30, C30/37, C40/50, and C50/60 the concrete strength take the average value (5-1) and elastic modulus take from the formula(5-2), as shown in Table 5.8

$$f_{cm} = f_{ck} + 8 \text{ [N/mm}^2\text{]} \quad (5-5)$$

$$E_{cm} = 22.000 \cdot \left[\frac{f_{cm}}{10} \right]^{0.3} \text{ [N/mm}^2\text{]} \quad (5-6)$$

Where

f_{cm} the characteristic value to the average value of the cylindrical strength.

f_{ck} characteristic compressive strength of the cylindric.

E_{cm} value for design of elastic modulus.

Table 5.8 The average concrete strength and elastic modulus

No. model	Model-4	Model-5	Model-6	Model-7
concrete classification	C25/30	C30/37	C40/50	C50/60
f_{cm} Mpa	33	38	48	58
E_{cm} [N/mm ²]	31475	32836	35220	37277

5.3.1 The analysis model based on the seismic vulnerability analysis of IDA method

Due to an IDA curve is not a good predictor of the damage of the structure, so we need to select a series of ground motion recorded separately for each model(model-4, model-5, model-6, model-7) to analyze based on IDA method, access to a number of IDA curves. to get the 10 different IDA curve from each ground motion, the 10 IDA curves are summarized in the same IM-DM coordinate system, as shown in Figure 5.15 -5.18

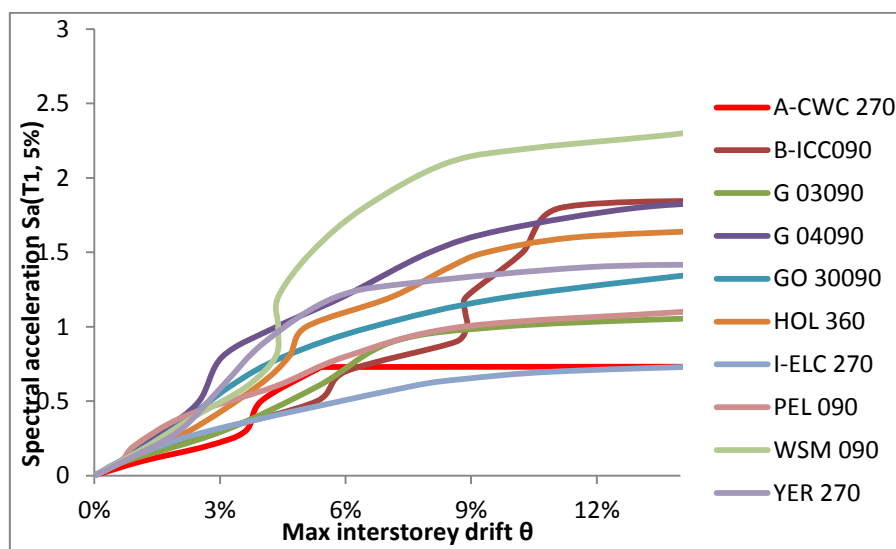


Figure 5.15 IDA curves of model-4

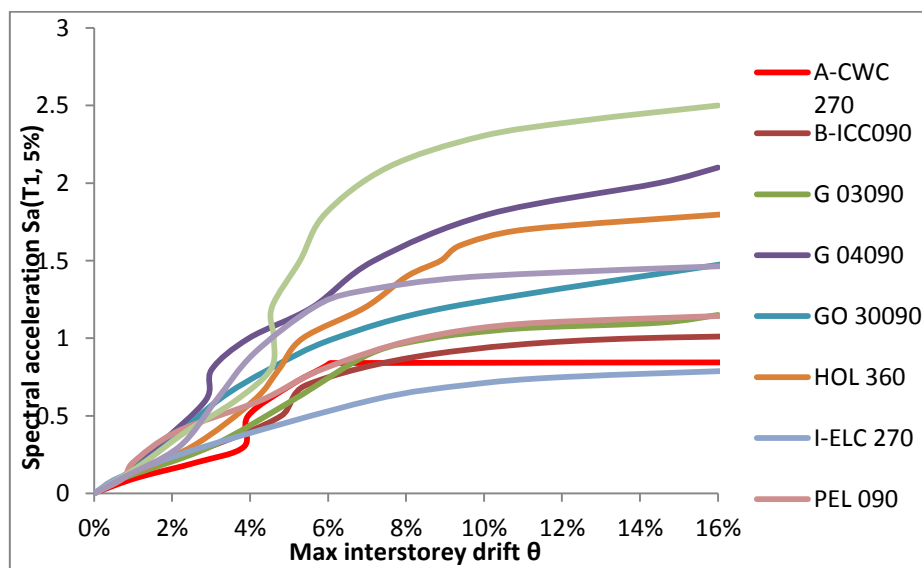


Figure 5.16 IDA curves of model-5

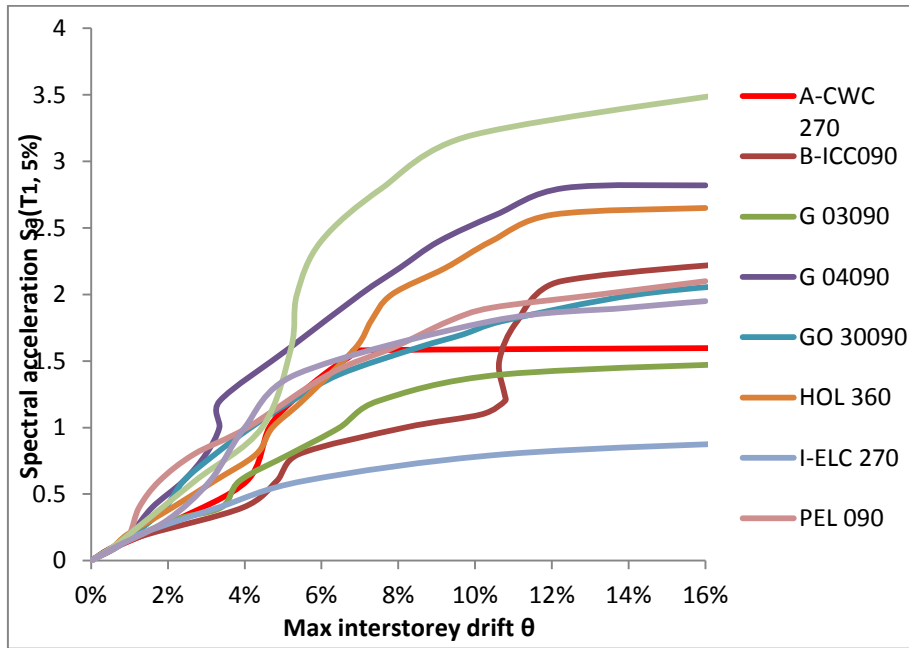


Figure 5.17 IDA curves of model-6

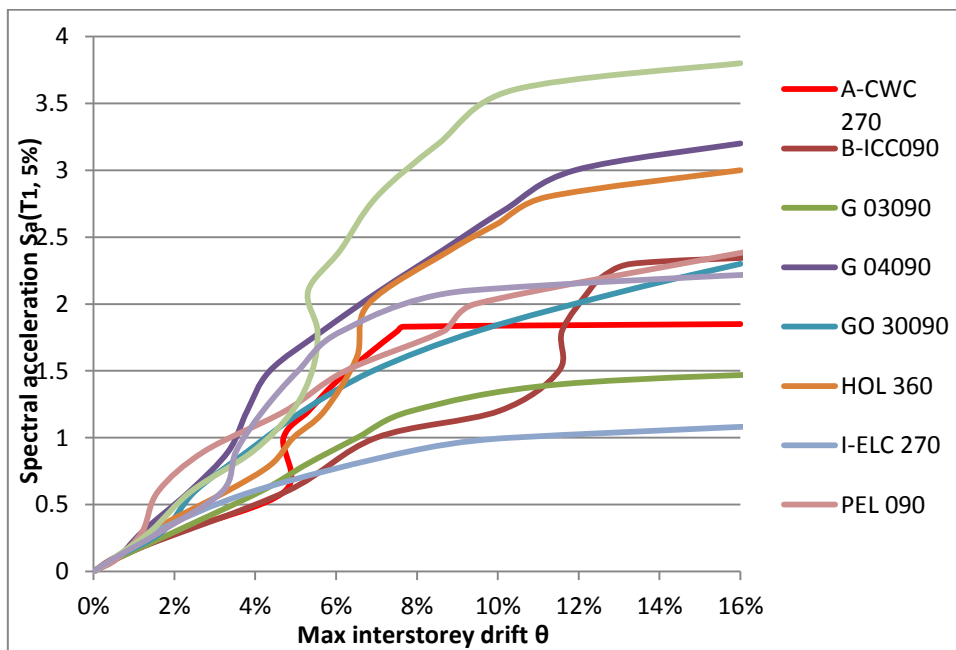


Figure 5.18 IDA curves of model-7

Due to the shape of the IDA curve are related by the selected made ground motion records, The reaction of the same structure when selected a different ground motion records also have certain discrete, so it is necessary to use the median to summarize these different curves to reduce the difference. In Figure 5.19 – 5.22.

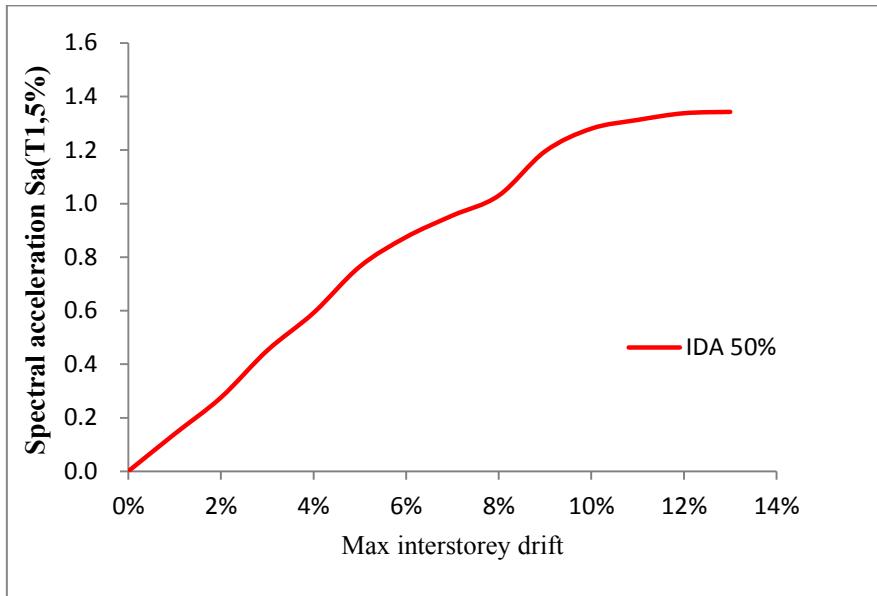


Figure 5.19 Median of IDA curve for model-4

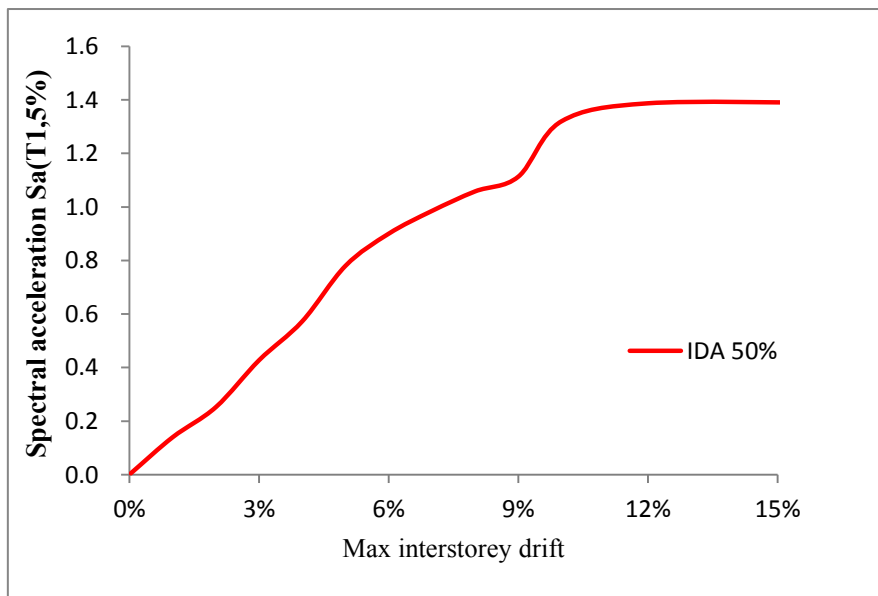


Figure 5.20 Median of IDA curve for model-5

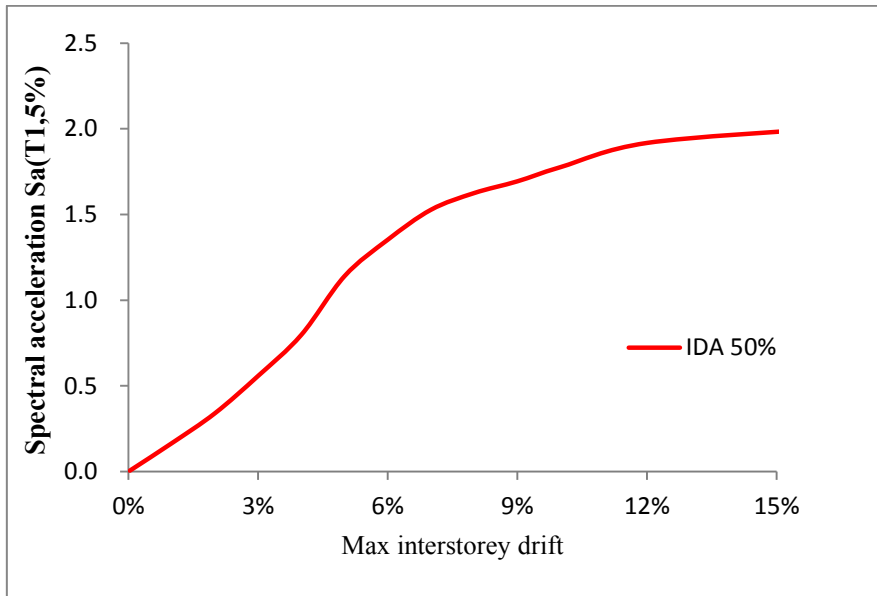


Figure 5.21 Median of IDA curve for model-6

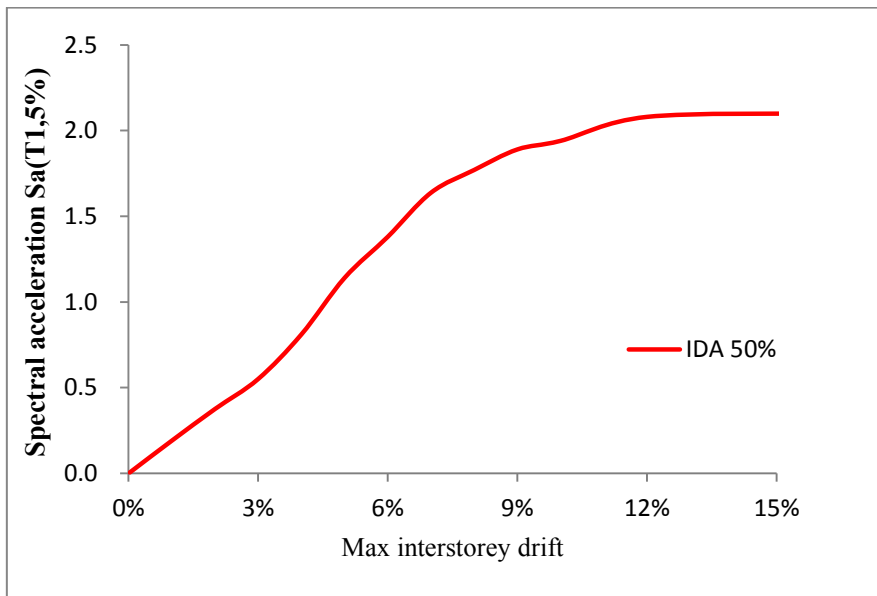


Figure 5.22 Median of IDA curve for model-7

Define the limit of the state point on median of IDA curves, for model-4, model-5, model-6, model-7, Respectively. Show on the table 5.9-5.12

Table 5.9 3 limit state point for model-4 on median curves.

IO		LS		CP	
θ_{max}	Sa (T1, 5%)	θ_{max}	Sa (T1, 5%)	θ_{max}	Sa (T1, 5%)
1.00%	0.14	2.00%	0.276	10.00%	1.28

Table 5.10 3 limit state point for model-5 on median curves.

IO		LS		CP	
θ_{max}	Sa (T1, 5%)	θ_{max}	Sa (T1, 5%)	θ_{max}	Sa (T1, 5%)
1.00%	0.14	2.00%	0.263	7.76%	1.3

Table 5.11 3 limit state point for model-6 on median curves.

IO		LS		CP	
θ_{max}	Sa (T1, 5%)	θ_{max}	Sa (T1, 5%)	θ_{max}	Sa (T1, 5%)
1.00%	0.165	2.00%	0.34	10.00%	1.777

Table 5.12 3 limit state point for model-7 on median curves.

IO		LS		CP	
θ_{max}	Sa (T1, 5%)	θ_{max}	Sa (T1, 5%)	θ_{max}	Sa (T1, 5%)
1.00%	0.19	2.00%	0.375	10.00%	1.94

Take logarithmic from each Intensity measure and damage measure, respectively. And according to the formula of the chapter 3 in the form of incremental dynamic analysis of the data obtained by linear regression analysis. Take $\ln(Sa)$ as independent variables and logarithm of structural response $\ln(\theta_{max})$ as the dependent variable establish the coordinate system, $\ln(\theta_{max}) - \ln(Sa)$, and regression analysis results shown in Figure 5.23-5.26.

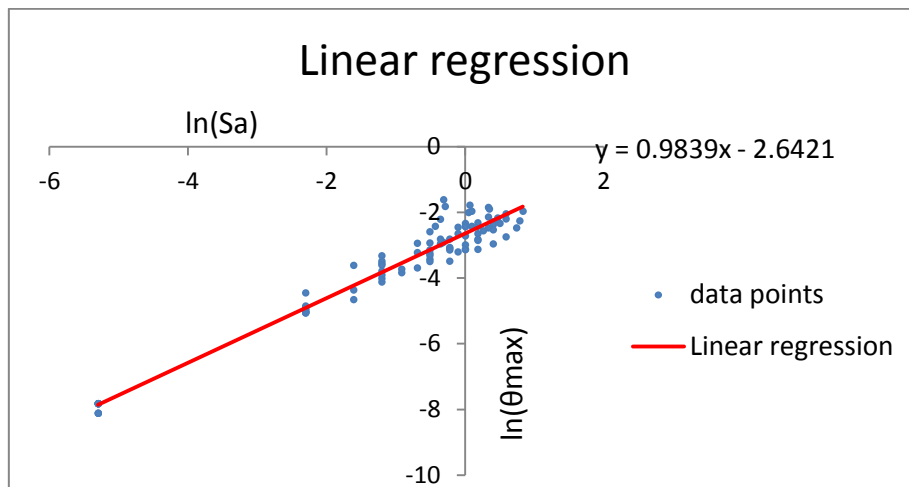


Figure 5.23 regression analysis results on model-4

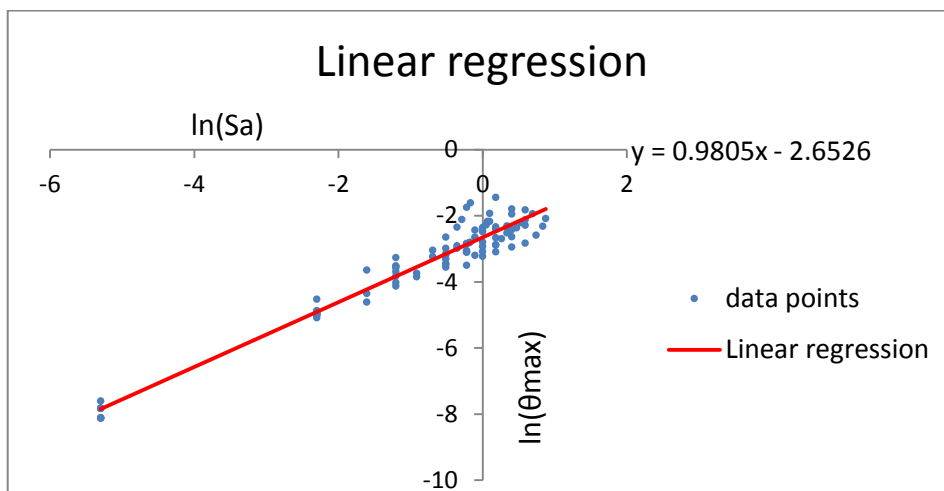


Figure 5.24 regression analysis results on model-5

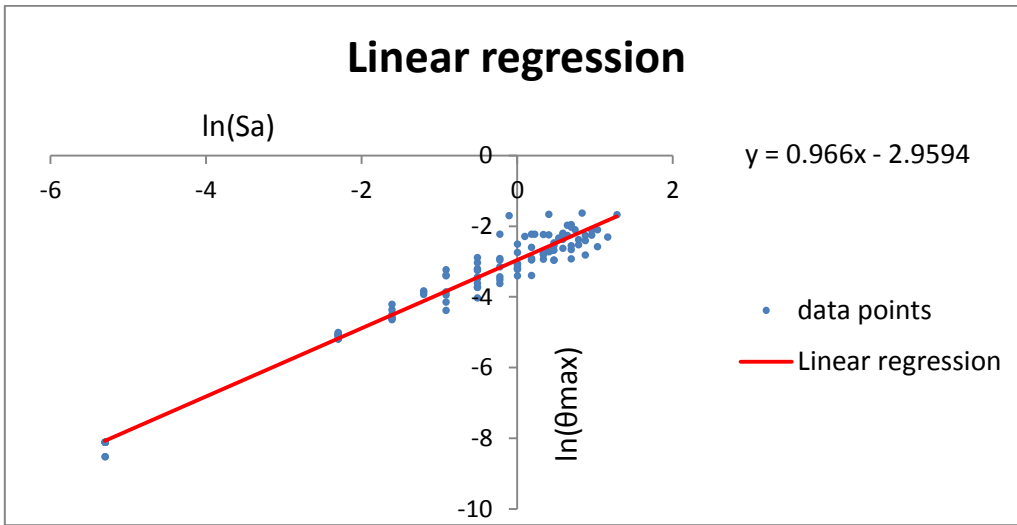


Figure 5.25 regression analysis results on model-6

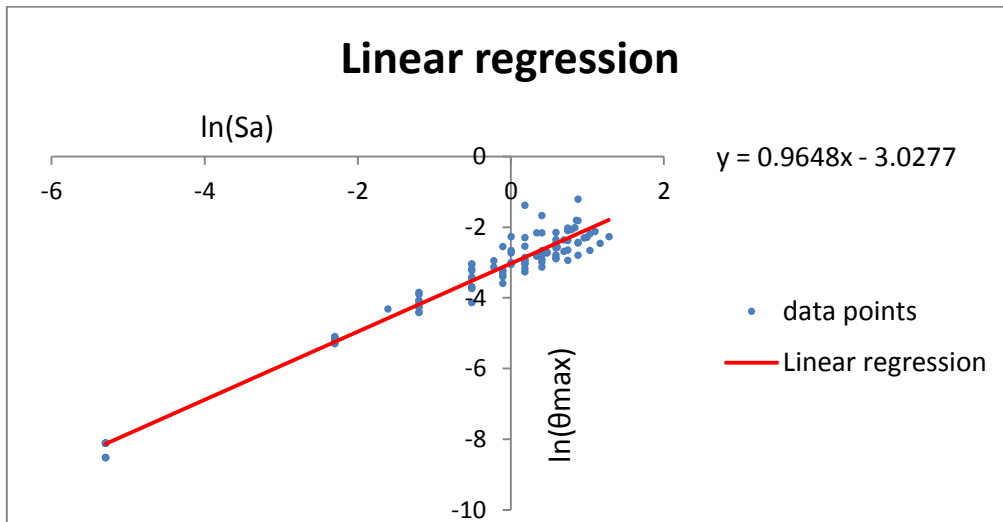


Figure 5.26 regression analysis results on model-7

The probability of Seismic demand model is express on table 5.13-5.16

$$\ln(\alpha) = a \quad \beta = b$$

Table 5.13 The probability of seismic demand model-4

$LN(\theta_{max})=0.9839LN(Sa)-2.6421$		
$\ln(\alpha)=-2.6421$	α	0.07121
$b=0.9839$	β	0.9839

Table 5.14 The probability of seismic demand model-5

$LN(\theta_{max})=0.9805LN(Sa)-2.6526$		
$\ln(\alpha)=-2.6526$	α	0.070468
$b=0.9805$	β	0.9805

Table 5.15 The probability of seismic demand model-6

$LN(\theta_{max})=0.966LN(Sa)-2.9594$		
$\ln(\alpha)=-2.9594$	α	0.05185
$b=0.966$	β	0.966

Table 5.16 The probability of seismic demand model-7

$LN(\theta_{max})=0.9648LN(Sa)-3.0277$		
$\ln(\alpha)=-3.0277$	α	0.048427
$b=0.9648$	β	0.9648

From above table we can get each value of α , β , and then take α , β , into equation (3-1) obtained the failure probability of fundamental period of structure corresponding the acceleration response spectrum $Sa(T1,5\%)$ in the limit state. as shown by formula (5-1) and to get the failure probability of the structure for each limit state.

$$P_f = \Phi \left[\frac{\ln \left[\alpha (S_a(T_{1,5\%}))^\beta / S_c \right]}{\sqrt{\beta_d^2 + \beta_c^2}} \right] \quad (5-7)$$

The failure probability of the structure for each limit state on model-4

$$P_f = \Phi \left[\frac{\ln \left[0.07121 (S_a(T_{1,5\%}))^{0.9839} / S_c \right]}{\sqrt{\beta_d^2 + \beta_c^2}} \right] \quad (5-8)$$

The failure probability of the structure for each limit state on model-5

$$P_f = \Phi \left[\frac{\ln \left[0.070468 (S_a(T_{1,5\%}))^{0.9805} / S_c \right]}{\sqrt{\beta_d^2 + \beta_c^2}} \right] \quad (5-9)$$

The failure probability of the structure for each limit state on model-6

$$P_f = \Phi \left[\frac{\ln \left[0.05185 (S_a(T_{1,5\%}))^{0.966} / S_c \right]}{\sqrt{\beta_d^2 + \beta_c^2}} \right] \quad (5-10)$$

The failure probability of the structure for each limit state on model-7

$$P_f = \Phi \left[\frac{\ln \left[0.048427 (S_a(T_{1,5\%}))^{0.9648} / S_c \right]}{\sqrt{\beta_d^2 + \beta_c^2}} \right] \quad (5-11)$$

The composite logarithmic standard deviation $\sqrt{\beta_d^2 + \beta_c^2}$, known as the dispersion, is taken from values recommended in HAZUS 99, $\sqrt{\beta_d^2 + \beta_c^2} = 0.4$, S_c is the capacity parameters of structure under the different limit state. $\Phi[*]$ is the standard normal distribution function, the value checking the table of the standard normal distribution to determine. Obtained the probability of corresponding to different levels of damage, this curve is the

fragility curve of structure. The abscissa indicates the intensity of ground motion $Sa(T1,5\%)$, and the vertical axis represents the probability of damage state exceeded. Seismic fragility curves shown in Figure 5.27-5.30.

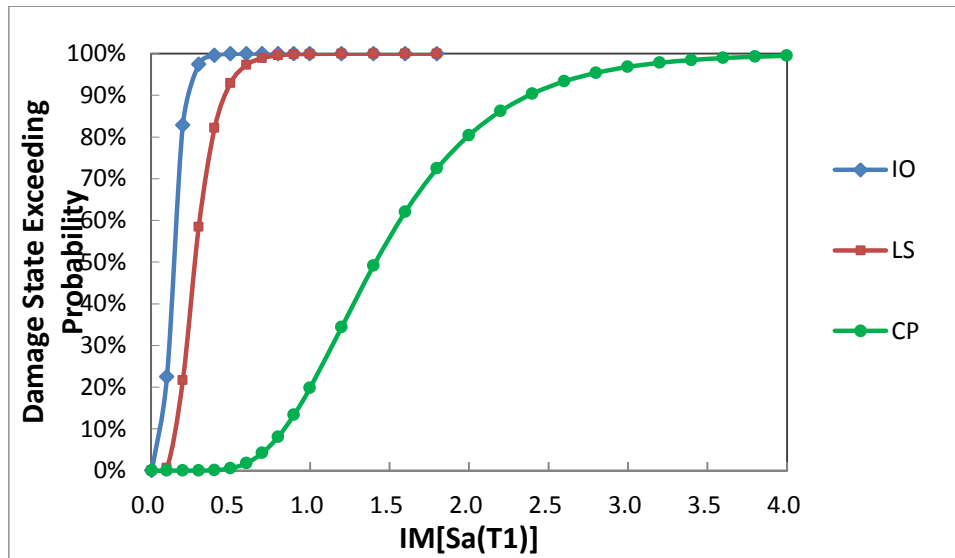


Figure 5.27 Fragility curves of model-4

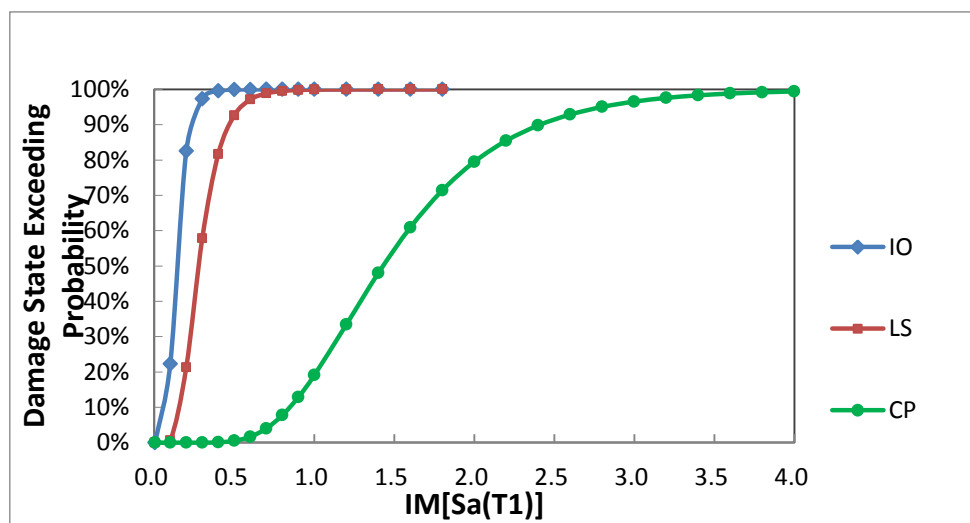


Figure 5.28 Fragility curves of model-5

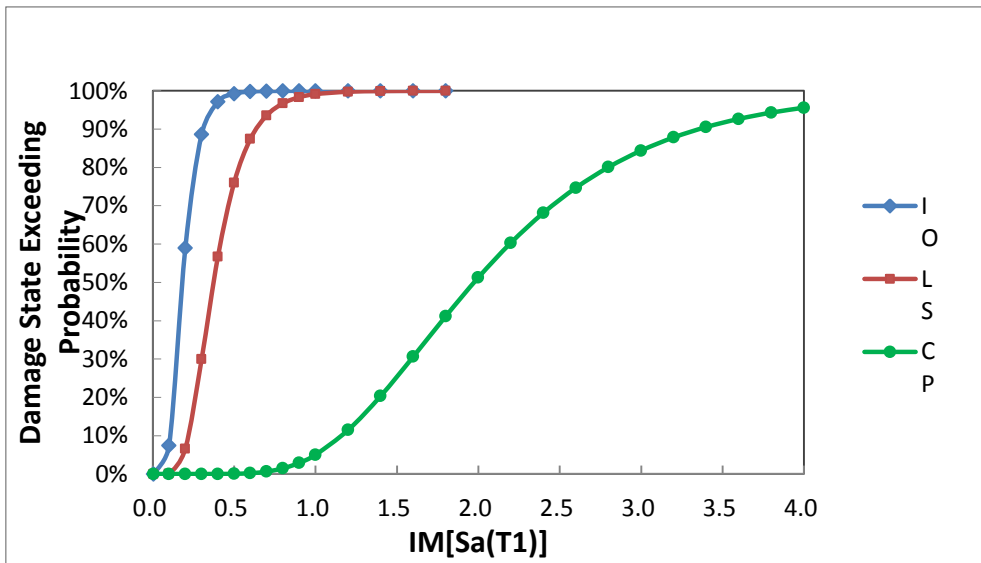


Figure 5.29 Fragility curves of model-6

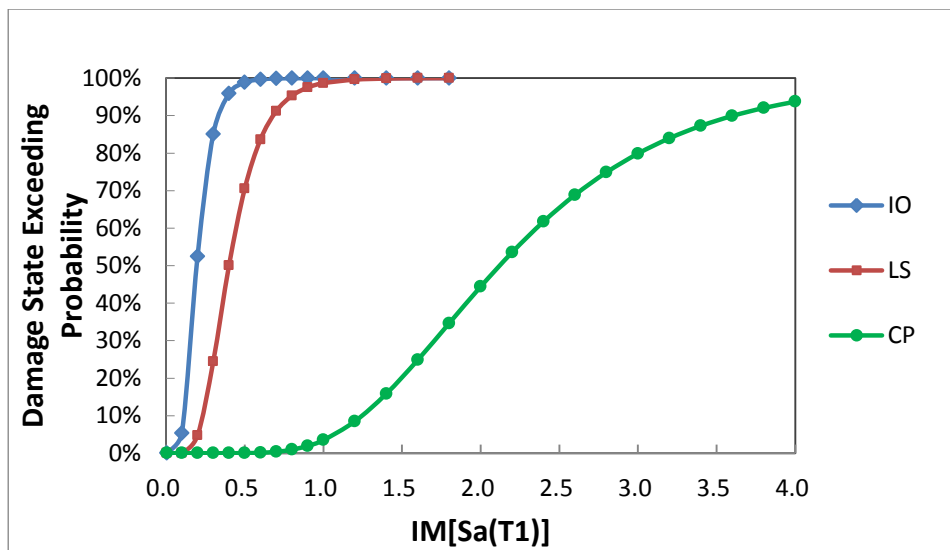


Figure 5.30 Fragility curves of model-7

5.3.2 Results analysis

By comparing the model-4, model-5, model-6, and model-7 of the seismic fragility curves, found that, with the increase the concrete strength of RC frame structure, the smaller the probability of the IO state, LS state and CP state with the same intensity earthquake. The probability of the model-4 and model-5 is very similar either in the IO state or LS state, and have a small difference in CP state. but the probability of the model-6 and model-7 are very different compared to the model-4 and model-5 in IO, LS and CP state. Means the smaller the strength of concrete, under the same seismic intensity, the structure more prone to slight damage and moderate damage, but also easier to achieve the collapse. As shown in Figure 5.31-5.33.

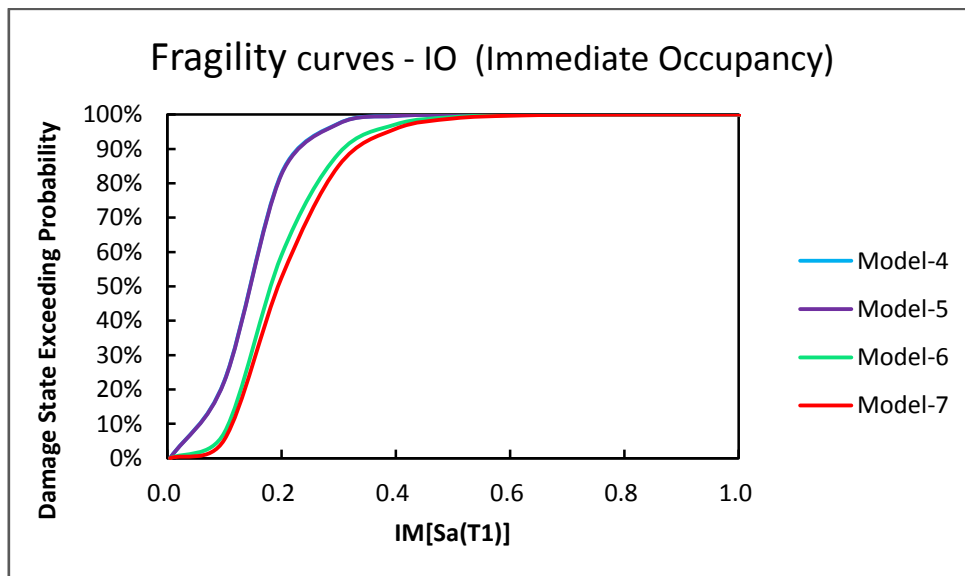


Figure 5.31 compare the different concrete strength on IO state.

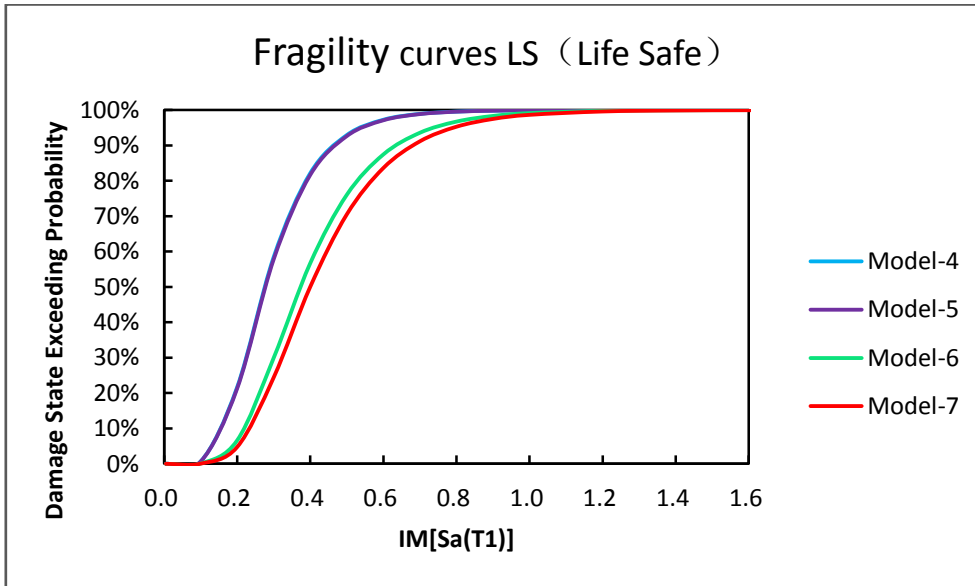


Figure 5.32 compare the different concrete strength on IO state.

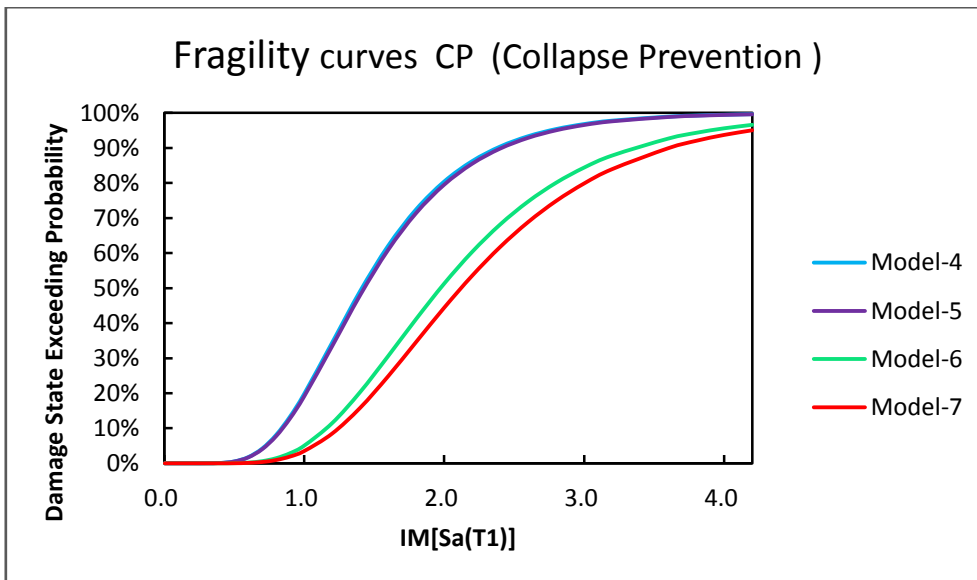


Figure 5.33 compare the different concrete strength on IO state.

5.4 The aspect ratio of the column cross-section

To study the influence of the aspect ratio of the column cross-section of RC frame structure on the seismic vulnerability, this paper designed 3 RC frame structure according to the Italian code (NTC2008), with the different aspect ratio of the columns cross-section and keep the same cross-sectional area in order to maintain constant axial compression ratio. In addition to the various the aspect ratio of the column cross-section of each model and the basic properties of other materials are kept the same with basic model. The concrete use C25/30 and the steel use B 450C. The 3 aspect ratio of the column cross-section as shown in Figure 5.43.

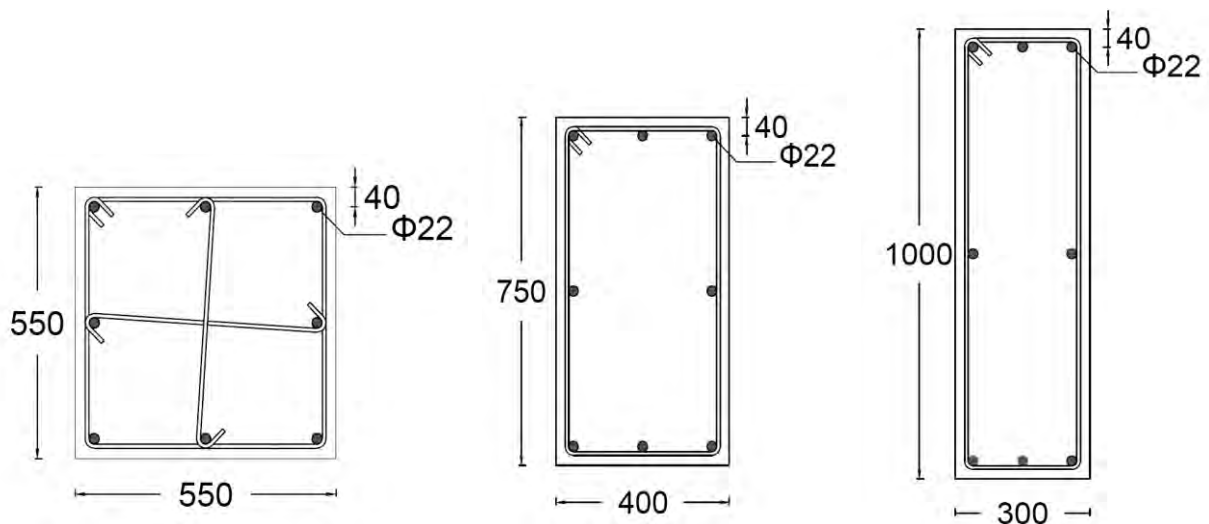


Figure 5.43 The 3 aspect ratio of the column cross-section

5.4.1 The analysis model based on the seismic vulnerability analysis of IDA method

Due to an IDA curve is not a good predictor of the damage of the structure, so we need to select a series of ground motion recorded separately for each model(model-4, model-8, model-9) to analyze based on IDA method, access to a number of IDA curves. to get the 10 different IDA curve from each ground motion, the 10 IDA curves are summarized in the same IM-DM coordinate system, as shown in Figure 5.44 – 5.46.

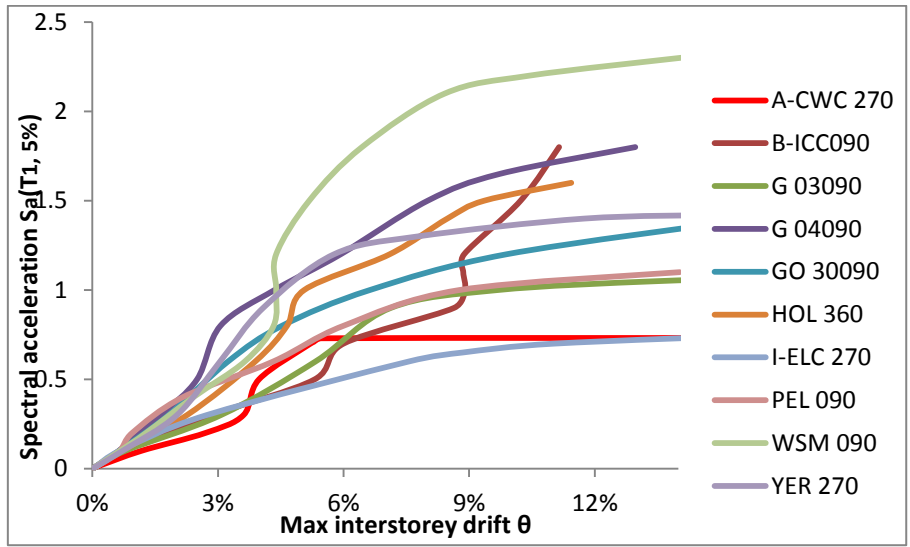


Figure 5.44 IDA curves of model-4

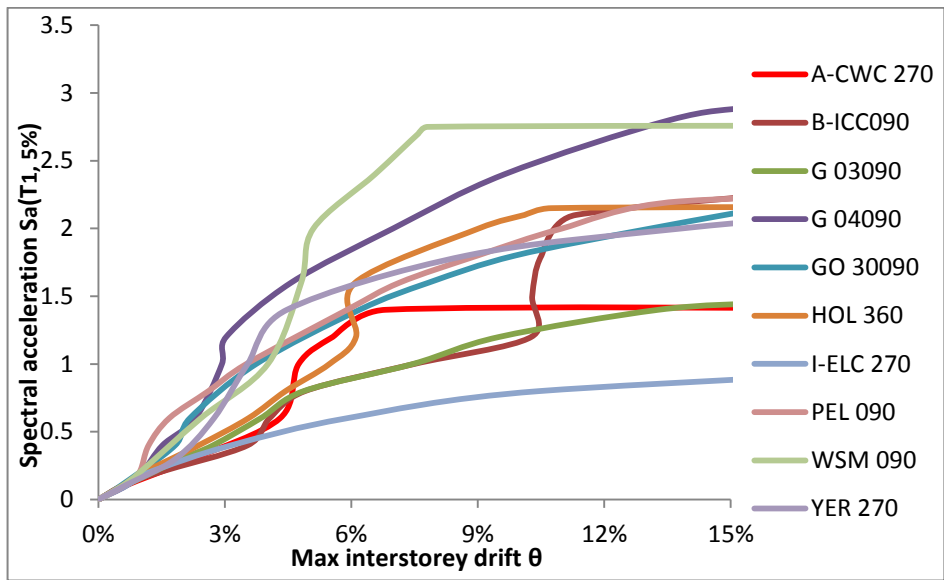


Figure 5.45 IDA curves of model-8

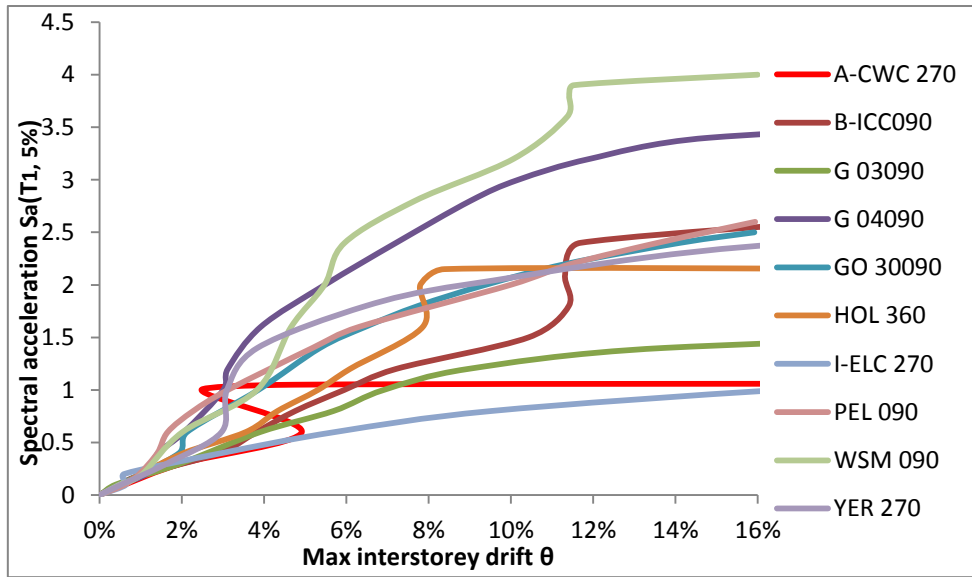


Figure 5.46 IDA curves of model-9

Due to the shape of the IDA curve are related by the selected made ground motion records, The reaction of the same structure when selected a different ground motion records also have certain discrete, so it is necessary to use the median to summarize these different curves to reduce the difference. In Figure 5.47 – 5.49.

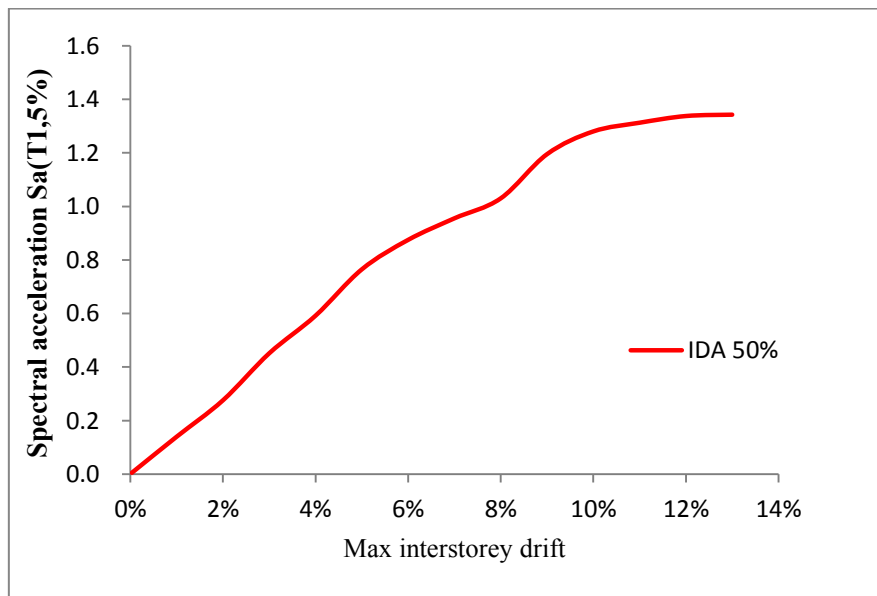


Figure 5.47 Median of IDA curve for model-4

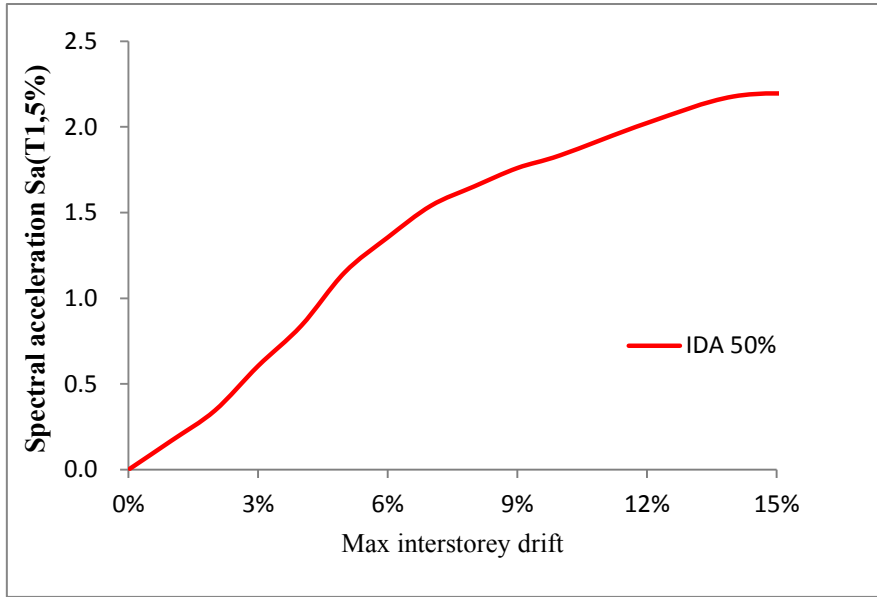


Figure 5.48 Median of IDA curve for model-8

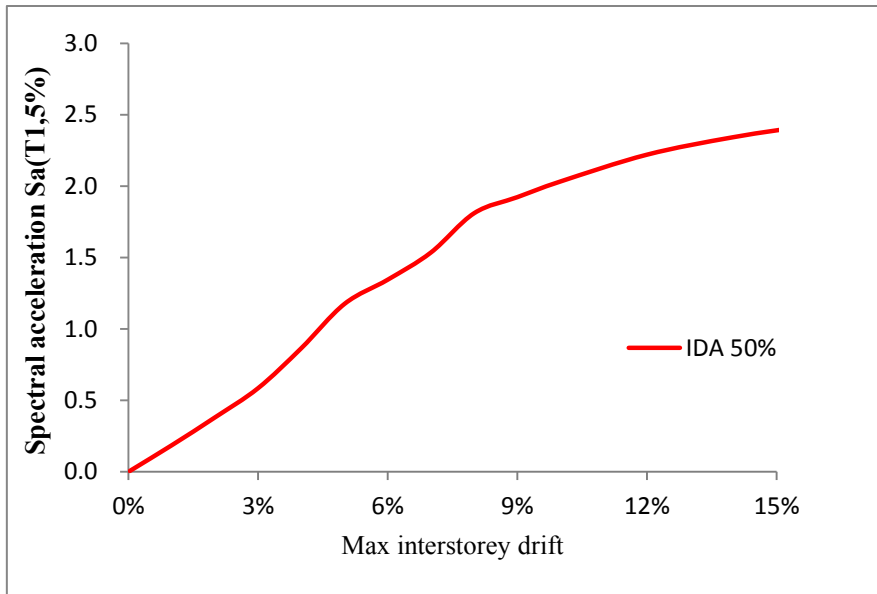


Figure 5.49 Median of IDA curve for model-9

Define the limit of the state point on median of IDA curves, for model-4, model-8, model-9, Respectively. Show on the table 5.17-5.19

Table 5.17 3 limit state point for model-4 on median curves.

I0		LS		CP	
θ_{max}	Sa (T1, 5%)	θ_{max}	Sa (T1, 5%)	θ_{max}	Sa (T1, 5%)
1.00%	0.14	2.00%	0.276	10.00%	1.28

Table 5.18 3 limit state point for model-8 on median curves.

I0		LS		CP	
θ_{max}	Sa (T1, 5%)	θ_{max}	Sa (T1, 5%)	θ_{max}	Sa (T1, 5%)
1.00%	0.17	2.00%	0.345	10.00%	1.835

Table 5.19 3 limit state point for model-9 on median curves.

I0		LS		CP	
θ_{max}	Sa (T1, 5%)	θ_{max}	Sa (T1, 5%)	θ_{max}	Sa (T1, 5%)
1.00%	0.185	2.00%	0.38	10.00%	2.033

Take logarithmic from each Intensity measure and damage measure, respectively. And according to the formula of the chapter 3 in the form of incremental dynamic analysis of the data obtained by linear regression analysis. Take $\ln(Sa)$ as independent variables and logarithm of structural response $\ln(\theta_{max})$ as the dependent variable establish the coordinate system, $\ln(\theta_{max}) - \ln(Sa)$, and regression analysis results shown in Figure 5.50-5.52..

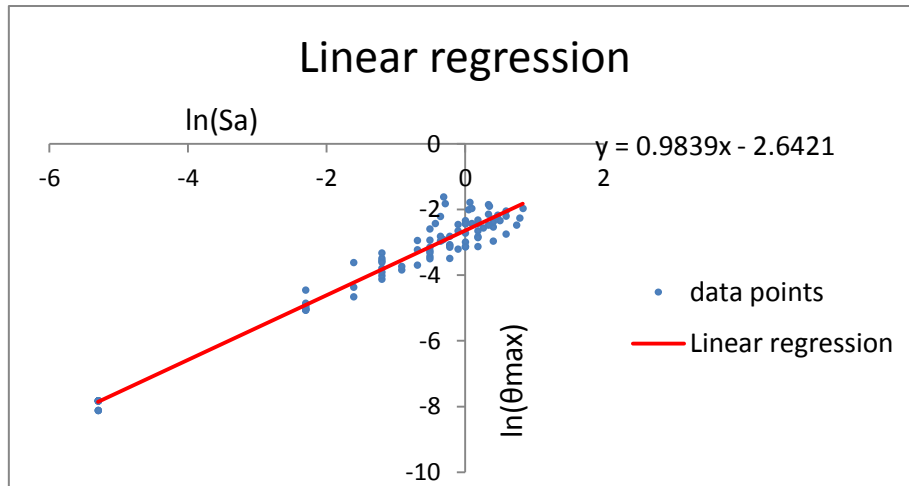


Figure 5.50 regression analysis results on model-4

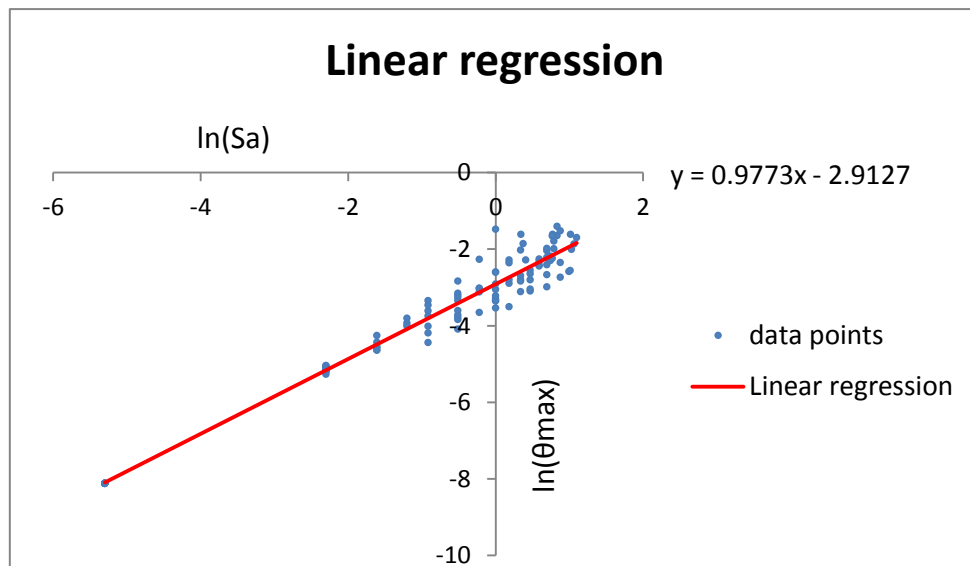


Figure 5.51 regression analysis results on model-8

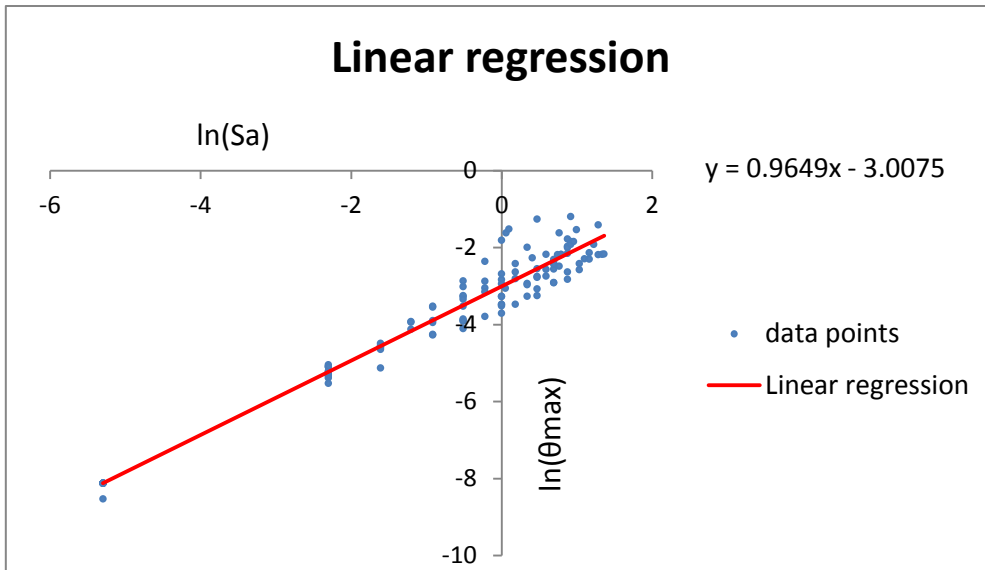


Figure 5.52 regression analysis results on model-9

The probability of Seismic demand model is express on table 5.20-5.22.

$$\ln(\alpha) = a \quad \beta = b$$

Table 5.20 The probability of seismic demand model-4

$LN(\theta_{max}) = 0.9839LN(Sa) - 2.6421$		
$\ln(\alpha) = -2.6421$	α	0.07121
$b = 0.9839$	β	0.9839

Table 5.21 The probability of seismic demand model-8

$LN(\theta_{max}) = 0.9773LN(Sa) - 2.9127$		
$\ln(\alpha) = -2.9127$	α	0.054329
$b = 0.9773$	β	0.9773

Table 5.22 The probability of seismic demand model-9

$LN(\theta_{max}) = 0.9649LN(Sa) - 3.0075$		
$\ln(\alpha) = -3.0075$	α	0.049415
$b = 0.9649$	β	0.9649

From above table we can get each value of α , β , and then take α , β , into equation (3-1) obtained the failure probability of fundamental period of structure corresponding the acceleration response spectrum $S_a(T_{1,5\%})$ in the limit state. as shown by formula (5-13) and to get the failure probability of the structure for each limit state.

$$P_f = \Phi \left[\frac{\ln \left[\alpha (S_a(T_{1,5\%}))^\beta / S_c \right]}{\sqrt{\beta_d^2 + \beta_c^2}} \right] \quad (5-13)$$

The failure probability of the structure for each limit state on model-4

$$P_f = \Phi \left[\frac{\ln \left[0.07121 (S_a(T_{1,5\%}))^{0.9839} / S_c \right]}{\sqrt{\beta_d^2 + \beta_c^2}} \right] \quad (5-14)$$

The failure probability of the structure for each limit state on model-5

$$P_f = \Phi \left[\frac{\ln \left[0.054329 (S_a(T_{1,5\%}))^{0.9773} / S_c \right]}{\sqrt{\beta_d^2 + \beta_c^2}} \right] \quad (5-15)$$

The failure probability of the structure for each limit state on model-6

$$P_f = \Phi \left[\frac{\ln \left[0.049415 (S_a(T_{1,5\%}))^{0.9649} / S_c \right]}{\sqrt{\beta_d^2 + \beta_c^2}} \right] \quad (5-16)$$

The composite logarithmic standard deviation $\sqrt{\beta_d^2 + \beta_c^2}$, known as the dispersion, is taken from values recommended in HAZUS 99 , $\sqrt{\beta_d^2 + \beta_c^2} = 0.4$, S_c is the capacity parameters of structure under the different limit state. $\Phi[*]$ is the standard normal distribution function, the value checking the table of the standard normal distribution to determine. Obtained the

probability of corresponding to different levels of damage, this curve is the fragility curve of structure. The abscissa indicates the intensity of ground motion $Sa(T1,5\%)$, and the vertical axis represents the probability of damage state exceeded. Seismic fragility curves shown in Figure 5.53-5.55.

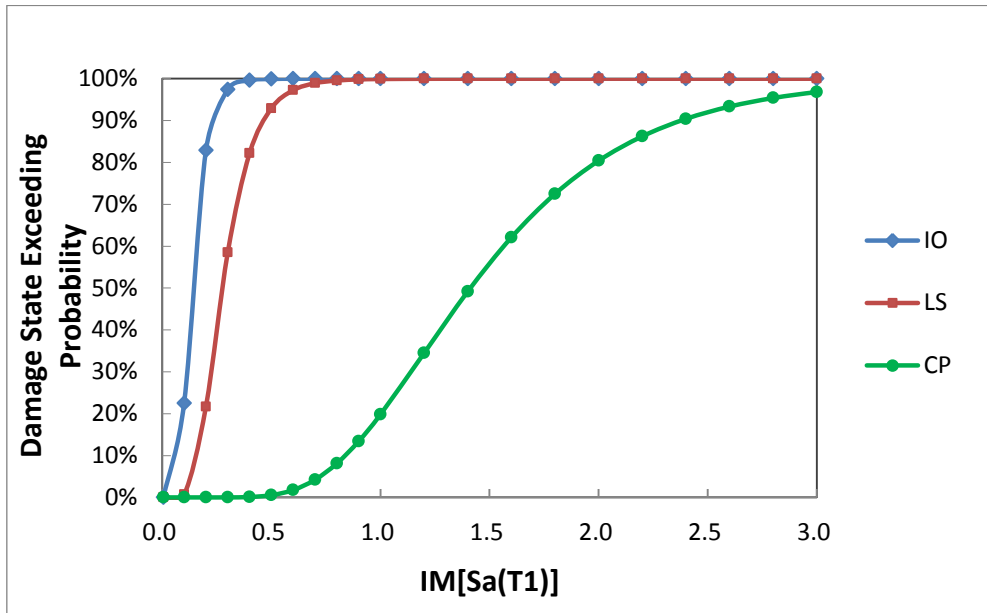


Figure 5.53 Fragility curves of model-4

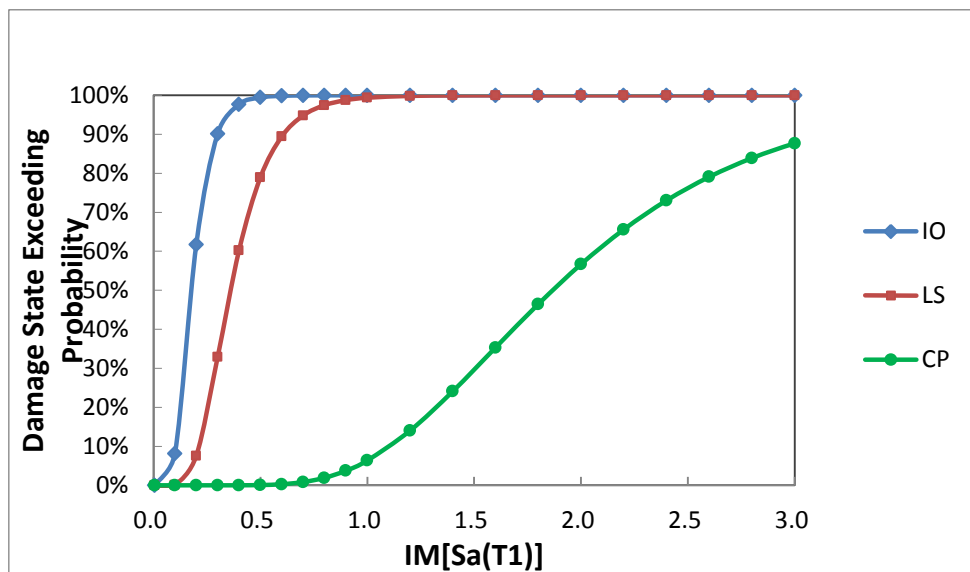


Figure 5.54 Fragility curves of model-8

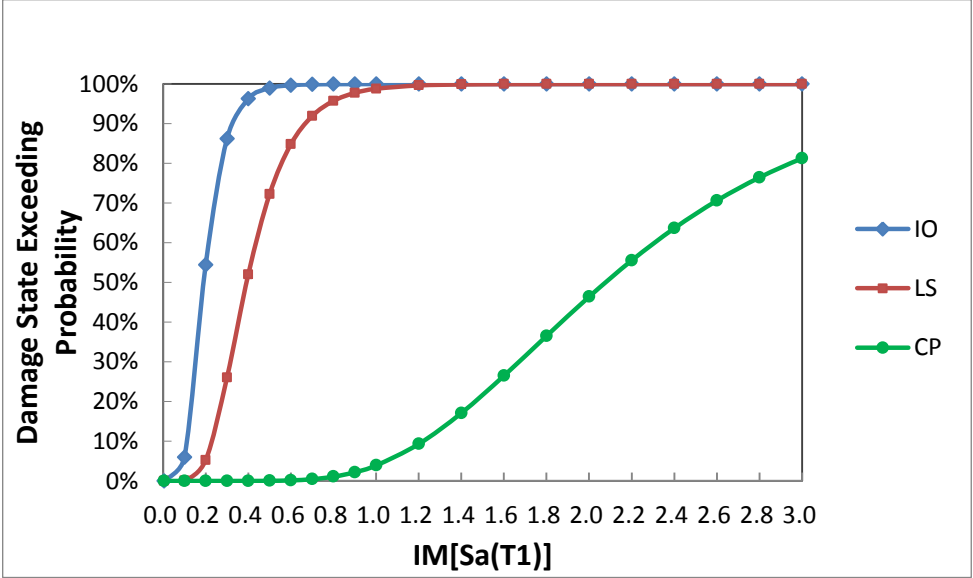


Figure 5.55 Fragility curves of model-9

5.4.2 Results analysis

By comparing the model-4, model-8, and model-9 of the seismic fragility curves, found that, with the increase the aspect ratio of RC frame structure, The probability of the model-4 and model-8 are substantially the same in the IO state, a little different compare to the model-9 in the CP state, and the probability of the model-8, model-9 are very different compared to the model 4 in LS,CP state.

For example when $S_a=0.4g$ the probability of model-4 is 92.92%, the probability of model-8 is 78.95%, and the probability of model-9 is smallest, about 70% in the LS state. Means to increase the aspect ratio of RC frame, ductility and lateral deformation capacity also increased, easy to form a "strong column weak beam" yield mechanism. The resistance of structure and structural collapse resistance increased. So the aspect of model-8 and model-9 is better to be used in Earthquake area. Comparing with probability of 3 models as shown in Figure 5.56-5.58.

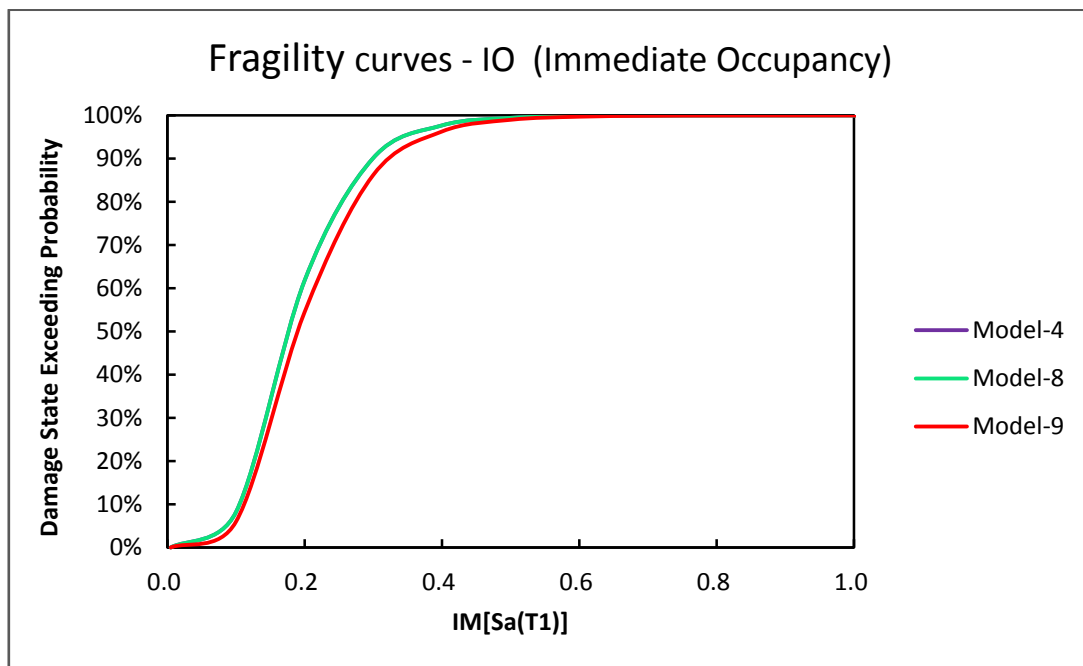


Figure 5.56 compare the different aspect ratio on IO state.

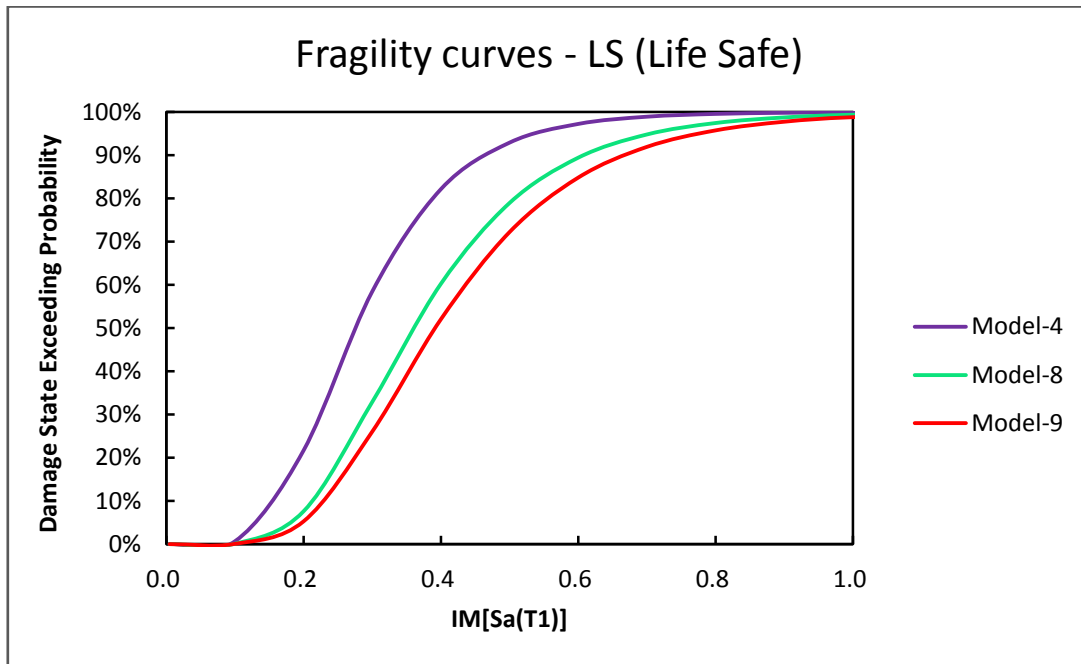


Figure 5.57 compare the different aspect ratio on LS state.

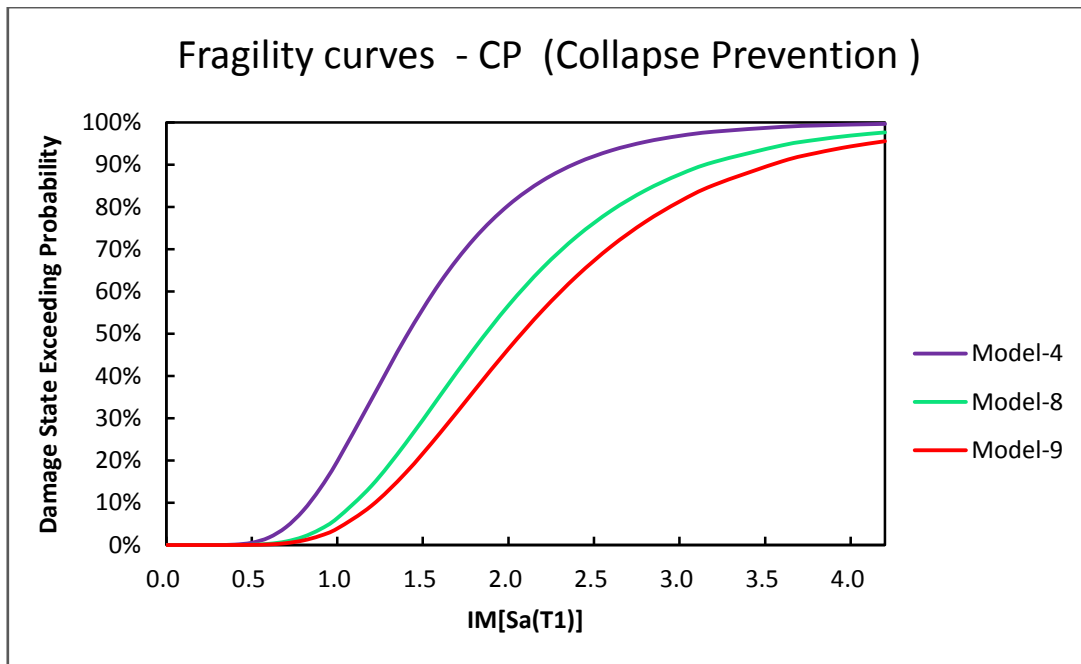


Figure 5.58 compare the different aspect ratio on CP state.

Chapter 6 CONCLUSIONS AND PROSPECT

6.1 The main results and conclusions of this paper

This paper is mainly to study the impact of three factors (the longitudinal reinforcement strength, the concrete strength and the aspect ratio of cross-section column) on the seismic performance of RC frame structure, especially against the influence of the collapse. Through analyzing the seismic vulnerability based on IDA method for the 6 story RC plane frame of structure, the conclusions can be summarized as follows:

- 1) In order to perform the performance calculations needed for Performance Based Engineering Earthquake (PBEE), the limit-states on the IDA curves have been defined, three of which are going to be demonstrated: Immediate Occupancy, Life Safe, and Collapse Prevention. Immediate Occupancy is violated at $\theta_{\max}=1\%$, Life Safe at $\theta_{\max}=2\%$ according to FEMA 350. On the other hand, when the local tangent reaches 20% of the elastic slope (Figure 3.34) or $\theta_{\max}=10\%$, Collapse Prevention exceeds the IDA curve immediately. Finally, the global dynamic instability shows up when the flatline is reached and any increase in the IM results in practically infinite DM response.
- 2) The increase of the concrete strength of RC frame structure brings no change in the probability of the IO state corresponding to the same intensity earthquake, although a little difference in the LS state. At the CP limit state, the probabilities of the 3 models are very different. When under a small earthquake, the damage of the structure is similar, because the steel has not yet reached the state yield due to the small deformation of the structure. Under a great earthquake, along with the increase of the steel strength, the probability in the CP state is getting lower, which means the smaller the strength of steel, the more prone to collapse for the structure of RC frame. That is the reason that the Italian code (NTC 2008) suggested the B 450C steel was very good to be used in the earthquake areas.
- 3) Corresponding to the same intensity of earthquake, when the concrete strength of RC frame structure is increased, the probabilities of the IO state, LS state and CP state become smaller. The probability of the model-4 and model-5 is very similar either in the IO state or LS state, and have a small difference in CP state. However, the probability of the model-6 and model-7 are very different compared to the model-4 and model-5 in IO, LS and CP states, which means the structure is more prone to collapse for small concrete strength when under the same seismic intensity. Therefore, the concretes C40/50, C50/60 are

suggested to be used in the earthquake areas.

- 4) When increasing the aspect ratio of RC frame structure, the probabilities of the model-4 and model-8 remain the same in the IO state, the probability of the model-9 is a little different in the CP state, and the probabilities of the model-8, model-9 are very different compared to the model-4 in the LS, CP states. That means it is easy to form a "strong column weak beam" yield mechanism when increasing the aspect ratio of RC frame, ductility and lateral deformation capacity. The resistance of structure and structural collapse resistance increase. Rectangular cross-section is better than a square cross-section, which is the reason that the aspect of model-8 and model-9 is better to be used in the Earthquake areas.

6.2 Prospect

Due to the limited research time of this work, there are still some problems left worthy to study further.

- 1) Due to the large calculations numbers of IDA method, it takes much time to finish all the works in the OpenSEES considering the 9 related models used in this work. Although it is theoretically possible to do IDA analysis of 3D frame in OpenSEES, planar analysis is used here because of the limited time. However, it is recommended to build 3D models to do simulation in the future work, which should be more accurate considering the effects of floorslabs and walls.
- 2) When doing the IDA analysis, the thesis simplify the earthquake force into one direction, in fact the real force should be in multi-direction, so it is still needed to consider those multiple Impact Factors.
- 3) This thesis only consider three impact factors to RC frame structure, which are the aspect ratio, the concrete strength and the longitudinal reinforcement strength. Stirrup restrain, seismic fortification intensity and the condition of the base are not under consideration.

REFERENCES

1. Ghobarah a. Performance based design in earthquake engineering state of development [J] . Engineering structures ,2001 ,23 (3) :878 -884
2. FEMA273/FEMA274, NEHRP guide lines for the seismic rehabilitation of buildings [S]. Washington D C, 1996.
3. SEAOC Vision 2000 Committee. Performance based seismic engineering of building[R]. April 3 1995.
4. Shinozuka M,Feng MQ,Jee L.Statistic analysis of fragility curves. Journal of Engineering Mechanics, ASCE, 2000, 126(20):1224-1231.
5. Lupoi A,Franchin P,Schotanus MIJ. Seismic risk evaluation of RC bridge structures.Earthquake Engineering and Structural Dynamics,2003,32:1275-1290
6. ATC-63, Quantification of building seismic performance factors, ATC-63 Project Report(90% Draft),FEMA P695/April 2008.
7. VamvatsikosD, Cornell C A. Incremental Dynamic Analysis[J].Earthquake Engineering and Structural Dynamics,2002,31(3):491-514.
8. Federal Emergency Management Agency (FEMA). Recommended Seismic Design Criteria for New Steel Moment-Frame Buildings.SAC Joint Venture, Washington D C:FEMA 350,2000
9. Federal Emergency Management Agency (FEMA).Moment-Frame Buildings. SAC Joint Venture, Washington D C: FEMA 351, 2000
10. IBC, (2006). International Building Code. International Code Council, 2006, USA.
11. FEMA 356 , Prestandard and commentary for the seismic rehabilitation of builings [S]. Washington D C,2000.
12. Vamvatsikos D.and Cornell C.A. Applied incremental dynamic analysis[J] . Earthquake Spectra, 2004, 20 (2): 523-553
13. Vamvatsikos D. and Cornell C. A. . The incremental dynamic analysis and its application to performance- based earthquake engineering[C] 12th European Conference on Earthquake Engineering, London, 2002.
14. Farzin Zareian1,and Helmut Krawinkler. Assessment of probability of collapse and design for collapse safety.
15. Zareian F. Simplified performance-based earthquake engineering. *Ph.D. Dissertation* (under supervision of Prof. Helmut Krawinkler), Stanford University, Stanford, CA,2006.
16. Cornell CA, Jalayer F, Hamburger RO, Foutch DA. Probabilistic basis for 2000 SAC Federal Emergency Management Agency steel moment frame guidelines. Journal of Structural

Engineering (ASCE) 2002; 128(4): 526–533.

17. Shinozuka M, Feng M, Jongheon L, Naganuma T. Statistical analysis of fragility curves. *Journal of Structural Engineering (ASCE)* 2000; 126(12):1224–1232.
18. Ibarra LF, Krawinkler H. 2005. Global collapse of frame structures under seismic excitations. Report No. PEER 2005/06, Pacific Earthquake Engineering Research Center, University of California at Berkeley, Berkeley, California.
19. Jamie E. Padgett¹, and Reginald DesRoches Methodology for the development of analytical fragility curves for retrofitted bridges. *Earthquake Engineering and Structural Dynamics*. 2008; 37:1157–1174.
20. Chopra AK. *Dynamics of Structures: Theory and Applications to Earthquake Engineering*. Prentice-Hall: Englewood Cliffs, NJ, 1995.
21. John B. Mander, *Fragility Curve Development for Assessing the Seismic Vulnerability of Highway Bridges* University at Buffalo, State University of New York.
22. Singhal, A., and Kiremidjian, A. S. 1998. "Bayesian updating of fragilities with application to RC frames." *J. Struct. Eng.*, 1248, 922–929.
23. Wen, Y. K., Ellingwood, B. R., and Bracci, J. M. 2004. "Vulnerability functions." Mid-America Earthquake Center, Univ. of Illinois, Technical Rep. No. DS-4, Champaign, Ill.
24. Italian code NTC 2008
25. Federal Emergency Management Association FEMA. 2000. "Prestandard and commentary for the seismic rehabilitation of buildings." FEMA 356, ASCE, Reston, Virginia.
26. Hamburger R, Rojahn C, Moehle J, Bachman R, Comartin C, Whittaker A. The ATC-58 Project: development of next-generation performance-based earthquake engineering design criteria for buildings. In: *Proceedings of the 13th world conference on earthquake engineering*, Vancouver, Canada, 2004. Paper 1819.
27. Wai-Fah Chen Charles Scawthorn. *Earthquake Engineering handbook*. Boca Raton London New York Washington, D.C.
28. OpenSees Tutorial. Nonlinear Structural Analysis by Quan Gu, Andre Barbosa, and Joel Conte.
29. Marko Brozovič, Matjaž Dolšek. Seismic risk assessment of reinforced concrete frames by employing different methods for determination of seismic response parameters. 2011. University of Ljubljana, Faculty of Civil and Geodetic Engineering, Jamova 2, 1000 Ljubljana, Slovenia.
30. M. Dolšek, Development of computing environment for the seismic performance assessment of reinforced concrete frames by using simplified nonlinear models, *Bulletin of Earthquake Engineering* 8:1309-1329, doi:10.1007/s10518-010-9184-8, 2010.

31. A. M. Breipohl [1970] Probabilistic Systems Analysis, John Wiley & Sons, Inc.
32. A. Coburn and R. Spence [2002] *Earthquake Protection*, second edition, Wiley, England
33. S. Akkar, H. Sucuoglu and A. Yakut [2005] –Displacement-based fragility functions for low- and mid-rise ordinary concrete buildings,” *Earthquake Spectra* , 21(4), 901-927
34. G. M. Calvi, R. Pinho, G. Magenes, J. J. Bommer, L. F. Restrepo-Velez and H. Crowley [2006] –Development of seismic vulnerability assessment methodologies over the past 30 years”, *Journal of Earthquake Technology*, Paper No. 472, Vol. 43, No. 3, September 2006, pp 75-104
35. M. A. Erberik [2008] –Fragility based assessment of typical mid-rise and low-rise RC buildings in Turkey”, *Engineering Structures* 30(5), 1360-1374
36. M. Oropeza, C. Michel and P. Lestuzzi [2010] –A simplified analytical methodology for fragility curves estimation in existing buildings” 14th European Conference on Earthquake Engineering, Ohrid
37. B. Özer AY and M. A. Erberik [2008] –Vulnerability of Turkish low-rise and mid-rise reinforced concrete frame structures” *Journal of Earthquake Engineering*, 12(S2):2-11,2008. doi: 10.1080/13632460802012687
38. A. Singhal and A. Kiremidjian [1995] –Method for developing motion damage relationships for reinforced concrete frames” *Report No.115*, Blume Earthquake Engineering Centre, Department of Civil and Environmental Engineering, Stanford University, Stanford
39. R. Vacareanu, R. Radoi, C. Negulescu and A. Aldea [2004] –Seismic Vulnerability of RC Buildings in Bucharest, Romania”, *13th World Conference on Earthquake Engineering*, Paper No.1796, Vancouver, Canada

APPENDIX

Table 6.1 Normal standard distribution and the value of Probability (Model-1)

Normal standard distribution and the value of Probability							
Sa	IO ($\theta_{\max}=1\%$)	LS ($\theta_{\max}=2\%$)	CP ($\theta_{\max}=10\%$)	Sa	Pf ($\theta=1\%$)	Pf ($\theta=2\%$)	Pf ($\theta=10\%$)
0.005	-8.549	-10.282	-14.306	0.005	0.0000	0.0000	0.0000
0.100	-1.240	-2.973	-6.997	0.100	0.1074	0.0015	0.0000
0.200	0.451	-1.282	-5.306	0.200	0.6739	0.0999	0.0000
0.300	1.440	-0.293	-4.317	0.300	0.9251	0.3848	0.0000
0.400	2.142	0.409	-3.615	0.400	0.9839	0.6587	0.0002
0.500	2.686	0.953	-3.070	0.500	0.9964	0.8298	0.0011
0.600	3.131	1.398	-2.625	0.600	0.9991	0.9190	0.0043
0.700	3.507	1.774	-2.249	0.700	0.9998	0.9620	0.0122
0.800	3.833	2.100	-1.924	0.800	0.9999	0.9821	0.0272
0.900	4.120	2.387	-1.636	0.900	1.0000	0.9915	0.0509
1.000	4.377	2.644	-1.379	1.000	1.0000	0.9959	0.0839
1.200	4.822	3.089	-0.934	1.200	1.0000	0.9990	0.1751
1.400	5.198	3.465	-0.558	1.400	1.0000	0.9997	0.2884
1.600	5.524	3.791	-0.232	1.600	1.0000	0.9999	0.4081
1.800	5.811	4.079	0.055	1.800	1.0000	1.0000	0.5219
2.000	6.068	4.336	0.312	2.000	1.0000	1.0000	0.6225
2.200	6.301	4.568	0.545	2.200	1.0000	1.0000	0.7070
2.400	6.513	4.780	0.757	2.400	1.0000	1.0000	0.7754
2.600	6.709	4.976	0.952	2.600	1.0000	1.0000	0.8295
2.800	6.889	5.156	1.133	2.800	1.0000	1.0000	0.8714
3.000	7.058	5.325	1.301	3.000	1.0000	1.0000	0.9034
3.200	7.215	5.482	1.459	3.200	1.0000	1.0000	0.9277
3.600	7.503	5.770	1.746	3.600	1.0000	1.0000	0.9596
3.800	7.634	5.902	1.878	3.800	1.0000	1.0000	0.9698
4.000	7.760	6.027	2.003	4.000	1.0000	1.0000	0.9774
4.200	7.879	6.146	2.122	4.200	1.0000	1.0000	0.9831

Table 6.1 Normal standard distribution and the value of Probability (Model-2)

Normal standard distribution and the value of Probability							
Sa	IO(θ max=1%)	LS(θ max=2%)	CP(θ max=10%)	Sa	Pf(θ =1%)	Pf(θ =2%)	Pf(θ =10%)
0.005	-8.608	-10.341	-14.101	0.005	0.0000	0.0000	0.0000
0.100	-1.238	-2.971	-6.732	0.100	0.1078	0.0015	0.0000
0.200	0.467	-1.266	-5.026	0.200	0.6796	0.1027	0.0000
0.300	1.464	-0.269	-4.029	0.300	0.9284	0.3941	0.0000
0.400	2.172	0.439	-3.321	0.400	0.9851	0.6697	0.0004
0.500	2.721	0.988	-2.772	0.500	0.9967	0.8384	0.0028
0.600	3.169	1.436	-2.324	0.600	0.9992	0.9246	0.0101
0.700	3.548	1.816	-1.945	0.700	0.9998	0.9653	0.0259
0.800	3.877	2.144	-1.616	0.800	0.9999	0.9840	0.0530
0.900	4.167	2.434	-1.326	0.900	1.0000	0.9925	0.0924
1.000	4.426	2.693	-1.067	1.000	1.0000	0.9965	0.1430
1.200	4.874	3.142	-0.619	1.200	1.0000	0.9992	0.2681
1.400	5.254	3.521	-0.239	1.400	1.0000	0.9998	0.4054
1.600	5.582	3.849	0.089	1.600	1.0000	0.9999	0.5355
1.800	5.872	4.139	0.379	1.800	1.0000	1.0000	0.6476
2.000	6.131	4.398	0.638	2.000	1.0000	1.0000	0.7383
2.200	6.366	4.633	0.872	2.200	1.0000	1.0000	0.8085
2.400	6.580	4.847	1.087	2.400	1.0000	1.0000	0.8614
2.600	6.776	5.044	1.283	2.600	1.0000	1.0000	0.9003
2.800	6.959	5.226	1.466	2.800	1.0000	1.0000	0.9286
3.000	7.129	5.396	1.635	3.000	1.0000	1.0000	0.9490
3.200	7.287	5.554	1.794	3.200	1.0000	1.0000	0.9636
3.600	7.577	5.844	2.084	3.600	1.0000	1.0000	0.9814
3.800	7.710	5.977	2.217	3.800	1.0000	1.0000	0.9867
4.000	7.836	6.103	2.343	4.000	1.0000	1.0000	0.9904
4.200	7.956	6.223	2.463	4.200	1.0000	1.0000	0.9931

Table 6.1 Normal standard distribution and the value of Probability (Model-3)

Normal standard distribution and the value of Probability							
Sa	IO (θ max=1%)	LS (θ max=2%)	CP (θ max=10%)	Sa	Pf (θ =1%)	Pf (θ =2%)	Pf (θ =10%)
0.005	-8.608	-10.341	-13.807	0.005	0.0000	0.0000	0.0000
0.100	-1.215	-2.948	-6.414	0.100	0.1121	0.0016	0.0000
0.200	0.495	-1.238	-4.703	0.200	0.6898	0.1079	0.0000
0.300	1.496	-0.237	-3.703	0.300	0.9326	0.4063	0.0001
0.400	2.206	0.473	-2.993	0.400	0.9863	0.6818	0.0014
0.500	2.756	1.023	-2.442	0.500	0.9971	0.8470	0.0073
0.600	3.206	1.473	-1.992	0.600	0.9993	0.9297	0.0232
0.700	3.587	1.854	-1.612	0.700	0.9998	0.9681	0.0535
0.800	3.916	2.183	-1.282	0.800	1.0000	0.9855	0.0999
0.900	4.207	2.474	-0.992	0.900	1.0000	0.9933	0.1607
1.000	4.467	2.734	-0.732	1.000	1.0000	0.9969	0.2322
1.200	4.917	3.184	-0.282	1.200	1.0000	0.9993	0.3890
1.400	5.297	3.564	0.099	1.400	1.0000	0.9998	0.5393
1.600	5.627	3.894	0.428	1.600	1.0000	1.0000	0.6657
1.800	5.917	4.185	0.719	1.800	1.0000	1.0000	0.7639
2.000	6.177	4.445	0.979	2.000	1.0000	1.0000	0.8362
2.200	6.413	4.680	1.214	2.200	1.0000	1.0000	0.8876
2.400	6.627	4.894	1.429	2.400	1.0000	1.0000	0.9235
2.600	6.825	5.092	1.626	2.600	1.0000	1.0000	0.9480
2.800	7.008	5.275	1.809	2.800	1.0000	1.0000	0.9648
3.000	7.178	5.445	1.979	3.000	1.0000	1.0000	0.9761
3.200	7.337	5.604	2.139	3.200	1.0000	1.0000	0.9838
3.600	7.628	5.895	2.429	3.600	1.0000	1.0000	0.9924
3.800	7.761	6.028	2.563	3.800	1.0000	1.0000	0.9948
4.000	7.888	6.155	2.689	4.000	1.0000	1.0000	0.9964
4.200	8.008	6.275	2.810	4.200	1.0000	1.0000	0.9975

Table 6.1 Normal standard distribution and the value of Probability (Model-4)

Normal standard distribution and the value of Probability							
Sa	IO (θ max=1%)	LS (θ max=2%)	CP (θ max=10%)	Sa	Pf (θ =1%)	Pf (θ =2%)	Pf (θ =10%)
0.005	-8.125	-9.858	-13.881	0.005	0.0000	0.0000	0.0000
0.100	-0.756	-2.489	-6.513	0.100	0.2248	0.0064	0.0000
0.200	0.949	-0.784	-4.808	0.200	0.8286	0.2165	0.0000
0.300	1.946	0.213	-3.810	0.300	0.9742	0.5844	0.0001
0.400	2.654	0.921	-3.103	0.400	0.9960	0.8215	0.0010
0.500	3.203	1.470	-2.554	0.500	0.9993	0.9292	0.0053
0.600	3.651	1.918	-2.105	0.600	0.9999	0.9725	0.0176
0.700	4.030	2.297	-1.726	0.700	1.0000	0.9892	0.0422
0.800	4.359	2.626	-1.398	0.800	1.0000	0.9957	0.0811
0.900	4.648	2.916	-1.108	0.900	1.0000	0.9982	0.1339
1.000	4.908	3.175	-0.849	1.000	1.0000	0.9993	0.1980
1.200	5.356	3.623	-0.400	1.200	1.0000	0.9999	0.3444
1.400	5.735	4.002	-0.021	1.400	1.0000	1.0000	0.4915
1.600	6.064	4.331	0.307	1.600	1.0000	1.0000	0.6207
1.800	6.353	4.621	0.597	1.800	1.0000	1.0000	0.7247
2.000	6.613	4.880	0.856	2.000	1.0000	1.0000	0.8040
2.200	6.847	5.114	1.091	2.200	1.0000	1.0000	0.8623
2.400	7.061	5.328	1.305	2.400	1.0000	1.0000	0.9040
2.600	7.258	5.525	1.501	2.600	1.0000	1.0000	0.9334
2.800	7.440	5.707	1.684	2.800	1.0000	1.0000	0.9539
3.000	7.610	5.877	1.853	3.000	1.0000	1.0000	0.9681
3.200	7.769	6.036	2.012	3.200	1.0000	1.0000	0.9779
3.600	8.058	6.326	2.302	3.600	1.0000	1.0000	0.9893
3.800	8.191	6.459	2.435	3.800	1.0000	1.0000	0.9926
4.000	8.318	6.585	2.561	4.000	1.0000	1.0000	0.9948
4.200	8.438	6.705	2.681	4.200	1.0000	1.0000	0.9963

Table 6.1 Normal standard distribution and the value of Probability (Model-5)

Normal standard distribution and the value of Probability							
Sa	IO (θ max=1%)	LS (θ max=2%)	CP (θ max=10%)	Sa	Pf (θ =1%)	Pf (θ =2%)	Pf (θ =10%)
0.005	-8.106	-9.839	-13.863	0.005	0.0000	0.0000	0.0000
0.100	-0.763	-2.496	-6.519	0.100	0.2228	0.0063	0.0000
0.200	0.936	-0.797	-4.820	0.200	0.8254	0.2129	0.0000
0.300	1.930	0.197	-3.826	0.300	0.9732	0.5782	0.0001
0.400	2.635	0.903	-3.121	0.400	0.9958	0.8166	0.0009
0.500	3.182	1.449	-2.574	0.500	0.9993	0.9264	0.0050
0.600	3.629	1.896	-2.127	0.600	0.9999	0.9710	0.0167
0.700	4.007	2.274	-1.749	0.700	1.0000	0.9885	0.0401
0.800	4.334	2.602	-1.422	0.800	1.0000	0.9954	0.0775
0.900	4.623	2.890	-1.133	0.900	1.0000	0.9981	0.1285
1.000	4.881	3.149	-0.875	1.000	1.0000	0.9992	0.1908
1.200	5.328	3.595	-0.428	1.200	1.0000	0.9998	0.3343
1.400	5.706	3.973	-0.050	1.400	1.0000	1.0000	0.4800
1.600	6.034	4.301	0.277	1.600	1.0000	1.0000	0.6091
1.800	6.322	4.589	0.566	1.800	1.0000	1.0000	0.7142
2.000	6.581	4.848	0.824	2.000	1.0000	1.0000	0.7950
2.200	6.814	5.081	1.058	2.200	1.0000	1.0000	0.8549
2.400	7.027	5.295	1.271	2.400	1.0000	1.0000	0.8981
2.600	7.224	5.491	1.467	2.600	1.0000	1.0000	0.9288
2.800	7.405	5.672	1.649	2.800	1.0000	1.0000	0.9504
3.000	7.574	5.842	1.818	3.000	1.0000	1.0000	0.9655
3.200	7.733	6.000	1.976	3.200	1.0000	1.0000	0.9759
3.600	8.021	6.288	2.265	3.600	1.0000	1.0000	0.9882
3.800	8.154	6.421	2.397	3.800	1.0000	1.0000	0.9917
4.000	8.280	6.547	2.523	4.000	1.0000	1.0000	0.9942
4.200	8.399	6.666	2.643	4.200	1.0000	1.0000	0.9959

Table 6.1 Normal standard distribution and the value of Probability (Model-6)

Normal standard distribution and the value of Probability							
Sa	IO(θ max=1%)	LS(θ max=2%)	CP(θ max=10%)	Sa	Pf(θ =1%)	Pf(θ =2%)	Pf(θ =10%)
0.005	-8.681	-10.414	-14.437	0.005	0.0000	0.0000	0.0000
0.100	-1.446	-3.179	-7.203	0.100	0.0740	0.0007	0.0000
0.200	0.228	-1.505	-5.529	0.200	0.5900	0.0661	0.0000
0.300	1.207	-0.526	-4.550	0.300	0.8863	0.2994	0.0000
0.400	1.902	0.169	-3.855	0.400	0.9714	0.5670	0.0001
0.500	2.440	0.708	-3.316	0.500	0.9927	0.7604	0.0005
0.600	2.881	1.148	-2.876	0.600	0.9980	0.8745	0.0020
0.700	3.253	1.520	-2.503	0.700	0.9994	0.9358	0.0062
0.800	3.576	1.843	-2.181	0.800	0.9998	0.9673	0.0146
0.900	3.860	2.127	-1.896	0.900	0.9999	0.9833	0.0289
1.000	4.114	2.382	-1.642	1.000	1.0000	0.9914	0.0503
1.200	4.555	2.822	-1.202	1.200	1.0000	0.9976	0.1147
1.400	4.927	3.194	-0.829	1.400	1.0000	0.9993	0.2034
1.600	5.249	3.517	-0.507	1.600	1.0000	0.9998	0.3061
1.800	5.534	3.801	-0.223	1.800	1.0000	0.9999	0.4119
2.000	5.788	4.056	0.032	2.000	1.0000	1.0000	0.5127
2.200	6.019	4.286	0.262	2.200	1.0000	1.0000	0.6034
2.400	6.229	4.496	0.472	2.400	1.0000	1.0000	0.6816
2.600	6.422	4.689	0.666	2.600	1.0000	1.0000	0.7471
2.800	6.601	4.868	0.844	2.800	1.0000	1.0000	0.8008
3.000	6.768	5.035	1.011	3.000	1.0000	1.0000	0.8440
3.200	6.923	5.191	1.167	3.200	1.0000	1.0000	0.8784
3.600	7.208	5.475	1.451	3.600	1.0000	1.0000	0.9267
3.800	7.338	5.606	1.582	3.800	1.0000	1.0000	0.9432
4.000	7.462	5.729	1.706	4.000	1.0000	1.0000	0.9560
4.200	7.580	5.847	1.824	4.200	1.0000	1.0000	0.9659

Table 6.1 Normal standard distribution and the value of Probability (Model-7)

Normal standard distribution and the value of Probability							
Sa	IO(θ max=1%)	LS(θ max=2%)	CP(θ max=10%)	Sa	Pf(θ =1%)	Pf(θ =2%)	Pf(θ =10%)
0.005	-8.836	-10.569	-14.592	0.005	0.0000	0.0000	0.0000
0.100	-1.610	-3.343	-7.367	0.100	0.0537	0.0004	0.0000
0.200	0.062	-1.671	-5.695	0.200	0.5246	0.0473	0.0000
0.300	1.040	-0.693	-4.717	0.300	0.8508	0.2441	0.0000
0.400	1.734	0.001	-4.023	0.400	0.9585	0.5003	0.0000
0.500	2.272	0.539	-3.485	0.500	0.9885	0.7050	0.0002
0.600	2.712	0.979	-3.045	0.600	0.9967	0.8361	0.0012
0.700	3.083	1.351	-2.673	0.700	0.9990	0.9116	0.0038
0.800	3.405	1.673	-2.351	0.800	0.9997	0.9528	0.0094
0.900	3.690	1.957	-2.067	0.900	0.9999	0.9748	0.0194
1.000	3.944	2.211	-1.813	1.000	1.0000	0.9865	0.0349
1.200	4.383	2.651	-1.373	1.200	1.0000	0.9960	0.0849
1.400	4.755	3.022	-1.001	1.400	1.0000	0.9987	0.1584
1.600	5.077	3.344	-0.679	1.600	1.0000	0.9996	0.2485
1.800	5.361	3.629	-0.395	1.800	1.0000	0.9999	0.3464
2.000	5.616	3.883	-0.141	2.000	1.0000	0.9999	0.4440
2.200	5.845	4.113	0.089	2.200	1.0000	1.0000	0.5355
2.400	6.055	4.322	0.299	2.400	1.0000	1.0000	0.6175
2.600	6.248	4.516	0.492	2.600	1.0000	1.0000	0.6886
2.800	6.427	4.694	0.671	2.800	1.0000	1.0000	0.7488
3.000	6.594	4.861	0.837	3.000	1.0000	1.0000	0.7987
3.200	6.749	5.016	0.993	3.200	1.0000	1.0000	0.8396
3.600	7.033	5.300	1.277	3.600	1.0000	1.0000	0.8992
3.800	7.164	5.431	1.407	3.800	1.0000	1.0000	0.9203
4.000	7.287	5.555	1.531	4.000	1.0000	1.0000	0.9371
4.200	7.405	5.672	1.649	4.200	1.0000	1.0000	0.9504

Table 6.1 Normal standard distribution and the value of Probability (Model-8)

Normal standard distribution and the value of Probabilitys							
Sa	IO(θ max=1%)	LS(θ max=2%)	CP(θ max=10%)	Sa	Pf(θ =1%)	Pf(θ =2%)	Pf(θ =10%)
0.005	-8.714	-10.447	-14.470	0.005	0.0000	0.0000	0.0000
0.100	-1.395	-3.127	-7.151	0.100	0.0816	0.0009	0.0000
0.200	0.299	-1.434	-5.458	0.200	0.6175	0.0758	0.0000
0.300	1.290	-0.443	-4.467	0.300	0.9014	0.3288	0.0000
0.400	1.992	0.260	-3.764	0.400	0.9768	0.6024	0.0001
0.500	2.538	0.805	-3.219	0.500	0.9944	0.7895	0.0006
0.600	2.983	1.250	-2.773	0.600	0.9986	0.8944	0.0028
0.700	3.360	1.627	-2.397	0.700	0.9996	0.9481	0.0083
0.800	3.686	1.953	-2.070	0.800	0.9999	0.9746	0.0192
0.900	3.974	2.241	-1.783	0.900	1.0000	0.9875	0.0373
1.000	4.231	2.498	-1.525	1.000	1.0000	0.9938	0.0636
1.200	4.677	2.944	-1.080	1.200	1.0000	0.9984	0.1401
1.400	5.053	3.320	-0.703	1.400	1.0000	0.9996	0.2410
1.600	5.380	3.647	-0.377	1.600	1.0000	0.9999	0.3531
1.800	5.667	3.934	-0.089	1.800	1.0000	1.0000	0.4645
2.000	5.925	4.192	0.168	2.000	1.0000	1.0000	0.5668
2.200	6.158	4.425	0.401	2.200	1.0000	1.0000	0.6558
2.400	6.370	4.637	0.614	2.400	1.0000	1.0000	0.7303
2.600	6.566	4.833	0.809	2.600	1.0000	1.0000	0.7908
2.800	6.747	5.014	0.990	2.800	1.0000	1.0000	0.8390
3.000	6.915	5.182	1.159	3.000	1.0000	1.0000	0.8768
3.200	7.073	5.340	1.317	3.200	1.0000	1.0000	0.9060
3.600	7.361	5.628	1.604	3.600	1.0000	1.0000	0.9457
3.800	7.493	5.760	1.736	3.800	1.0000	1.0000	0.9588
4.000	7.618	5.885	1.862	4.000	1.0000	1.0000	0.9687
4.200	7.737	6.005	1.981	4.200	1.0000	1.0000	0.9762

Table 6.1 Normal standard distribution and the value of Probability (Model-9)

Normal standard distribution and the value of Probability							
Sa	IO(θ max=1%)	LS(θ max=2%)	CP(θ max=10%)	Sa	Pf(θ =1%)	Pf(θ =2%)	Pf(θ =10%)
0.005	-8.787	-10.520	-14.543	0.005	0.0000	0.0000	0.0000
0.100	-1.560	-3.293	-7.317	0.100	0.0594	0.0005	0.0000
0.200	0.112	-1.621	-5.645	0.200	0.5445	0.0525	0.0000
0.300	1.090	-0.643	-4.667	0.300	0.8621	0.2601	0.0000
0.400	1.784	0.051	-3.973	0.400	0.9628	0.5203	0.0000
0.500	2.322	0.589	-3.434	0.500	0.9899	0.7222	0.0003
0.600	2.762	1.029	-2.995	0.600	0.9971	0.8483	0.0014
0.700	3.134	1.401	-2.623	0.700	0.9991	0.9194	0.0044
0.800	3.456	1.723	-2.301	0.800	0.9997	0.9576	0.0107
0.900	3.740	2.007	-2.016	0.900	0.9999	0.9776	0.0219
1.000	3.994	2.261	-1.762	1.000	1.0000	0.9881	0.0390
1.200	4.434	2.701	-1.322	1.200	1.0000	0.9965	0.0930
1.400	4.806	3.073	-0.951	1.400	1.0000	0.9989	0.1709
1.600	5.128	3.395	-0.629	1.600	1.0000	0.9997	0.2648
1.800	5.412	3.679	-0.344	1.800	1.0000	0.9999	0.3653
2.000	5.666	3.933	-0.090	2.000	1.0000	1.0000	0.4640
2.200	5.896	4.163	0.140	2.200	1.0000	1.0000	0.5555
2.400	6.106	4.373	0.350	2.400	1.0000	1.0000	0.6367
2.600	6.299	4.566	0.543	2.600	1.0000	1.0000	0.7063
2.800	6.478	4.745	0.721	2.800	1.0000	1.0000	0.7647
3.000	6.644	4.911	0.888	3.000	1.0000	1.0000	0.8127
3.200	6.800	5.067	1.044	3.200	1.0000	1.0000	0.8516
3.600	7.084	5.351	1.328	3.600	1.0000	1.0000	0.9079
3.800	7.215	5.482	1.458	3.800	1.0000	1.0000	0.9276
4.000	7.338	5.605	1.582	4.000	1.0000	1.0000	0.9432
4.200	7.456	5.723	1.699	4.200	1.0000	1.0000	0.9554